Predicting the Effects of Interaction Between Multiple Impacts on the Residual Strength in Metallic Honeycomb Sandwich Aircraft Panels Subject to Low-Velocity Impact Damage

Prédire les Effets de l'Interaction entre les Impacts Multiples sur la Résistance Résiduelle des Panneaux en nid d'abeille sandwich métallique d'avions Soumis à des Dommages d'Impact à Faible Vitesse

A Thesis Submitted to the Division of Graduate Studies
of the Royal Military College of Canada
By

Mark Boctor, BSc

In Partial Fulfillment of the Requirement for the Degree
of Master of Applied Science in Mechanical Engineering

September 2021

"Who can find a virtuous woman? For her price is far above rubies."

In The Loving Memory of My Beautiful Darling Mother
To the one who bears the sweetest name,
To the most precious and unique person in my life,
I want you to know that though you are out of sight, you will always be in my heart,
I still see you in the light, you are always on my mind,
I missed you, and I wish that you were here.

To My Beloved Father

Father is a man like no other,
You believed in me, protected, strengthened, and loved me,
There are not enough words to describe what you mean to me and what an influence you have on my life.

Acknowledgements

Successful researchers often build their academic and professional life upon three main pillars: a strong research group with similar research interests, an institution with a clear vision, and supportive family and friends. The guidance provided by Dr. Diane Wowk has been exceptional and extremely valuable for me. I would like to express my sincerest gratitude for Dr. Wowk's support and patience in every stage of my thesis. I would also like to thank my friends, sponsors, research group, and all the teaching and administrative staff at Royal Military College of Canada, who supported and encouraged me to achieve my ambitions. Last but not least, I am indebted to my family for their love, prayers, encouragement and unconditional support.

Abstract

Honeycomb sandwich structures are common in aerospace applications due to their high in-plane strength and bending stiffness to weight ratios. An aircraft vehicle is likely to experience some form of impact loading throughout its lifetime, during maintenance (e.g., tool drops) or in-service activity (e.g., runway debris). Impact damage can cause significant reductions in structural stiffness and strength, leading to in-flight structural failures. All structural panels developed for aircraft must survive numerous impacts of various energies with distinct damage characteristics. The size, number, and proximity of these events may have a unique influence on the panel's residual strength.

Current literature shows that even low-velocity impact damage can result in significant losses in residual strength. However, no comprehensive studies have been done on the proximity of multiple impact sites on the residual strength of metallic sandwich panels under in-plane compression. The current work presents a method for predicting the residual strength for a panel with two dents loaded in compression using finite element (FE) modelling. Specifically, the effect of spacing between dents on the residual strength was determined using a two-stage loading simulation, consisting of a dynamic impact event to create the dents, followed by an in-plane applied compressive load.

It was found that two impact sites in close proximity may interact to produce a deeper dent with a larger area. This leads to a reduction in the residual strength of up to 13%, compared to a single dent. The residual strength is sensitive to the dent depth, as deeper dents initiate the failure earlier, while the planar area of the dent does not affect the residual strength. In addition, dents that are sufficiently separated so that their edges are not touching behave individually and have a minimal reduction in the residual strength in the range of 1-2%, compared to a single dent.

Résumé

Les structures sandwich en nid d’abeille sont courantes dans les applications aérospatiales grace a leur résistance élevée dans les avions et de leur rapport rigidité/poids en flexion. Un véhicule d’avion est susceptible de subir une certaine forme de charge d’impact tout au long de sa durée de vie, pendant l’entretien (p. ex., chute d’outils) ou l’activité en service (p. ex., débris de piste). Les dommages causés par les chocs peuvent causer des réductions significatives de la rigidité et de la résistance structurelle, causant des défaillances structurelles en vol. Tous les panneaux structurels développés pour les avions doivent survivre à de nombreux impacts de diverses énergies avec des caractéristiques de dommages distinctes. La taille, le nombre et la proximité de ces événements peuvent avoir une influence unique sur la résistance résiduelle du panneau

La littérature actuelle montre que même les dommages causés par un impact à faible vitesse peuvent causer des pertes importantes de résistance résiduelle. Cependant, aucune étude approfondie a été completée pour étudier la proximité de sites d'impacts sur la resistance résiduelle des panneaux sandwich metalliques sous compression dans un avion. Ce travail présente une méthode pour prédire la résistance résiduelle d’un panneau avec deux échancrure chargées en compression à l’aide de la modélisation par éléments finis (FE). Plus précisément, l’effet de l’espacement entre les échancrure sur la résistance résiduelle a été déterminé à l’aide d’une simulation de charge en deux étapes, consistant en un événement d’impact dynamique pour créer les échancrure, suivi d’une charge de compression appliquée dans l'avion.

On a trouvé que de deux sites d’impact à proximité peuvent interagir et produire une échancrure plus profonde avec une plus grande surface. Cela cause une réduction de la résistance résiduelle allant jusqu’à 13%, par rapport à une seule bosse. La résistance résiduelle est sensible à la profondeur de la échancrure, car des échancrure plus profondes initient la défaillance plus tot, tandis que la zone plane de la échancrure n’affecte pas la résistance résiduelle. De plus, les échancrure suffisamment éloignées les unes des autres que leurs bords ne se touchent pas, se comportent individuellement et ont une réduction minimale de la résistance résiduelle de l’ordre de 1 à 2%, par rapport à une seule échancrure.

Table of Contents

List of Figures

List of Tables

List of abbreviations

BVID	Barely Visible Impact Damage.
CAI	Compression-After-Impact.
FE	Finite Element.
OEM	Original Equipment Manufacturer.
SRM	Standard Repair Manual.
UK	United Kingdom.
CFRP	Carbon Fibre Reinforced Polymers.
FEA	Finite Element Analysis.
NDI	Non-Destructive Inspection.

1. Introduction

The use of honeycomb sandwich structures is rapidly increasing in the aerospace, marine, automotive and industrial fields due to their high stiffness and strength-to-weight ratios. Honeycomb panelling is often the lightest option for in-plane compression and bending-specific applications. However, these structures are extremely vulnerable to impact damage, reducing their residual strength and compromising their structural integrity [1]. In aerospace applications, honeycomb sandwich panels are used widely in fixed and rotary-wing aircraft within commercial and military sectors as floors that support the weight of transport personnel and cargo and cover panels that cover and protect the underlying structures. Two examples of honeycomb sandwich panels retired from service are shown in Figure 1-1.

Figure 1-1: Examples of dented aerospace honeycomb sandwich panels [1].

Honeycomb structures are subjected to low-velocity impact damage from tool drops during maintenance, from runway debris during takeoff or taxiing and from hail due to their poor out-of-plane resistance to deformation. Impact damage is defined here as residual deformation of

either the facesheet or core material. This damage takes the form of dents that may be visible on the surface of the panel, as shown in Figure 1, as well as core damage beneath the dent, as shown in Figure 1-2.

Figure 1-2: Surface denting and core damage due to impact [2, 3].

The Structural Repair Manual (SRM), which is provided by the Original Equipment Manufacturer (OEM), defines the damage limits based on surface damage characteristics such as dent area, diameter, depth, and the distance between the edges of the dents. These limits are necessary for categorizing the dents into being negligible or allowable and state the amount of damage that can be present in honeycomb sandwich panels before they need repairing or replacing. Dents beyond the allowable limits may reduce the residual strength of the panel by local facesheet wrinkling, disbonding and localized buckling in the core. Residual strength hereby refers to the dented panel's residual capacity to support in-service loads.

1.1. Motivation

This thesis is part of a larger research project aimed at more precisely assessing the damage limits specified in the SRM to reach important conclusions about extending the service life of honeycomb panels. The damage limits are thought to be conservative as they are based on assumptions such as circular dents and spacing, which do not account for dent profiles or shapes or orientation with respect to the loading direction. This thesis focuses on the damage limit that addresses the minimum distance between multiple impact sites. The majority of research on multiple impacts focuses on repeated events at a single location. However, in reality, dents are scattered across multiple locations on the panel, and the distance between impact sites could influence the panel's ability to carry in-service loads. Therefore, it is essential to investigate how the spacing between two dents affects the residual strength.

In reality, panels contain inherent variability in terms of cell size, cell shape, cell wall thickness and adhesive distribution. In addition, impacts can occur at different locations on the panel with respect to the cells, such as in the center of the cell or on top of a cell wall. All these potential variations mean that for the same impact scenario, the dent depth could vary at different impact locations on the panel. Preliminary studies showed that these variations could make it difficult to interpret the effect of spacing on the interaction between multiple dents. In order to isolate the effects of dent spacing and to explain how dents in close proximity interact, these variations should be removed if possible. In finite element simulations, all variations in the panel properties can be removed by using the same geometry for each simulation. However, a study was required to see whether a consistent impact location was required as the spacing between the multiple dents was altered.

The SRM specifies the minimum distance required between dents, but this does not consider the size, depth, or orientations of the dents. It is general and not optimal for each panel. A more comprehensive investigation into the mechanism by which two dents interact is required to potentially optimize this distance in the future. This thesis focuses on numerical simulations of low-velocity impacts on panels with aluminum facesheets and aluminum honeycomb core. The effect of the interaction between two dents in close proximity to each other on the residual strength of a panel subject to in-plane compression is studied.

1.2. Overall Approach and Constraints

The goal of the numerical simulations is to predict the peak in-plane compressive force that can be resisted by a panel with two dents. Dynamic finite element simulations of the impact stage followed by in-plane compressive loading were conducted on a honeycomb panel with a metallic honeycomb core and metallic facesheet. Multiple, low-velocity impacts that produced barely visible impact damage (BVID) were used to achieve the goal in two stages, as illustrated in Figure 1-3. The first stage consists of a finite element analysis of the impact event with two dent sites. In the second stage, the panel was loaded in compression, and the peak load at the point of localization was noted. Comparison between the peak load for a panel with a single dent versus a panel with two dents gave the reduction in residual strength.

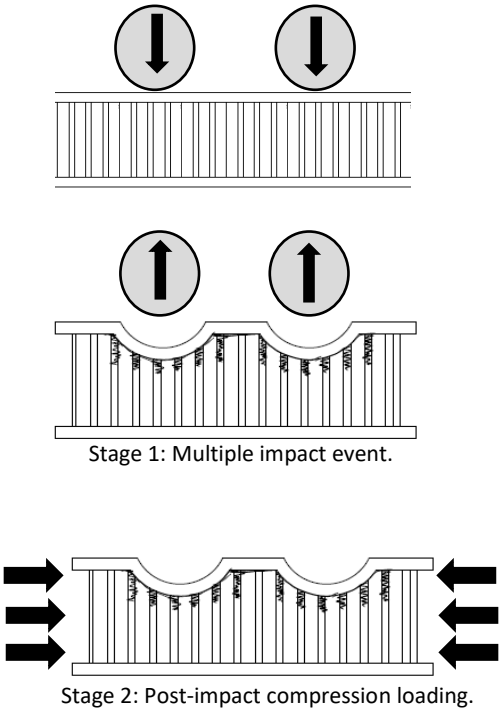

Figure 1-3: Steps of the overall approach.

As the distance between two dents changes, the dents could be located overtop of different parts of the cells, for example, the center of the cell or a cell wall. A study was first performed to determine how much the impact location affected the resulting dent depth. This will be referred to as Study 1. This study determined the method by which the spacing between dents was defined when looking at the effects of dent proximity. Study 2 determined the relationship between the dent spacing and the residual strength in in-plane compression.

1.3. Outline

This thesis is presented in an article-based format. It includes two separate studies, each a stand-alone document with its own literature review, conclusions, and references will be found at the end of the thesis. The thesis is outlined as the following:

- **Chapter 1: Introduction**
  - Provides a general overview of honeycomb sandwich panels and introduces the problems that were addressed by the work in this thesis.
- **Chapter 2: Background and Literature Review**
  - Provides a general overview of the necessary background on damage in honeycomb sandwich panels, focusing on barely visible impact damage (BVID) and the effects of this damage on the residual strength of these structures.
- **Chapter 3: Study 1**
  - "Effect of impact location on the variation of residual dent depth in metallic honeycomb sandwich panels".
- **Chapter 4: Study 2**
  - "Effect of the interaction between multiple dents on the in-plane compressive residual strength in aluminum honeycomb sandwich panels."
- **Chapter 5: Summary**
  - Discusses the key findings of both studies in the context of the larger goal of evaluating the SRM dent limits and discuss areas for further research.

2. Honeycomb Sandwich Structures

Honeycomb sandwich structures consist of two facesheet layers bonded to a honeycomb core with adhesive layers, as shown in Figure 2-1. The facesheets are designed to carry the majority of the bending load, while the core is designed to carry the shear load and keep the facesheets separated [4]. The resulting structure significantly improved stiffness-to-weight ratio and bending strength compared to facesheets alone [5]. The core also increases the distance between the two facesheets and increases the second moment of area while optimizing the strength to weight ratio.

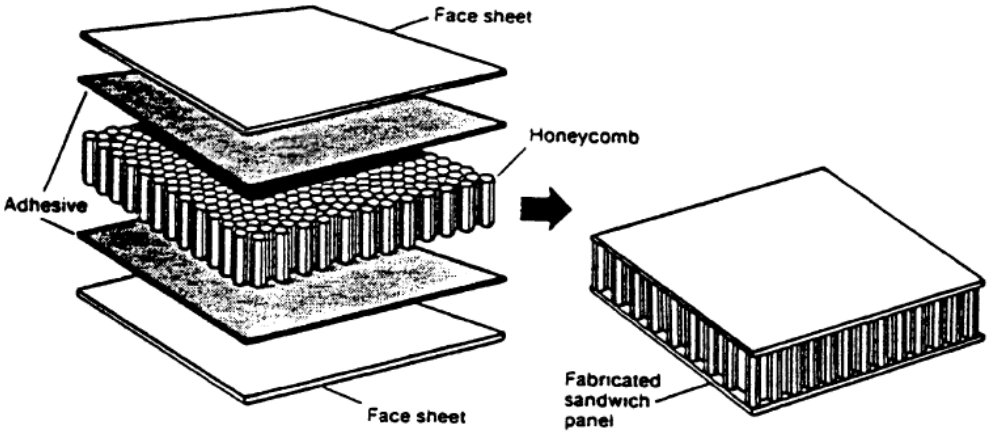

Figure 2-1: Honeycomb sandwich panel construction [4].

Sandwich panels are commonly found in aerospace, automotive and marine industries. Sandwich panels are used in aircraft structures for wing panels, cabin floors and flight control surfaces. Figure 2-2 illustrates an example of honeycomb sandwich panelling as used within an aircraft.

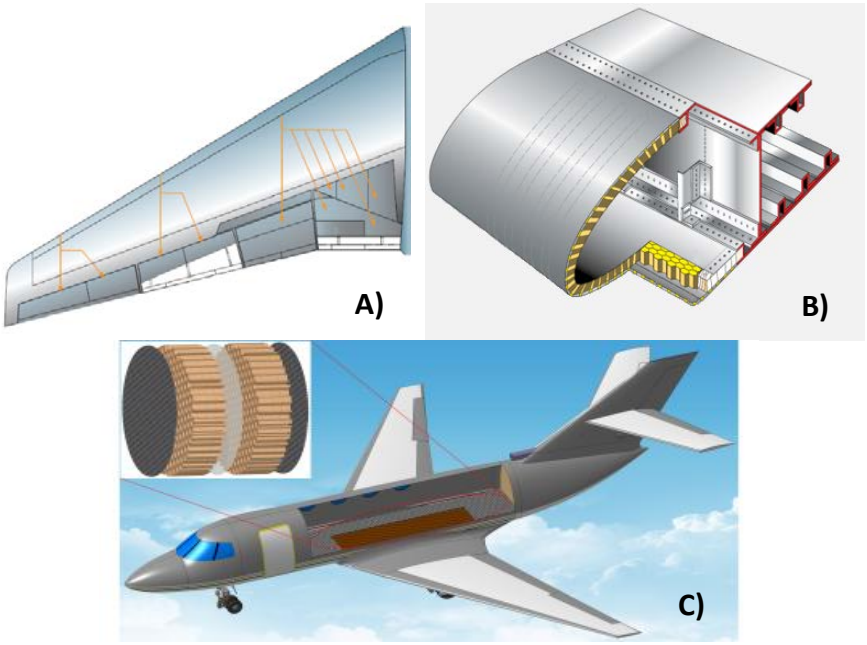

Figure 2-2: Honeycomb panels in aircraft structures a) Honeycomb wing construction on large jet aircraft [6], b) Wing leading edge formed from honeycomb bonded to aluminum spar structure [6], c) Aircraft cabin floor [7].

2.1.1. Materials and Manufacturing

Honeycomb sandwich panels have been made from a variety of materials since the 1940s. Metallic materials such as aluminum, stainless steel and titanium and non-metallic materials such as fiberglass, Nomex and Kraft paper being among the most commonly used today. Unusual materials such as copper, lead, asbestos, Kapton and Mylar have also been used [4]. Carbon fabric is a new material that produces honeycomb with exceptional mechanical properties, particularly for a non-metallic core. In fact, it is the first non-metallic core that has shear moduli as high as aluminum honeycomb [4]. The material for the honeycomb sandwich panel is chosen for its mechanical properties but may also be selected due to its fire-resistive or thermal properties [8]. Epoxy liquid/paste or film adhesive is commonly used to attach the core materials and facesheet together [9]. This adhesive is typically non-volatile to avoid the build-up of volatile substances during the curing phase [10]. The majority of research has been conducted on laminate facesheets such as CFRP rather than metallic facesheets. However, due to the continued use of these panels as secondary structures and on older aircraft that need maintenance, further investigation of panels with metallic facesheets is needed.

For metallic honeycomb cores, the expansion and corrugation methods are the most commonly used techniques for manufacturing. The metallic honeycomb cores in both methods are manufactured with multiple layers of aluminum foil, bonded with adhesive at the ribbon direction nodes, and then stacked and cured in an oven. This allows the cell walls in the ribbon direction to be doubled, as illustrated in Figure 2-3.

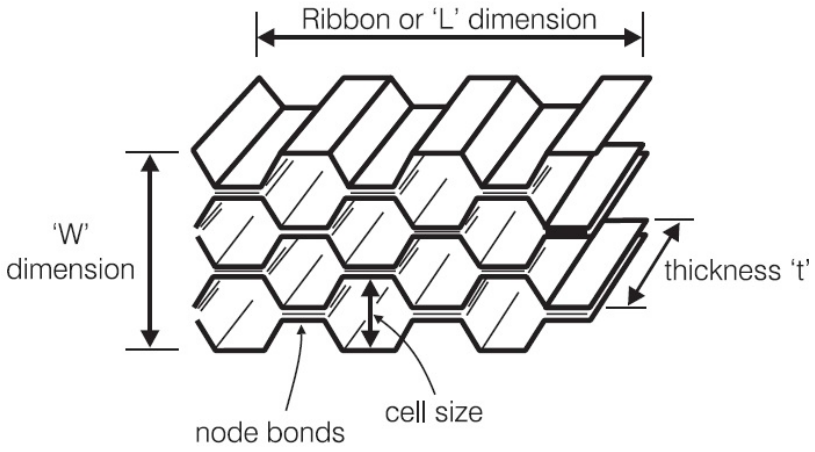

Figure 2-3: Honeycomb manufacturing process showing the ribbon direction [11].

2.1.2. Damage

Impact damage to aircraft honeycomb sandwich structures such as tool drops, or runway debris may occur during repair or operation. The facesheets and the core have minimal resistance to local out-of-plane deformation, making the panels susceptible to surface dents and localized buckling of the core upon impact. Figure 2-4 shows a surface dent as well as core damage.

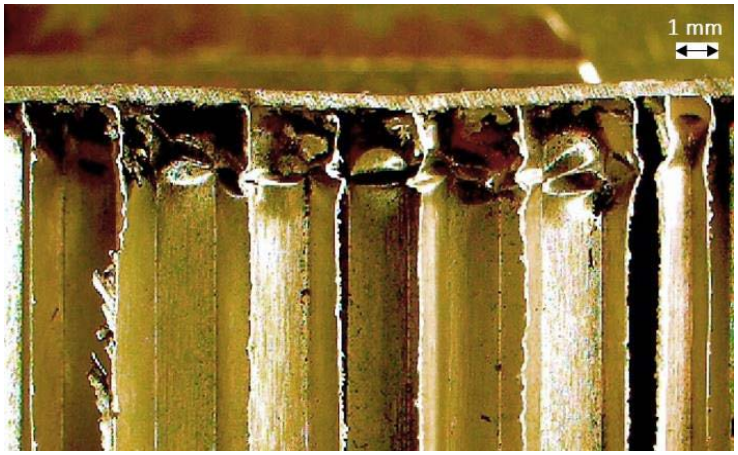

Figure 2-4: Surface denting and core damage [2]

Impact damage is typically confined to the top facesheet, core material, and the adhesive between them, whereas the bottom facesheet usually remains undamaged [1]. For aluminum-faced aircraft panels, both low- and high-velocity projectiles produce impact damage.

Low-velocity impacts are often a result of tool drops and runway debris, which result in both facesheet denting and honeycomb core crushing. It is not only the velocity of the impactor that determines whether an impact is considered low-velocity or not, but also the ratio of the mass of the impactor to the mass of the panel is a factor that is considered. A ratio of at least 10:1 is

sufficient to be considered low-velocity [12]. Low-velocity impacts are usually characterized as having contact durations long enough that the stress and shock waves caused by the impact reach the boundaries of the panel before the contact with the impacting body has finished. Following the elastic spring-back of the facesheet, these impacts often produce BVID, which can mask extensive core damage. This phenomenon has been observed frequently in honeycomb sandwich panels with laminate facesheets [13], as laminate facesheets have greater spring-back than metallic facesheets. Panels subjected to low-velocity impact are often able to remain in service if the damage falls within the allowable limits specified in the SRM. However, more severe impact damage can reduce the strength in compression, tension, fatigue and bending by as much as 50% [13]. This may further reduce airfoil stiffness, leading to unfavourable aeroelastic phenomena and a significantly reduced fatigue life [14].

High-velocity impacts are often a result of birds, hailstorms, ballistics (e.g., small arms fire) or hypervelocity impacts (e.g., space debris). These impacts typically result in severe surface denting or through-facesheet penetration, as well as severe core crushing for both composite and aluminum honeycomb sandwich panels, necessitating panel replacement as specified by the SRM. This type of impact damage is not considered in this thesis.

2.2. Low-Velocity Impact Damage Mechanism

A low-velocity impact event on an aluminum honeycomb panel with aluminum facesheets involves three separate stages, as illustrated in Figure 2-5.

1) **Initial contact between impactor and facesheet**.

   The facesheet starts to bend as the point of contact is displaced toward the core. The honeycomb core starts to deform as well, although it may not be experiencing any permanent damage at this point.

2) **Continued indentation until maximum displacement**.

   The impactor indents the panel until its kinetic energy is dissipated. Depending on the facesheet's bending stiffness, core density and the impactor's shape, this may cause a sharp indentation, or the deformation may be smoother and spread over a wider area [15]. During this denting process, the honeycomb core underneath absorbs most of the impact energy and gets damaged through localized folding of the walls, which continues to progressive crumpling and crushing.

3) **Impactor rebounding and facesheet spring-back**.

   The elastic strain energy in the core and the facesheet releases, transforming back into kinetic energy, pushing the impactor away from the facesheet at a reduced velocity from the initial impact. As the elastic strain energy is released, the facesheet springs back, resulting in a final dent shape that is less deep than the maximum indentation position during the impact. The spring-back of the facesheet can induce residual tensile loads in the honeycomb core because of the larger degree of plastic deformation that is present in the core. Adhesive failure may occur between the facesheet and core.

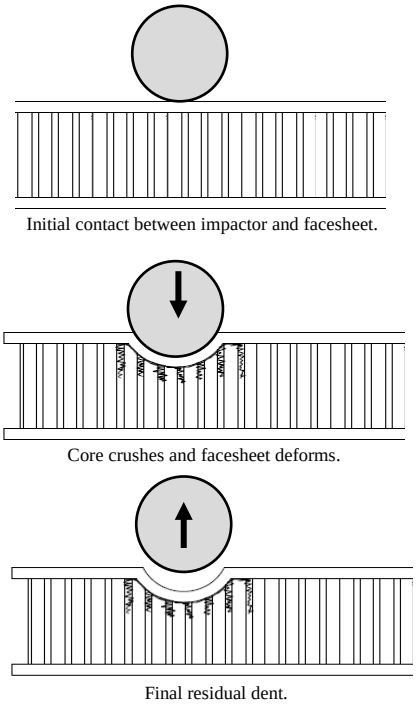

Figure 2-5: Stages of impact damage.

2.3. Impact Damage Detection

Visual inspection is the most common method of locating impact damage in metallic honeycomb sandwich panels. Once located, a dial depth gauge and a ruler are used to determine the maximum dent depth and measure the dent length. The damaged area is evaluated by approximating the dent perimeter as a circle and using the dent length as the diameter [16]. The length measurement is rounded up to give a more conservative area measurement [16]. It is more difficult to detect damage to sandwich panels when significant relaxation of the facesheet occurs. Impact damage in the core can be detected using tap testing, requiring experienced technicians with a trained ear for the tonal differences between damaged and undamaged areas. Human factors cause much variation in these methods. Figure 2-6 illustrates examples of these tools as used within the Royal Canadian Air Force [16].

Figure 2-6: Dial depth gauge (left) and tap tester (right) [16].

Other commonly used NDT methods include thermography, which measures the effect of damage on heat transfer rate through a panel. Shearography identifies defects by measuring variations in the reflection of the laser on the panel's surface before and after a load is applied to it. Radiography uses x-ray imaging to provide a detailed view of the interior of a honeycomb panel [11]. 3D laser scanning can be used to measure surface damage, including dent profiles. Eddy current testing can be used at different frequencies to measure surface and subsurface damage [1]. Finally, Transmission Ultrasonic C-Scan measurements can detect underlying damage by identifying the changes in the propagation of sound waves through a crushed honeycomb core, as was used by Tomblin et al. [17]. These techniques can be used to detect the presence of damage. However, none can accurately distinguish between different types of damage, such as disbonding, crumpling, or cracking of the core, and none can tell the depth or severity of the core damage.

2.4. Allowable Damage Limits

The definitions of allowable damage limits for honeycomb sandwich panels are specified within the SRM of an aircraft. This manual, which is issued by the manufacturer and approved by the regulatory authority (Transport Canada), details the specific repairs approved for a specific aircraft structure. This manual describes what constitutes negligible and allowable damage. In this context, negligible damage is defined as damage that does not necessitate consideration or documentation, whereas allowable damage is defined as damage that it needs to be noted during an inspection.

Damage that is more severe than allowable damage requires panel repair or replacement. The damage limits, in general, are different for different regions of the aircraft or different types of aircraft.

2.4.1. Negligible Damage:

For negligible damage, there is no limitation on the number of these dents per panel, or the distance between these dents and fasteners or edges as long as there is no delamination, disbond, cracking or puncturing identified visually or by tap test. Negligible damage may be based on a metric such as maximum dent diameter or maximum dent depth, and there is no requirement to report dents that are below this threshold.

2.4.2. Allowable Damage:

Allowable damage is defined by a maximum diameter and maximum dent depth, which could be a function of the total panel thickness. For example, the SRM for one model of Gulfstream aircraft states that the maximum depth of any dent shall not exceed 20% of the total panel thickness [18]. The total area of all combined dents (not including negligible damage) must be less than a certain percentage of the panel area. A minimum distance from the dent edge to a fastener, adjacent skin, edge, or hole is specified (less than 25.4mm (1in) for the Gulfstream [18]). A minimum distance for two dents between the edges of individual dents is also given. For example, the SRM for the Gulfstream states that the distance between two dents shall not be less than 101.6mm (4in) [18].

2.4.3. Additional Information:

It is recommended to repair allowable damage during major inspections, especially if the damaged area approaches the limit or if mapping history indicates that damage will exceed the limit of the total damage area before the next major inspection. No disbonding is permitted, which constitutes either failure of the adhesive at the facesheet-core interface or tearing/cracking of the honeycomb core. There is no distinction made between sharp and smooth dents, as significant differences in residual strength have not been observed in practice.

2.5. Barely Visible Impact Damage (BVID)

Low-velocity impact is considered in this thesis because it results in dents within the allowable damage limits, which are free of punctures or cracks that would otherwise necessitate panel repair or replacement. BVID is simply a type of low-velocity impact damage that usually falls within the allowable damage category and is characterized by dents that are difficult to detect solely by visual inspection [17]. The criterion for classifying BVID is loosely based on dent depth as opposed to dent diameter for the damage limits outlined previously. According to Tomblin et al. [19], BVID is identified as standing below the allowable damage limits for the aircraft as detailed in the structural repair manual, and these limits may differ between aircraft and between components. The generally accepted threshold for what is determined to be BVID is a residual indentation depth of 1.27 mm (0.05") [19], and lower values are used by some [20]. As an example, the National Physical Laboratory in the United Kingdom (UK) defined BVID as damage causing a dent depth of 0.5mm [21], whereas a NASA report defined BVID as having a dent depth within the range of 1.27mm to 2.54mm [22]. In contrast, Boeing considers dents in the 0.25 to 0.5 mm depth range to

be the threshold for BVID [20]. Reference [16] uses dent depths in the range of 0.14-1.01mm, while reference [2] uses dent depths in the range of 0.15-1.13mm based on dent depth which coincided with the deepest dent in a retired aircraft panel. Given the lack of an official definition for BVID in terms of accepted measurements, the numerical models in the current work used dent depths in the range of 0.18-1.25mm. These respect the allowable damage limits and are considered as BVID.

2.6. Impact Damage in Honeycomb Panels

While in maintenance or service, honeycomb sandwich panels are susceptible to low-velocity impact damage, which results in a variety of damage found in both the facesheet and the honeycomb core, depending on the material used. For example, metallic panels typically experience facesheet deformation and core crushing, while composite panels see matrix cracks, delamination or fibre fracture and core crushing or cracking. The primary parameters influencing impact damage are those of the panel, such as facesheet thickness and core density via cell size and cell wall thickness, and those of the impactor, such as impactor size as well as impact energy via impactor mass and velocity. The effect of these parameters on low-velocity impact damage has been studied to varying degrees by researchers.

2.6.1. Dent depth

The dent depth has been shown to be primarily affected by such parameters as impact energy, impactor shape, core density and facesheet thickness.

The effect of impact energy on dent depth has been studied by varying the impactor mass and velocity [23-28]. It was found that increasing the impact energy results in a larger contact force and facesheet deformation; the greater the impact velocity, the more energy is absorbed by the panel, which results in deeper dents. For aluminum-aluminum honeycomb panels, Zhang et al. [3] concluded that dent depth increased non-linearly with impact energy, while Clarke [23] and Foo et al. [25] showed a linear increase.

The shape and size of the impactor determine the contact area with the surface of the panel. Larger radius impactors have larger contact areas that distribute the impact energy over a larger surface, resulting in smaller residual dents [17, 24, 29]. For impactor shapes, Zhou et al. [29] found that a flat-ended impactor will result in deeper dents than a spherical-ended impactor due to larger contact forces and greater stress concentrations around the edge of the impactor.

Denser honeycomb cores will result in smaller dent depths as they are capable of absorbing more energy with less deformation than less dense cores [25, 27, 28]. Wowk et al. [30] showed that denser cores also had increased elastic energy absorption, resulting in greater spring-back capacity and contributing to smaller residual dent depths.

As is the case with denser cores, thicker facesheets can absorb more energy than thin facesheets and produce smaller dent depths. In addition, the increased spring-back capacity of thicker facesheets can effectively pull upwards on the crushed core and cause the residual dent depth to be much smaller than the maximum dent depth during impact [30]. Clarke [23] discovered that changes in the facesheet thickness for aluminum panels could result in changes in the dent depth

without necessarily changing the dent diameter, thus causing the dent depth and width to behave independently.

2.6.2. Dent Area

The dented area has been shown to be affected by parameters such as impact energy, impactor shape, core density and facesheet thickness.

The effect of impact energy on dent area has been studied by varying the impactor mass and velocity [23-25]. The greater the impact energy, the larger the contact forces on the panel, which results in a larger damaged area. For aluminum-aluminum honeycomb panels, Clarke [23] and Foo et al. [25] showed the dented area increased logarithmically with increasing impact energy for the same impactor size.

The shape and size of the impactor determine the contact area with the surface of the panel; a larger radius impactor results in a larger contact area that distributes the impact energy over a wider area resulting in a larger damaged area of the panel [23, 24, 31]. For impactor shape, impactors with larger contact surfaces produce bigger damage area and shorter contact duration. Flat-ended impactors produce larger impact damage areas, while conical impactors localize the damaged area and result in surface penetration [32, 33].

Lower density honeycomb cores are more easily deformed, allowing the impactor to travel deeper into the panel before spring-back. For spherical impactors, travelling deeper into the panel will result in a larger contact area between the impactor and the panel, thus producing a larger dent area [30]. For aluminum honeycomb panels, it was found that the residual dent width increases linearly with increasing facesheet thickness for the same impactor size. This is a result of thicker facesheets being less able to conform to the shape of the impactor, therefore producing a dent with a more gradual profile and larger width [23, 29, 30]. A stiffer impactor will also tend to result in a smaller dent area as the impact is more localized.

2.6.3. Facesheet and Core damage

Honeycomb panels are susceptible to impact damage in the facesheet or in the core. Sections 2.6.1 and 2.6.2 discussed the dent depth and dent area, which are examples of permanent deformation in the facesheet. Additional damage may occur in the facesheet depending on the material and the amount of impact energy. In metallic facesheets, cracking occurs if the impact energy is large enough. Composite facesheets are susceptible to matrix cracks, delamination, or fibre fracture. Aluminum cores crush and crumple similarly to Nomex cores, but Nomex cores have a higher tendency to fail via brittle fracture. Figure 2-7 shows different impact damage modes for the facesheet and honeycomb core. The allowable damage limits do not allow any failures in the facesheet or the adhesive, so these damage modes will not be discussed any further.

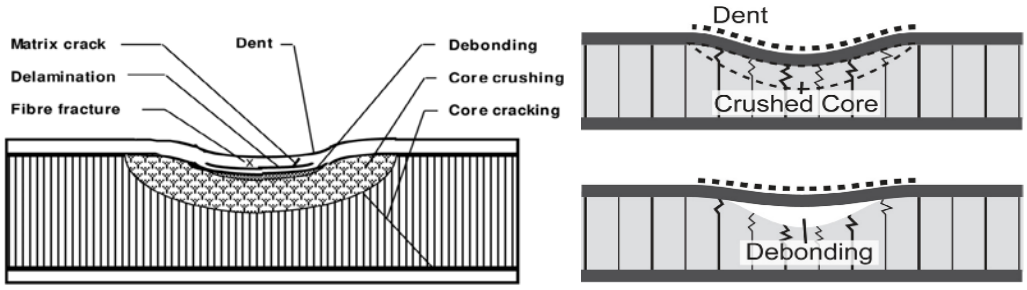

Figure 2-7: Impact damage mode for composite facesheet and honeycomb core [34, 35].

At the low-velocity impact energy that produces BVID, the damage to aluminum honeycomb cores is progressive in nature throughout the depth of the core, starting from the impacted facesheet and continuing downwards as the indentation progresses. Initially, facesheet bending compresses the honeycomb core elastically in the out-of-plane direction. As the impact progresses, the cell walls develop a wavelike pattern of displacement in the lateral directions. As these deflections increase, the cell walls deform plastically and buckle, leading to the appearance of lobes (folds). The core shows a clear division between the damaged upper part and the undamaged lower part. More deformation occurs only through the lobes near the top facesheet, buckling plastically and forming tighter folds rather than creating more lobes [2]. These folds continue to deepen until the initial crush region has fully flattened. This progression of damage happens because the number of lobes that develop in a cell wall is determined at the initiation of impact. The development of new lobes does not occur until the initial lobes have been completely crushed. As new folds are created and compacted in the section directly beneath the initially crushed region, a pattern of minor peaks and drops in the crushing load are seen. This progressive crushing pattern continues until the kinetic energy from the impactor has been entirely absorbed by the panel. Figure 2-8 shows the core damage and folding mechanism.

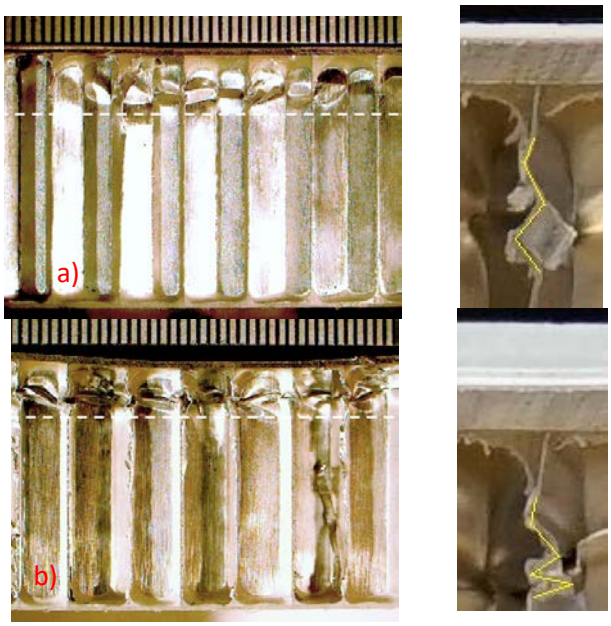

Figure 2-8: Core damage and folding mechanism a) Plastic folds and buckling of the cells walls, b) Tighter folds [2].

It was found that the depth of the core damage for all dents within a panel is constant, even for different impact configurations [2, 23, 36, 37] and is driven by the height of the adhesive fillet that joins the facesheet to the core. The larger adhesive fillets cause buckling of the cell walls to initiate deeper into the core, resulting in an increase in the depth of the core damage. The adhesive constrains the top of the cell walls, where the honeycomb core connects to the facesheet, and prevents the cell walls from buckling [2].

Denser cores resulting from increased cell wall thickness or smaller cell sizes exhibited higher peak loads, increased buckling resistance, and reduced damage profiles in the core and indented facesheet [23, 27, 28, 30]. It was found that when the core density increased, the depth of the core damage decreased. The core damage depth decreases with increasing core density because of the increased core stiffness on the damage progression in the cell walls. Cells that are larger in size or have smaller wall thicknesses are more flexible and experience more displacement before crumpling occurs; therefore, the dent depth will be larger. Larger cell sizes also result in larger core damage depth as they allow more room for cell wall buckling to occur.

When aluminum honeycomb panels are impacted at low-velocity, they will undergo damage in the form of a residual dent in the facesheet and cell wall buckling in the core that is confined to a region directly beneath the dent. The core damage diameter being equal to the dent diameter has been demonstrated numerically and experimentally [2, 23, 25]. This means that the width of the core damage can be determined by manually measuring the diameter of the surface dent without any requirements for advanced non-destructive inspection (NDI) methods [2]. This indicates that the cell walls in the core experience yielding only when the facesheet over them is deformed. Therefore, the damage in the honeycomb core does not extend further than the planar area of the dent.

2.7. Compressive Failure of Honeycomb Panels following Impact Damage

Aircraft sandwich panels will undergo different types of loading such as in-plane compression, tension, bending and shear depending on the type of aircraft manoeuvres and the location and purpose of each panel. When dents due to low-velocity impact are present, panels can fail prematurely due to the presence of localized damage. This thesis will focus on how the presence of dents can cause a reduction in the residual strength of a panel when loaded with an in-plane compressive force.

2.7.1. Failure Mode due to In-plane Compression Loading

In honeycomb sandwich panels subjected to in-plane compressive loading, different failure modes will occur depending on if there is a dent present or not and the characteristics of the panel. Figure 2-9 shows different failure modes such as general buckling, shear crimpling, face wrinkling and intracell buckling (dimpling) for undamaged panels.

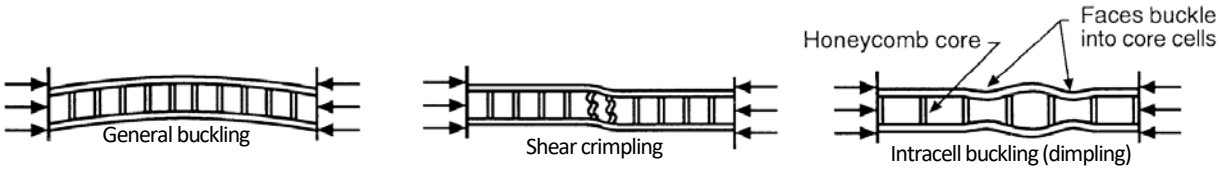

Figure 2-9: Different failure modes for undamaged honeycomb sandwich panel subjected to compressive load.

General buckling occurs for undamaged panels that have an inadequate panel thickness. Shear crimpling can occur if the core has a low shear modulus or low adhesive shear strength. Facesheet wrinkling and intracell buckling occur due to the compressive instability of the facesheet, as the core can no longer support the facesheet's normal load, which leads to inwards or outwards buckling depending on the core and bond properties. Moreover, the facesheet can buckle inward due to core compression failure or outwards due to adhesive bond failure, as shown in Figure 2-10.

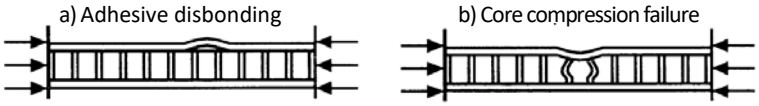

Figure 2-10: Facesheet wrinkling a) Buckle outwards (adhesive disbonding), and b) Buckle inwards (core crushing failure).

When a dent is present under compressive loading, the panel shows the phenomena of dent growth. The dent first experiences localized facesheet wrinkling and then grows and propagates to the edge of the panel. Figure 2-11 a) shows the initial circular dent in the panel, b) shows that under in-plane compression, the facesheet bends inwards towards the core and the dent deepens and becomes more elliptical, c)-d) shows the region expanding across the facesheet transverse to the

compressive loading direction, e) shows the overall general failure mode as the localization has propagated to the edges of the panel.

Figure 2-11: Phenomena of dent growth for sandwich panel [37].

2.7.2. Test Set-up

Post-impact loading tests are used to measure residual strength, such as a compression-after-impact (CAI) test that measures the residual strength of a dented panel under in-plane compression [37-42]. For CAI tests, a dent must be created first, and this can be achieved by a drop tower, or a pendulum, as shown in Figure 2-12. After the damage site has been created, the CAI test compresses the panel in the in-plane direction up to the point of failure. CAI produces the type of failures that each different panel is susceptible to, such as delamination in the case of laminate facesheets or facesheet wrinkling in the case of metallic facesheets.

Figure 2-12: Pendulum apparatus used to impact the honeycomb sandwich panel coupons.

The CAI test setup is defined in ASTM standard C364/C364M-07 [43]. CAI testing is typically performed by placing a honeycomb sandwich coupon under a uniaxial compressive load, as shown in Figure 2-13. The two opposite ends of the panel are gripped, and either a force or displacement can be prescribed. The end conditions are representative of clamped boundary conditions. The sides of the panels can either be left free or placed in a track to prevent early bucking failure at the grips as a result of the stress concentrations near the loading region. Typically, the impact damage is located in the center of the test coupon, and strain gauges are placed on both sides of the sandwich panel. Multiple strain gauges as well as digital image correlation (DIC) may be used if a strain distribution is desired. Both the force and the applied displacement are recorded. A high-definition video recording system can be used to monitor the front and the rear of the coupon. CAI residual strength results are usually presented as a function of impact energy [41, 44, 45]. The peak force

measured at the grips is taken as the residual strength of the panel and can be compared between a dented and undented panel to determine the reduction in residual strength.

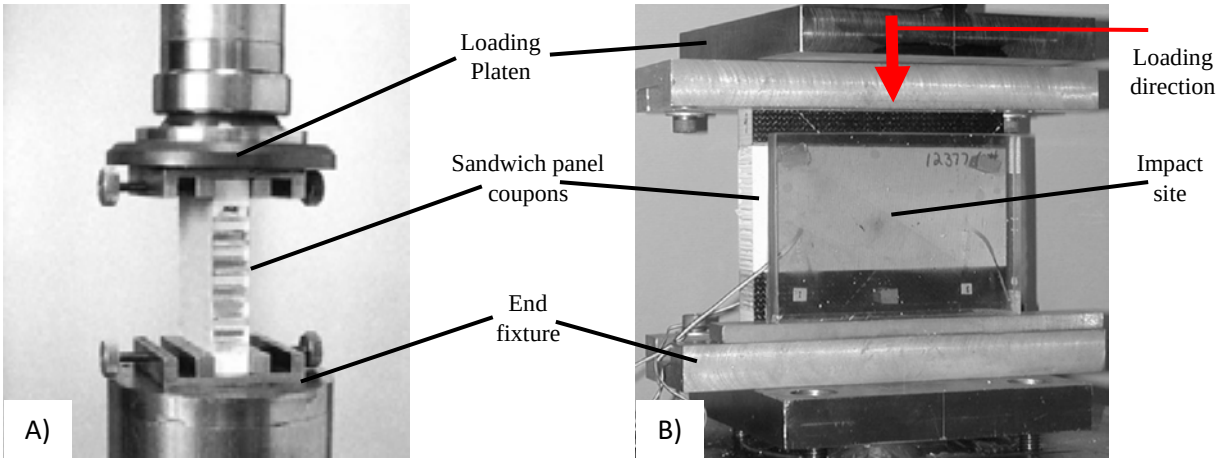

Figure 2-13: Test configuration of axial compressive test on a honeycomb sandwich panel specimen [43], a) The side view for test setup and b) The front view for test setup.

2.7.3. Residual Strength

The residual strength in compression is defined as the maximum compressive load that the impacted panel can withstand and is most commonly determined through CAI tests. As the dented panel is loaded in compression, the force increases linearly as it passes through the facesheets. Then the instability will typically occur through facesheet wrinkling, and this will coincide with the peak force. The force then drops as the wrinkle deepens and propagates perpendicular to the loading direction. Tomblin et al. [46] stated that these reductions in CAI are caused by buckling and crumpling in the core, which leaves the damaged facesheet unsupported and reduces its ability to carry loads, particularly in bending. The majority of the work has been on Nomex, and minimal work has looked into metallic panels.

CAI studies have been used to determine the effects of impact energy on the peak in-plane force resisted by panels. The effect of dent depth on the residual strength has been studied, and it was found that increasing the dent depth results in a reduction in residual strength [38, 40]. McQuigg et al. [37] showed a reduction in compressive strength of up to 25% when no surface damage was visible and up to 50% for higher impact energies with deeper surface dents. The failure is a result of facesheet buckling above an unsupported honeycomb core. These results are important to consider because, even though the surface damage was minimally visible, a reduction in the load-carrying capacity occurred. Aminanda et al. [40] also found that the residual strength decreased with dent depth due to the local instability; however, the load-displacement behaviour of the panel up to that point was not affected.

It has been determined that the size of the core damage region plays an important role in the residual strength of honeycomb panels as increasing the depth of the core damage results in a reduction in CAI strength [17, 46, 47]. Shyprykevich et al. [46] determined that damage propagation due to compressive loading will depend on the depth of the core crush as the core will not provide any

support until the facesheet has been displaced by the depth of the crushed core. It has been shown that the core damage could contribute up to 20% to the reduction in residual strength [47].

The properties of the sandwich panel also affect the CAI strength. For core density, it was found that increasing the core density results in increasing residual strength as it results in smaller dents [37, 45]. While for the facesheet thickness and core thickness, the researchers showed that increasing the skin thickness or core thickness can produce a stiffer structure with more bending resistance, resulting in a higher compressive strength for the undamaged panel [41, 44]. Gilioli et al. [41] showed that increasing the skin thickness from 1 to 1.5 mm leads to the edgewise strength increasing by 36%.

2.8. Modelling Methods

Finite element analysis is a numerical method that has been widely used for predicting the behaviour of honeycomb sandwich panels that have been damaged through impacts. Different approaches have been used to simplify the simulations because of the extremely long run times associated with modelling the cellular core in a geometrically accurate manner. For example, the core is often homogenized and represented by uniform properties. Run times could also be reduced by simulating the impact event as a quasi-static event.

2.8.1. Quasi-static versus Dynamic Simulations

Low-velocity impact damage can be modelled in two different ways: dynamic impact (drop-weight) or quasi-static indentation; both methods produce roughly the same damage except at lower energy levels where quasi-static indentation caused more damage [37]. Schubel et al.[48] investigated both methods of generating low-velocity impact damage. It was found that damage initiated sooner and was more severe for quasi-static indentation, especially in the indenter-facesheet contact region. The majority of researchers who have attempted to model low-velocity impact damage to honeycomb sandwich structures with lower energy have used explicit dynamic analyses rather than quasi-static analyses [3, 25-27, 36, 49-52].

The FE modelling software gives the user a choice of either an explicit or implicit solving option for modelling low-velocity impact damage. These two options are mainly different in the time integration scheme used. Explicit solvers are typically used for dynamic problems where the loading lasts less than a second, while the implicit solvers are usually used for static structural where the loading lasts longer than a second. Explicit solvers do so explicitly without iterating during time integration, while implicit solvers approximate the solution at discrete time steps using equilibrium iterations. Explicit solvers are generally better-suited for highly non-linear problems, while implicit solvers are generally better-suited for linear problems. Sun et al. [53] and Giglio et al. [54] used an explicit dynamic solver for modelling the impact damage stage and the post-impact loading stage and achieved good agreement with their experimental results with a relative error between 3 – 5% [53]. For these reasons, this thesis uses an explicit solver to model impact damage and post-impact loading.

2.8.2. Core Representation

When numerically modelling impact damage, there are two ways to represent the honeycomb core: realistic core representation and simplified core representation. The realistic core representation method uses complete core details such as cell geometry and material properties for the cell walls, producing cell wall buckling. This method accurately models both the impact response and damage modes caused by the low-velocity impact but at significantly longer solution times. For the simplified representation, the core is either homogenized as a single orthotropic material of solid elements with equivalent material properties determined through experimental testing or a grid of equivalent non-linear springs. The simplified core representation method is typically used to study the impact response of honeycomb structures and benefits from faster solution times.

2.8.2.1. Realistic Honeycomb Core Representation

Realistic representations of the honeycomb core consist of a full 3D cell geometry. This facilitates the investigation of damage and failure modes, such as localized buckling in the core, facesheet spring-back, and load path changes for post-impact loading. Researchers found that using the realistic honeycomb core representation gives agreement with the experimental results as the damage progression and failure in the honeycomb core are detailed with local damage distribution along the cells. Either the entire core can be represented at this level of detail, or it can be limited to the impact and failure region. Zhang et al. [3] modelled the entire panel structure in details such as the honeycomb core, facesheets, and adhesive layer, while Czabaj et al. [55] used a geometrically accurate representation of the honeycomb core in only the failure region to predict the CAI strength. The remainder of the core was simplified and modelled with solid orthotropic elements to increase the model's computational efficiency by reducing the run time.

All the numerical models created in this thesis used a 3D geometric representation of the cells to model the honeycomb cores. In doing so, this allowed for the analysis of damage and failure modes, localized buckling in the core, facesheet spring-back, and post-impact loading.

2.8.2.2. Simplified Honeycomb Core Representation

Simplified representations of the core are used to reduce the runtime by using a smaller number of elements than that of a realistic cellular core. The geometry is not accurate as the cells are not represented, but they are replaced with a single homogeneous solid block [28, 36, 56-58] or a grid of equivalent non-linear springs [59, 60] with equivalent material properties to represent the overall behaviour of the core.

For a single homogenous solid block, the material model must be orthotropic to account for the orthotropic behaviour of the core because of the ribbon direction and the orientation of the cells (in-plane or out-of-plane). The material model must also be able to represent the damage initiation and progression that occurs during the impact. The orthotropic properties are defined by determining an equivalent Young's modulus, E, and Poisson's ratio in each of the three orthogonal directions [28, 36, 56-58]. Researchers have demonstrated that representing the honeycomb structure as a homogeneous orthotropic solid with a progressive failure model provides results that are similar to experimental data [56, 57]. This was evaluated by comparing the force versus displacement graphs for the impactor as well as damage to the facesheet [56]. Aktay et al. [28]

showed the stages of core crush in Nomex and Aluminum honeycomb cores, including buckling initiation, progressive folding, and finally densification using experimental examples. Two numerical models were applied, one representing the detailed core structure and the other with homogenized material properties. The homogenized model used a semi-adaptive coupling (SAC) technique to eliminate failed elements and replace them with discrete particle elements defined by a plastic compression law. The SAC model agreed with experimental results and was more computationally efficient than the micromechanical model.

Another method for simplifying the core is to replace it with non-linear spring elements. Ratcliffe and Jackson [59] designed a FE model which includes a facesheet represented by shell elements and a core made of non-linear spring elements to provide elastic support. The impact damage was represented by a geometric dent in the facesheet, and a region of damaged core elements based on the idealized core crush response of the damaged honeycomb core. They found that the included "damaged" spring element core region resulted in a good agreement with the experimental results, but this comparison was limited due to the small amount of available experimental data. Castanié et al. [60] also studied the validity of using a grid of non-linear springs for modelling the low-velocity impact response of metal-skinned panels with a Nomex core. The springs were discovered to be incapable of modelling transverse shear in the core under bending. Because the honeycomb is composed of discrete cells, the simplified representation of the honeycomb core may have difficulty simulating the same damage progression.

2.9. Summary

Most of the studies in the literature have been focused on sandwich panels made of laminate facesheets and Nomex cores. The introduction of advanced FEA software packages capable of simulating the impact damage of sandwich panels occurred during the period when the aerospace industry was progressively shifting toward lighter composite panels instead of aluminum panels. As a result, researchers focused their efforts on studying the behaviour of these novel materials. As the damage modes in aluminum are different, it would be unreasonable to assume that results generated through testing of panels made of composite materials are applicable to aluminum panels. Metallic panels are still used widely in legacy aircraft fleets, and research into their properties is required to extend their life cycles, reduce the ongoing maintenance costs, and ensure the safe operations of ageing aircraft.

In service, aircraft panels will incur impact damage in random locations resulting in dents that could be spaced apart or could be overlapping. These dents may not be circular or have a spherical profile and will most likely be of different sizes and depths. If the dents are close enough that they interact, this results in increased dent depth and damage area, which are the main parameters affecting the residual strength in compression. The SRM specifies that dents that are within the allowable size metrics must have a minimum distance between them. This may be conservative as it does not account for the individual dent areas or depths, the panel properties such as facesheet thickness or the core density and it does not account for how the dents are positioned with respect to the loading direction. Currently, the published literature is almost solely focused on honeycomb structures with isolated impact sites using spherical impactors/indentors. Post-impact loading typically consists of in-plane compression in order to establish the residual strength. There are few studies that have investigated the effect of multiple impact sites on honeycomb panels. There have not been sufficient studies to quantify the relationship of the spacing between multiple dents on the

residual strength in honeycomb sandwich panels. This thesis aims to address this topic by using finite element simulations to quantify the effects of the interaction between multiple dents on the residual strength due to post-impact compressive loading.

3. Study 1

"Effect of Impact Location on The Variation of Residual Dent Depth in Metallic Honeycomb Sandwich Panels".

3.1. Introduction

Sandwich panels are used in aerospace applications due to their high stiffness and strength-to-weight ratios. Extensive experimental work and numerical simulations have been done to understand their impact damage response and their post-impact loading strength. For aircraft panels, the impact is frequently a result of events such as tool drops, runway debris and ground handling. These impacts are usually limited to the top facesheet, core material, and the adhesive between them. This type of damage which is produced from low-velocity impacts, is concerning as it may be difficult to detect and could reduce residual strength under in-plane compressive loading while aircraft are in service.

It has been noted that the scatter in experimental tests of honeycomb sandwich panels can be significant enough to obscure some of the trends of interest. A large portion of this scatter can be attributed to the imperfections and variations in the honeycomb panels due to the manufacturing process, such as non-uniform cell shape and size, adhesive fillets of varying sizes in different regions of the panel, inconsistent cell wall thickness, and inconsistent facesheet thickness as shown in Figure 3-1. Imperfections can be classified as global, local, or micro. Examples of global imperfections are irregular cell geometry, uneven or pre-buckled cell walls. Local imperfections on the macro level are surface roughness, wall thickness variation, and on the micro-level, they can be cracks and pores [61].

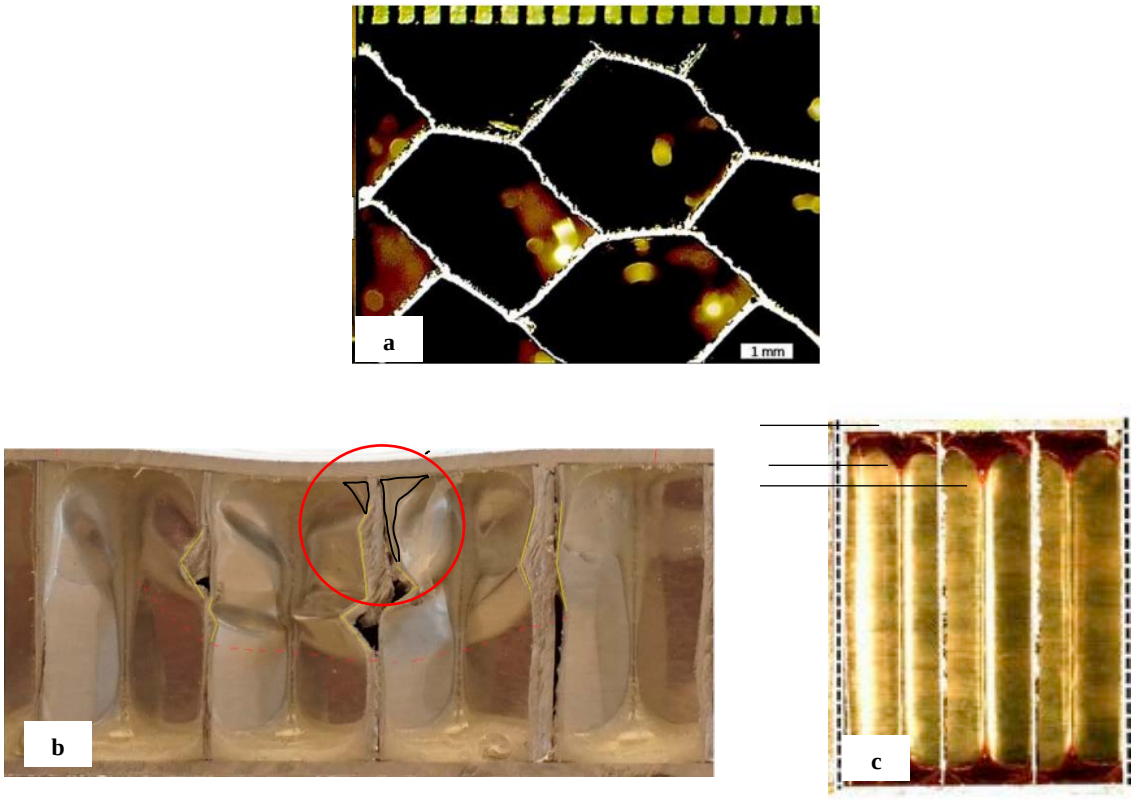

Figure 3-1: Examples of panel imperfections
a) Non-uniform cell size and shape [62], b-c) Non-uniform fillet height and thickness [2, 63].

Many researchers have used theoretical and numerical simulations to investigate the effects of different panel imperfections on honeycomb cores with irregular cell wall thicknesses, irregular cell geometries, uneven call walls, different thicknesses of cell wall junctions, and missing cell walls [64-66]. Yang and Huang et al. [66] investigated the effect of different thicknesses of cell wall junctions on the mechanical in-plane properties of honeycomb panels. The authors found the existing theoretical models for variable thickness cell edges predicted up to 33.75% higher elastic buckling strength than finite element analysis results for regular hexagonal honeycombs. Li et al. [64] investigated the effect of imperfections such as irregular cell wall thicknesses and irregular cell geometries on the mechanical in-plane properties of honeycomb panels. The authors found scatter up to 27% of their mean in the values of the nominal plateau stress for specimens with the same number of cells. Increasing the number of cells in the panel decreased the scatter variation, and they found that the minimum scatter could be 2% of their mean, and this variation was due to panel imperfections. Also, they found that for a given high impact velocity, the irregularity in cell shape increases the speed of the stress wave propagation by about 50%. In contrast, the non-uniformity of the cell wall thickness slows the stress wave propagation by approximately 20%. They showed a variation up to 10% in the presence of non-uniformity of the cell wall thickness on the plateau stress as the folds initiated at the thinnest cell can be easily spread to other adjacent thin cell walls.

Furthermore, determining trends using experimental tests could be difficult, even when identical panels are used due to scatter in the results from manufacturing imperfections or impact location within the cells. Gilioli et al. [41] found a significant amount of variation in measuring the peak load for CAI for undented aluminum-skinned honeycomb core panels. The variation could be up to 104% of the mean when the facesheet thickness was 1mm, while the variation decreased to 52% when the facesheet thickness was 1.5mm. This introduces the probability of minor manufacturer defects, material imperfections, or other defects that are not easily visible playing a significant part in the residual strength of aircraft structure. Also, Wowk et al. [2] found that identical repeats of the same impact test resulted in a variation of up to 0.179 mm in residual dent depths in the range of 0.846mm to 1.025mm and a significant variation of up to 0.205mm in residual dent depths range of 0.153mm and 0.358mm. All these variations in the same panel's configurations could be due to panel imperfections, slightly different impact energy, or impact location within the cells. Tomblin et al. [17, 67] showed up to a 57% scatter in their experimental results for CAI strength and a 30% scatter in the maximum residual indentation depth. Also, the authors mentioned that the thinner factsheets have higher scatter in residual dent depth compared to thicker facesheets.

In addition to panel imperfections, differences in the impact location with respect to the cells could also cause variations in experimental results. Lee et al. [51] found that in aluminum honeycomb sandwich panels at low impact energy (10J), the impact behaviours are similar for four different impact locations with minimal variation of 4% in the energy absorbed. However, for high-impact energy (32J), the absorbed energy is within 10% for different impact locations.

In real-life applications on an aircraft, impacts occur on random locations with respect to the cells, and the variation due to impact location can not be controlled. However, it can be minimized when performing physical tests so trends can be seen clearly. Also, it is necessary to know the worst-case scenario in terms of damage and residual panel strength when performing simulations. In this study, the focus will be on the variation due to impact location relative to the honeycomb cells, as this can be controlled in numerical models. All other sources of variation will be removed, leaving only the variation due to impact location. The main objective is to quantify the expected variation in dent depth based on the impact location and identify the critical location. Dynamic finite element simulations considering panels with aluminum facesheets, and aluminum cores were used to predict the dent depth resulting from low-velocity impacts at four different locations relative to the honeycomb cells. This was performed for different panel configurations with different cell sizes, facesheet thickness and cell wall thicknesses. Different impact configurations such as impactor size and impactor velocity were also considered. The maximum scatter that is expected for a wide variety of impact and panel configurations was determined, and configurations that are expected to have more scatter were identified. This could help in designing experiments so that the experimental scatter can be minimized.

3.2. Methodology

3.2.1. Introduction

In order to determine the effect of the impact location on the residual dent depth following low-velocity impacts, numerical simulations were used as they ensure ideal and perfect geometry for all panel features such as cell size, hexagonal shape, adhesive fillet size and wall thickness. Finite element modelling allowed the variations due to panel features to be removed, and the effect of impact location was isolated to be the only source of variation. These studies were conducted to predict the expected variation in dent depth that could be present in simulations, experimental testing, or the field due to impacts occurring at random locations on the panel surface. The study considers sandwich panels with aluminum facesheet and aluminum honeycomb core at energies that produce residual dent depths between 0.1mm and 1.25mm, which were categorized as BVID.

Explicit dynamic simulations were performed using the finite element analysis software ANSYS to predict the residual dent depth as a result of an impact by a spherical object at different positions on the honeycomb panel. The model simulation represented a 1.8ms impact run time where the core and facesheet had sprung-back and formed the residual dent. The simulations included a full geometric representation of the honeycomb core, the facesheet, the impactor and the adhesive. The solution included geometric and material non-linearity through local buckling of the core and plasticity in the facesheet and core. Contact was defined between all bodies to capture the interaction between the indentor and the facesheet, as well as the facesheet and cell walls and between the cell walls as they fold during crushing.

The analysis was performed on four different impact locations: the center of a double-wall in the ribbon direction (P1), the center of a single-wall (P2), the center of the cell (P3), and at the intersection between cells (P4), as shown in Figure 3-2. Refer to Section 2.1.1 for the definition of ribbon direction and double walls. The impactor radius, cell sizes, impactor velocity, facesheet thickness, and cell wall thickness were also varied for a total of 84 simulations.

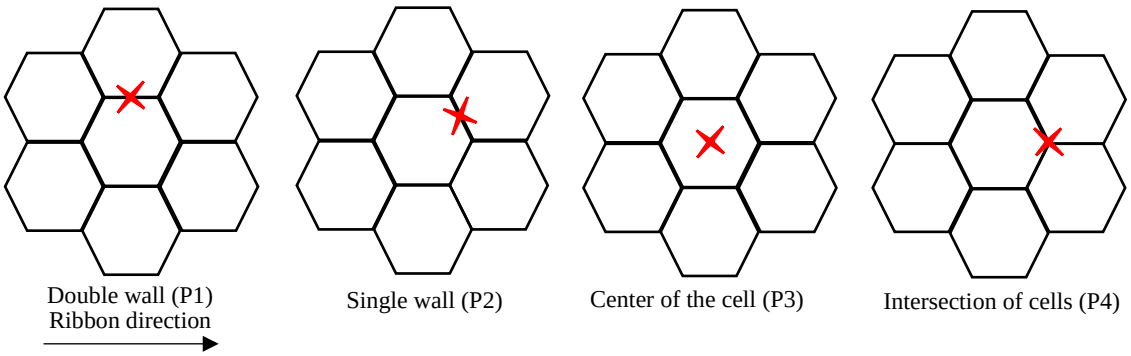

Figure 3-2: Four different impact locations on the honeycomb cell.

3.2.2. Baseline Model

Section 3.2.2 describes the baseline model that was created to run the initial study on the four impact locations. This baseline model was then altered to perform subsequent studies varying the impactor radius, core cell size, facesheet thickness and core cell wall thickness as described in Section 3.2.3.

All models consisted of a 69.85 mm x 69.85 mm (2.75" x 2.75") panel with a spherical surface impacting the top of the panel at four different locations relative to the cells. Figure 3-3 shows the four main components of the model: impactor, honeycomb core, facesheet and adhesive. Note that the facesheet located on the top of the panel is represented by a surface which is too thin to be visible in the cross-sectional view. This panel size was chosen to be large enough to capture the damage caused during the impact event and avoid edge effects. The initial impact velocity was chosen to produce dent depths between 0.1mm and 1.25mm, which would fall within the allowable dent limits of a typical aircraft panel [2].

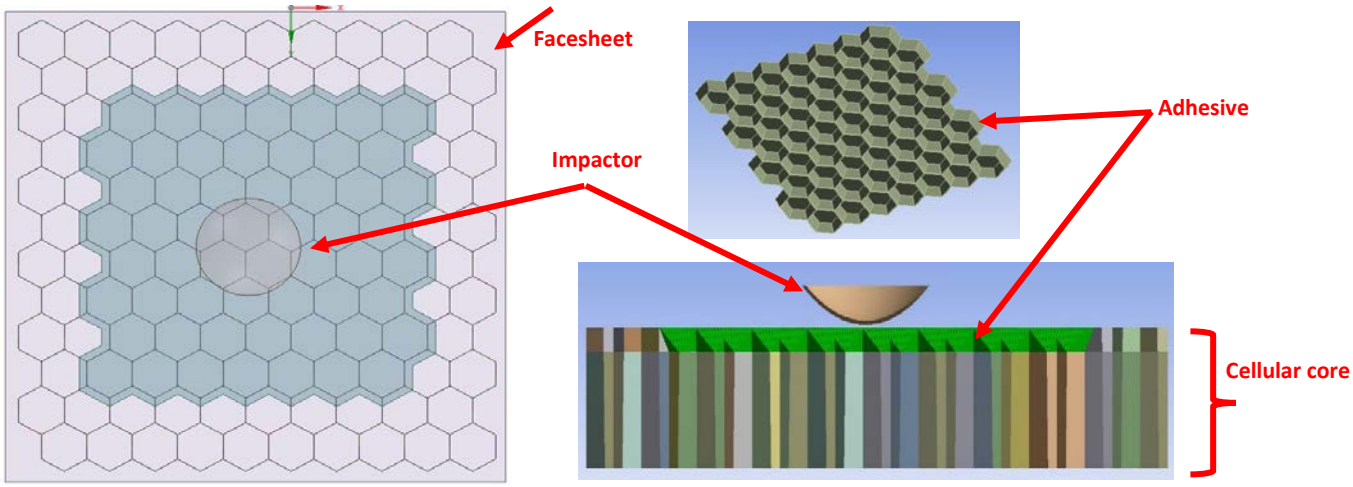

Figure 3-3: The four main components of the FE model.

3.2.2.1. Geometry

The geometry of the panel coupon consisted of one 0.508 mm (0.02") thick aluminum facesheet and a 12.7mm (0.5") thick aluminum honeycomb core; these are the typical panel configurations used previously within the research group for experimental tests [2]. The core has a hexagonal cell of size 6.35mm (0.25") measured across flats with a wall thickness of 0.0508mm (0.002") and a doubled thickness of 0.1016mm (0.004") in the ribbon direction. The adhesive layer encased the top 2.17mm of the core. The surface of the spherical indentor was modelled as a spherical shell with a radius of 9.3mm (0.37") and a shell thickness of 0.5mm (0.0197"). These dimensions are illustrated in Figure 3-4.

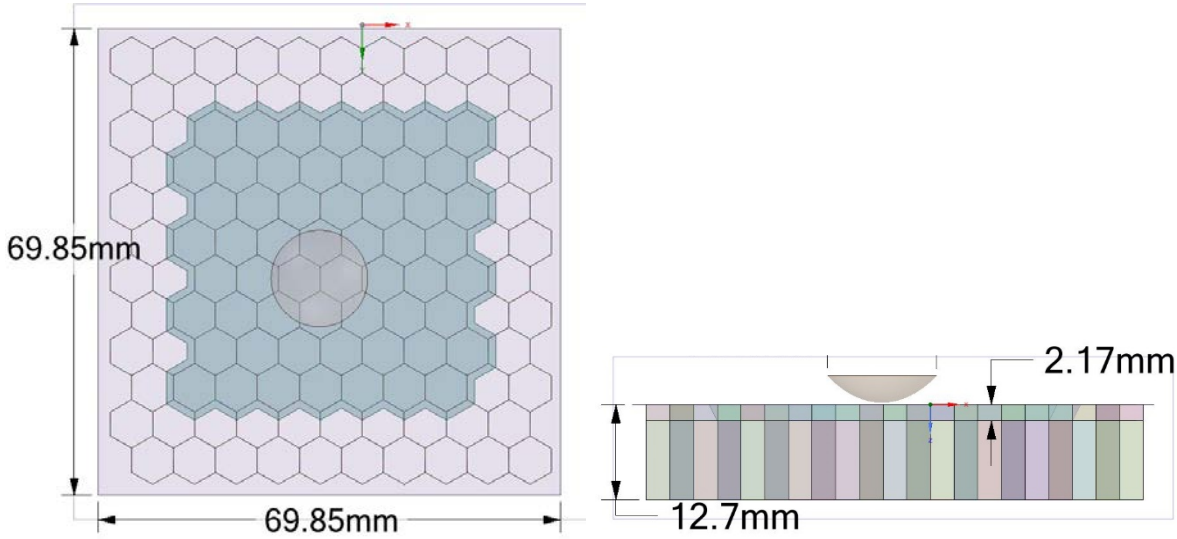

Figure 3-4: Model dimensions (mm).

The solid adhesive was modelled with a fillet height "R" of 2.17mm, a thickness of 0.1R and a width of 0.5R, as shown in Figure 3-5. All adhesive dimensions were idealized from measurements of commercially manufactured panels. The adhesive is essential to predict the correct residual dent depth as it prevents the top of the cells from crushing and provides stiffness to the facesheet. The adhesive was attached to the facesheet by bonded contact. However, due to the inability to attach the adhesive layer to the top of the cell walls, the solid adhesive representation was only used to contribute to the energy absorption of the panel. In order to prevent the top of the cell walls from crushing and buckling, the top of the cell walls was thickened and assigned calibrated material properties to obtain an equivalent stiffness. the process used to determine the equivalent stiffness is detailed in reference [2].

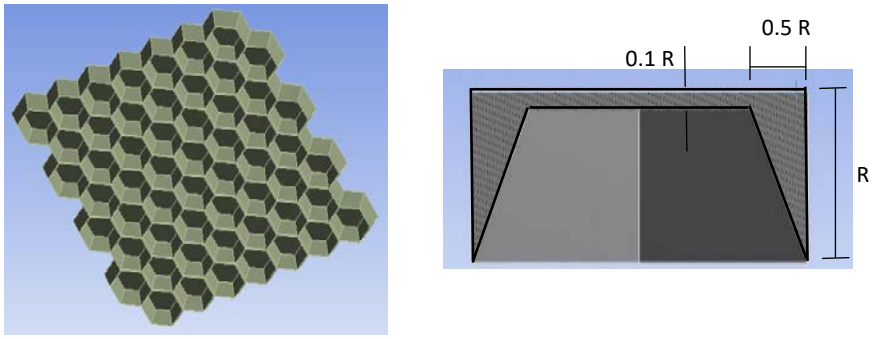

Figure 3-5: Solid adhesive dimensions.

3.2.2.2. Material Models

The facesheet was made of 2024-T3 aluminum and the honeycomb core of 5052- H34 aluminum. The spherical impactor was assumed to be made of steel, and the density was adjusted, so the impactor had a mass of 0.29kg. The impactor was modelled using a linear elastic material model, as the impactor was not supposed to yield given the relative stiffness of the two components in contact. Bilinear strain-hardening models were used for both the facesheet and core as the bilinear material model sufficiently captures the impact response while reducing the solver run times [5].

The top 2.17mm of the core geometry was prescribed linear elastic material properties to represent the constraint that the adhesive provides as this region was not expected to yield. This included one set of material properties for the regular cell walls (denoted by "Single-wall adhesive") and another for the doubled cell walls in the ribbon direction (denoted by "Double-wall adhesive"). The wall thickness and the material properties at the top of the cell walls were adjusted to reach a stiffness equivalent to the cell wall and the adhesive combined [2]. Table 3-1 shows the material properties of the model for the impactor, facesheet, core and adhesive.

Table 3-1: Material properties for the baseline model [2].

	Impactor, structural steel	Facesheet, 2024-T3 [68]	Core, 5052-H34 [63]	Adhesive, epoxy material [69]	Single-wall adhesive	Double-wall adhesive
Density [kg/mm^3]	0.00282079	2.78E-06	2.68E-06	1E-06	1E-06	1E-06
Young's Modulus [MPa]	2E+05	73100	71700	3700	6678	9402
Poisson's ratio [-]	0.3	0.33	0.33	0.3	0.3	0.3
Yield Strength [MPa]	-	345	345	-	-	-
Tangent Modulus [MPa]	-	811	305	-	-	-

3.2.2.3. Element Meshing

Lower-order elements were used in this simulation because the Explicit Dynamics solver in ANSYS does not support higher-order elements. Shell elements with 6 degrees of freedom were used for the facesheet and the honeycomb core cell walls, which allowed for the elements in those structures to carry axial, shear, torsional and bending loads. Solid hexahedral and tetrahedral elements were used to capture the adhesive fillet geometry. Figure 3-6 shows the free mesh used for the facesheet and adhesive and the mapped mesh used for the cell walls. Element sizes of 0.48 mm, 0.6 mm, 0.6 mm, and 1.5 mm were used for the core, adhesive, facesheet and indentor, respectively. The model had 123588 nodes and 187546 elements. The element size in the core was determined based on the result of convergence studies presented in Reference [2].

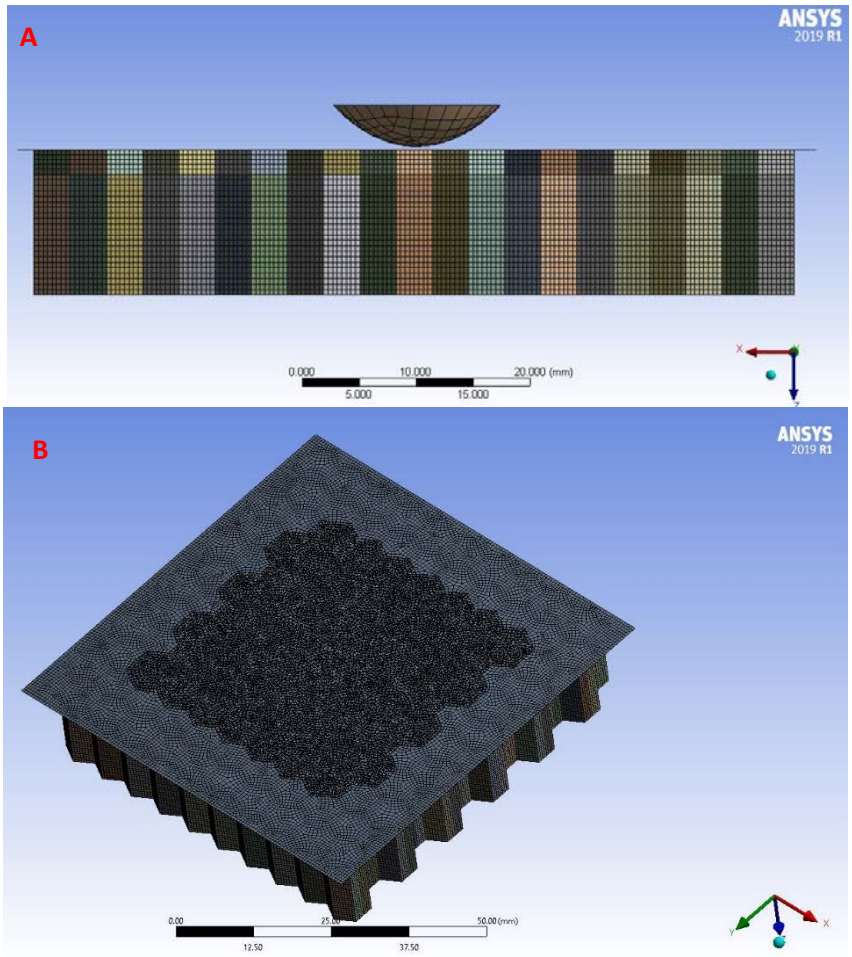

Figure 3-6: Final shape mesh a) Mesh in cell walls and b) Mesh in facesheet and adhesive.

3.2.2.4. Loading and Boundary Conditions

The impactor hit the facesheet with a prescribed initial velocity of 1354.3 mm/s in the facesheet normal direction and was constrained from moving in either lateral direction. This velocity was chosen to produce a residual dent within BVID limits. The effect of gravity was neglected, as its overall effect would be minimal given the short duration of the impact simulation.

The honeycomb core bottom was fixed in all degrees of freedom to prevent any rotation or displacement. This would be equivalent to a coupon-level test where the panel is clamped to a rigid platform. Although in reality, the bottom of an aircraft panel wouldn't be supported, however, with low impact velocities that produce BVID, the damage state is expected to be the same. The loading and boundary conditions are shown in Figure 3-7.

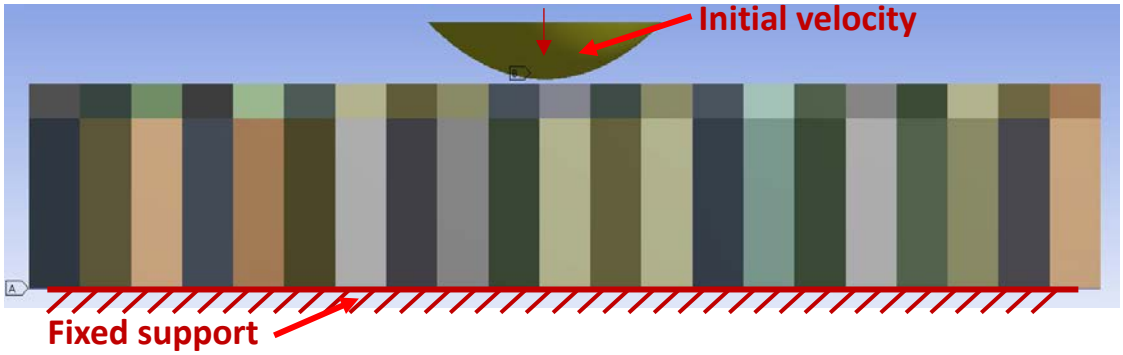

Figure 3-7: Loading and boundary conditions for the baseline model.

Automatic frictionless contact was defined between all the surfaces to capture the interactions between the impactor and facesheet, facesheet and cell walls, as well as self-contact between the folds in the cell walls during crushing. Since all the contact was expected to be between surfaces normal to each other rather than tangential, the effects of friction were expected to be negligible, and a frictionless contact model is considered for ease of convergence.

3.2.3. Variations to Baseline Simulation

A total of 84 simulations were conducted for five different studies at all impact locations, using various properties for the impact and the panel. The purpose was to determine the dent depth variation due to impact location changes for different panels and impact configurations. For each series, parameters of the baseline model were altered independently as outlined in Table 3-2, and any interaction between them is not considered. The range of values was chosen to match the typical configurations of commercially available panels. The five studies considered impactor radius, cell size, impactor velocity, facesheet thickness and cell wall thickness. For the impactor radius study, the impactor density was adjusted to maintain a constant mass and resulting impact energy level. The adhesive fillet size was kept the same as the baseline model for all simulations.

Table 3-2: Parameters varied for each series of simulations, with bold entries indicating the baseline model parameters.

	Impactor radius mm	Cell size mm (inch)	Impactor velocity mm/s	Facesheet thickness mm (inch)	Cell wall thickness mm (inch)	Study on position
Impactor radius	5.3 **9.3** 16 33.4	6.35 (1/4)	1354.3	0.508 (0.02)	0.0508 (0.002)	All positions 1- Double cell wall 2- Single-cell wall 3- The center of the cell 4- Intersection between cells
Cell size	9.3	3.175 (1/8) 4.725 (3/16) **6.35 (1/4)** 9.525 (3/8)	1354.3	0.508 (0.02)	0.0508 (0.002)	
Impactor velocity	9.3	6.35 (1/4)	677.15 **1354.3** 2031.45 2708.6	0.508 (0.02)	0.0508 (0.002)	
Facesheet thickness	9.3	6.35 (1/4)	1354.3	**0.508 (0.02)** 0.8128 (0.032) 1.016 **(**0.04)	0.0508 (0.002)	
Cell wall thickness	9.3	6.35 (1/4)	1354.3	0.508 (0.02)	0.0254 (0.001) **0.0508 (0.002)** 0.0762 (0.003) 0.1016 (0.004)	

3.3. Results

The results presented in this section show the variation in residual dent depth for different impact locations, panels, and impact configurations.

The overall mechanism for how damage is created from these low-velocity impacts can be seen in Figure 3-8. Initial contact between the impactor and facesheet causes bending of the facesheet. Then the section of the core underneath the impact area starts to deform (elastic deformation). With a further downward displacement of the impactor, the facesheet plastically deforms, and the honeycomb core crushes via localized buckling of the walls. Finally, after reaching maximum deflection, the impactor rebounds and the facesheet and core partially spring-back, resulting in the final residual dent.

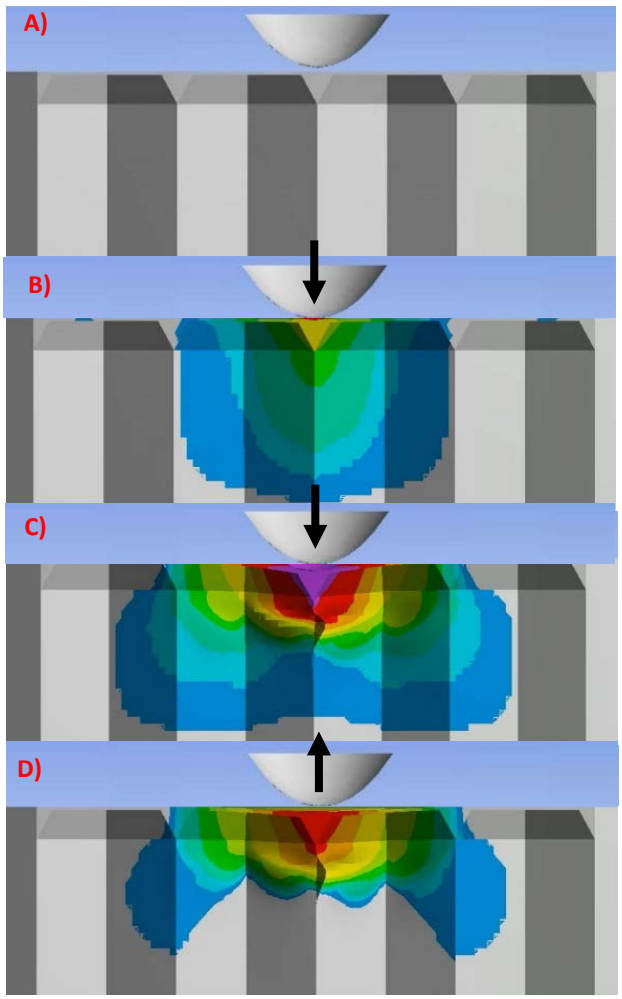

Figure 3-8: Impact damage mechanism. a) Undented panel. b) Initial contact between impactor and facesheet. c) Maximum point of indentation (facesheet plastically deforms and core crushes via localized bucking). d) Facesheet spring-back (final dent shape). Contour colour shows the vertical displacement, purple shows the maximum and grey shows deformation less than 0.01mm.

3.3.1. Baseline Simulation Results at 4 Impact Locations

This section presents the expected variation in dent depth with impact location for the baseline panel configuration. Figure 3-9 and Table 3-3 show that the four different impact positions result in different residual dent depths for the same panel and same impact configuration. For example, the impact at the center of the cell, P3 results in the largest residual depth of 0.324 mm, while the other three locations have residual dent depths between 0.157 and 0.164 mm. The variation in residual dent depth could be up to 0.167mm over this panel, depending on where the impact occurs.

Table 3-3: Residual dent depth for a baseline model.

Residual dent depth (mm)				
Model P1	Model P2	Model P3	Model P4	Max Variation of damage
0.163	0.164	0.324	0.157	0.167

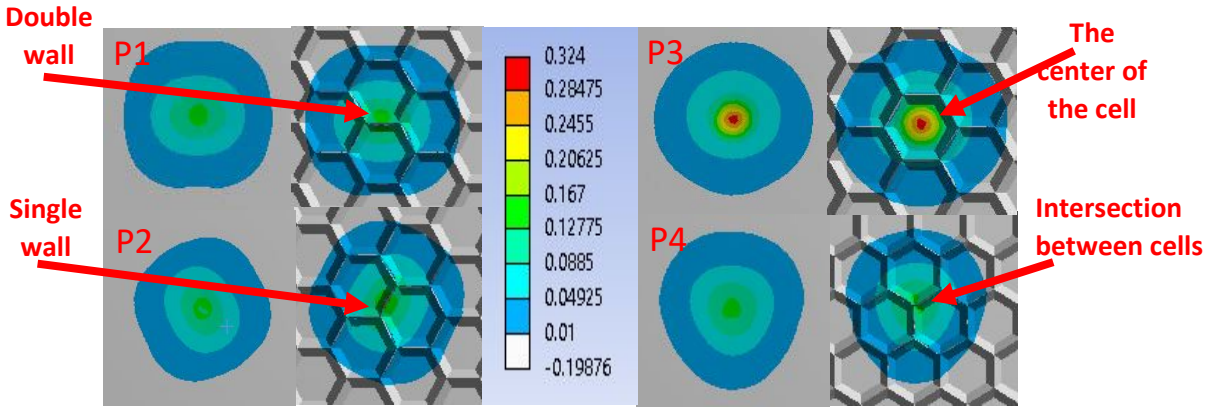

Figure 3-9: Residual dent depth for baseline model in mm and the contour values of residual dent depth, The red shows the deepest dent, and the grey shows deformation less than 0.01mm.

Figure 3-10 shows the mechanism of how dents are formed at different locations within the panel and how this contributes to differences in dent depth. Figure 26 a) shows that the center of the cell position, P3 forms dents primarily due to facesheet bending, and the residual dent depth will be more affected by the facesheet and any characteristics that localize the dent. Figure 26 b) shows that the cell wall positions P1, P2 and P4 form dents primarily due to cell wall buckling, and they all show the same results as each other in terms of residual dent depth and variation. There is no difference in the mechanism of dent formation between P1, P2 and P4 as proven by the minimal difference between the residual dent depths from Table 3-3.

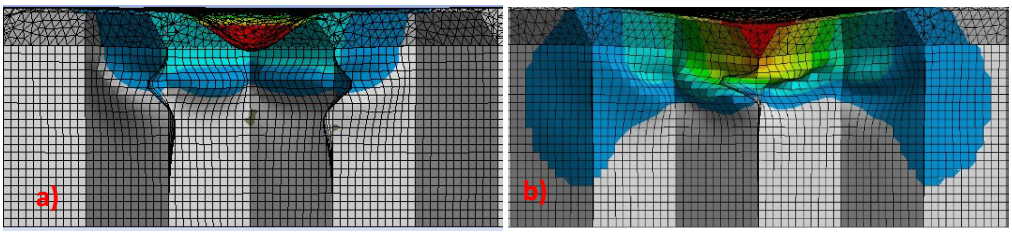

Figure 3-10: Deformation of the core and facesheet for different impact locations at a) The center of the cell (P3), b) The top of the cell wall (P1, P2 and P4).

3.3.2. Effect of Impact and Panel Parameters on Residual Dent Depth Variation

This section presents the effect of impactor radius, cell size, facesheet thickness, cell wall thickness and impact velocity on the variation in residual dent depth with impact location.

3.3.2.1. Impactor Size Study

Impactor radii of 5.3, 9.3, 16 and 33.4 mm were considered for all positions for this series of sixteen simulations. To ensure that the impactor size was the only factor being changed, the impactor density was adjusted. Hence, the mass of the impactor was the same as the baseline model, and the kinetic energy was kept constant.

Figure 3-11 shows the effect of impactor radius on impact damage for the same impact energy. The larger impactor radius distributes the impact energy over a larger panel area resulting in a smaller residual dent depth. Impactor size has a considerable effect on dent depth for P3 because when impacted at the center of the cell, a small impactor concentrates the impact energy into a smaller section of the facesheet between the cells causing more localized deformation.

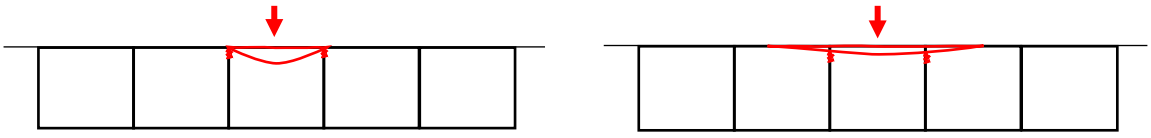

- Smaller impactor radius produced larger dent depths.

- Larger impactor radius produced small dent depths.

Figure 3-11: The difference between a small impactor size and a larger impactor size on impact damage.

Figure 3-12 a) shows how the residual dent depth changes with impactor size for the four impact locations. For all impact locations, the maximum dent depth decreases with increasing impactor size. Increasing the impactor radius while maintaining constant impact energy resulted in larger, shallower dents. At position P3, the residual dent depth decreases by 0.244mm as the impactor radius increases from 5.3mm to 33.4mm, while at positions P1, P2 and P4, the residual dent depth decreases by only 0.018mm. This shows that impacts occurring directly on top of cell walls are less sensitive to changes in the impactor size compared to impacts at the center of the cells.

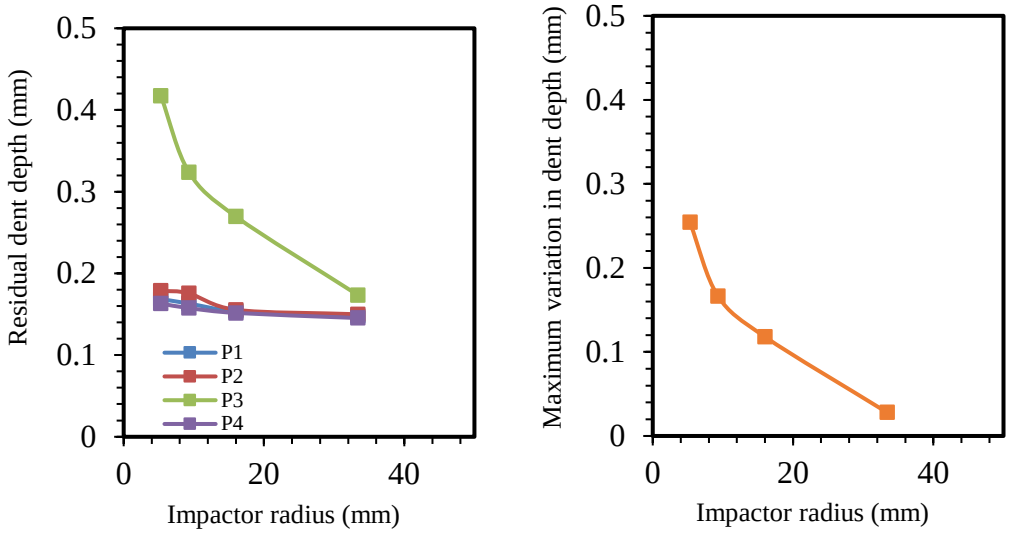

Figure 3-12: a) Residual dent depth and b) Maximum dent depth variation for different impactor radius and impact locations.

Figure 3-12 b) shows the maximum variation in dent depth (maximum dent depth from all four-impact locations – minimum dent depth from all four impact locations) for each impactor radius. The variation in dent depth decreases from 0.254mm to 0.028mm as the impactor radius increased from 5.3mm to 33.4mm.

3.3.2.2. Cell Size Study

Honeycomb cell sizes of 3.175mm (1/8"), 4.725mm (3/16"), 6.35mm (1/4") and 9.525mm (3/8") were considered for all positions for this series of sixteen simulations. To ensure that the cell size was the only factor being changed, all other base model parameters were kept constant.

Figure 3-13 a) shows how the residual dent depth changes with cell size for the four impact locations. For all impact locations, the maximum dent depth increases with increasing cell size. A larger cell size allows more of the deformation to be concentrated in the facesheet for P3 but does not change the mechanism for P1, P2 and P4 as much. P1, P2 and P4 are only affected because a larger cell size means more room for buckling (lowers the buckling load) and leads to more crumpling. At position P3, the residual dent depth increases by 0.296mm as the cell size increases from 3.175mm to 9.525mm, while at positions P1, P2 and P4, the residual dent depth increases by only 0.109mm. This shows that impacts occurring directly on top of cell walls are less sensitive to changes in the cell size than impacts at the center of the cells.

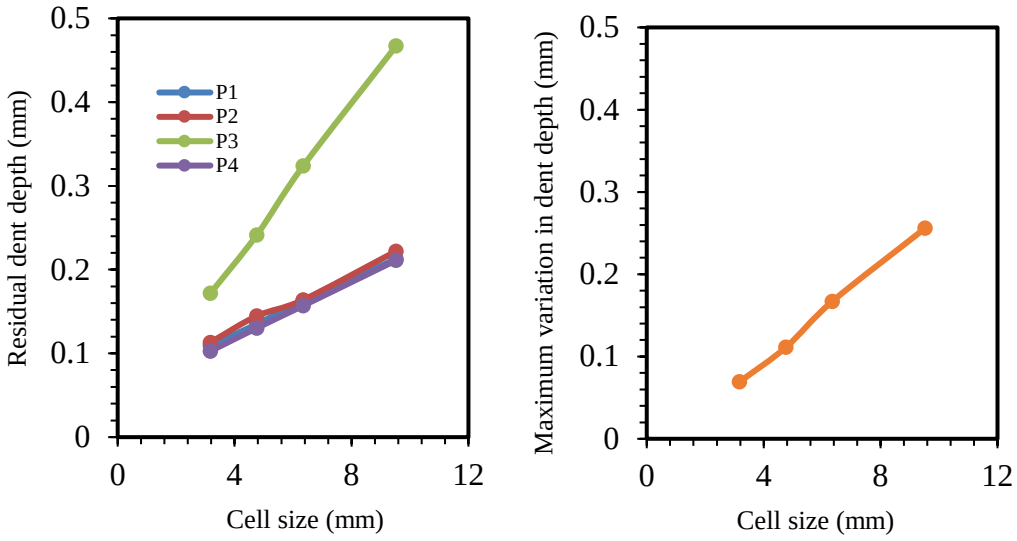

Figure 3-13: a) Residual dent depth and b) Maximum dent depth variation for different cell sizes and impact locations.

Figure 3-13 b) shows the maximum variation in dent depth for each cell size. The variation in dent depth increases from 0.069 to 0.256mm as the cell size increased from 3.175 to 9.525mm.

3.3.2.3. Facesheet Thickness Study

Facesheet thicknesses of 0.508mm (0.02"), 0.8128mm (0.032") and 1.016mm (0.04") were considered for all positions for this series of twelve simulations. To ensure that the facesheet thickness was the only factor being changed, all other base model parameters were kept constant.

Figure 3-14 a) shows how the residual dent depth changes with facesheet thickness for the four impact locations. The maximum dent depth decreases with increasing facesheet thickness for all impact locations due to the increased energy absorbed by the facesheet. Facesheet thickness has a larger effect on dent depth at location P3 because when impacted at the center of the cell, the dent depth is more sensitive to the deformation of the facesheet. At position P3, the residual dent depth decreases by 0.106mm as the facesheet increases from 0.508mm to 1.016mm, while at positions P1, P2 and P4, the residual dent depth decreases by only 0.033mm. This shows that impacts occurring directly on top of cell walls are less sensitive to changes in the facesheet thickness than impacts at the center of the cells.

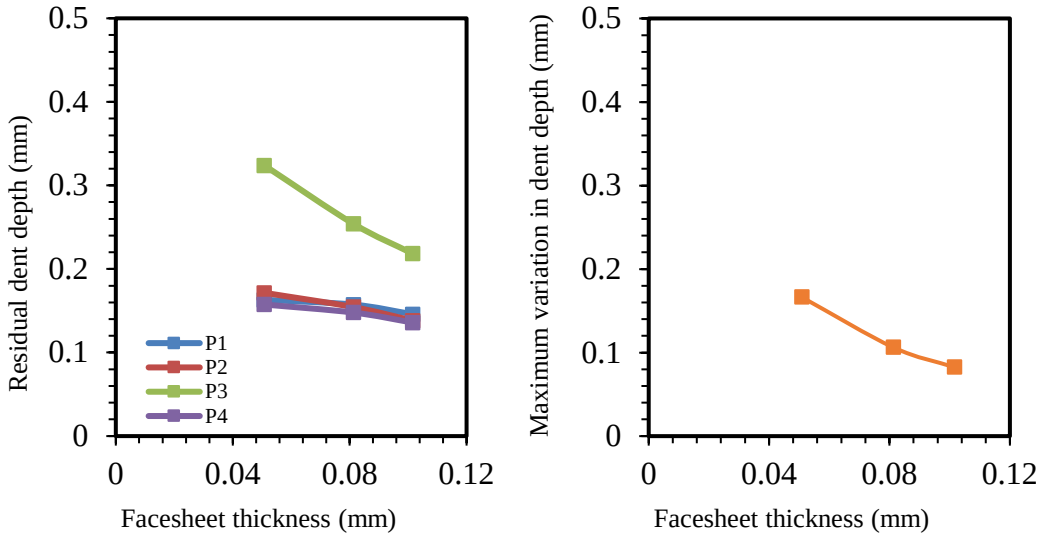

Figure 3-14: a) Residual dent depth and b) Maximum dent depth variation for different facesheet thickness and impact locations.

Figure 3-14 b) shows the maximum variation in dent depth for each facesheet thickness. The variation in dent depth decreases from 0.167 to 0.082mm as the facesheet thickness increased from 0.508 to 1.016mm.

3.3.2.4. Cell Wall Thickness Study

Cell wall thicknesses of 0.0254mm (0.001"), 0.0508mm (0.002"), 0.0762mm (0.003") and 0.1016mm (0.004") were considered for all impact positions for this series of sixteen simulations. To ensure that the cell wall thickness was the only factor being changed, all other base model parameters were kept constant.

Figure 3-15 a) shows how the residual dent depth changes with cell wall thickness for the four impact locations. For all impact locations, the maximum dent depth decreases with increasing cell wall thickness as stiffer core results in a smaller amount of core crushing and a smaller residual dent depth. At positions P1, P2 and P4, the residual dent depth decreases by 0.056mm as the cell wall thickness increases from 0.0254mm to 0.1016mm, while at position P3, the residual dent depth decreases by 0.038mm. This shows that the cell wall thickness does not have an effect on the variation in dent depth due to impact location, as the variation is the same for all positions.

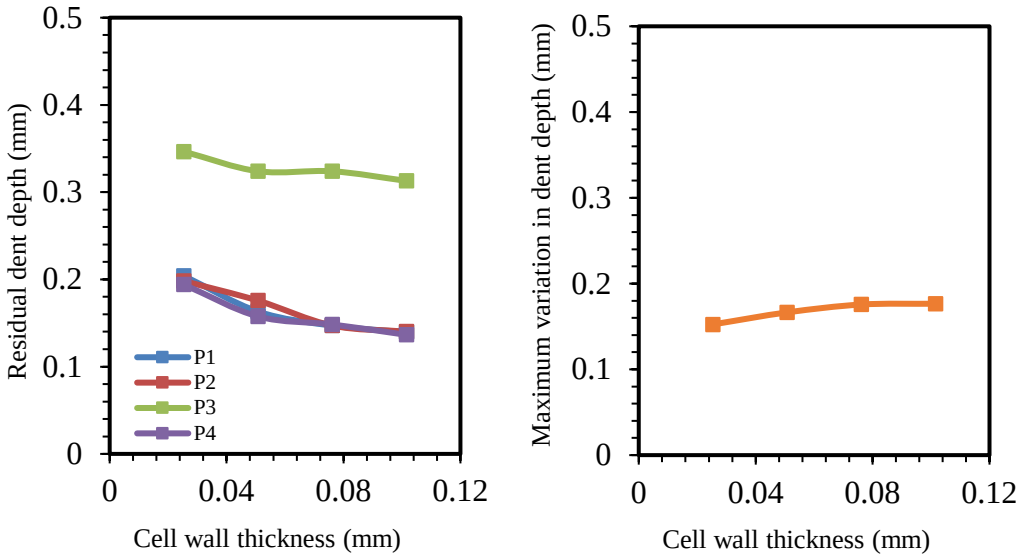

Figure 3-15: a) Residual dent depth and b) Maximum dent depth variation for different cell wall thickness and impact locations.

Figure 3-15 b) shows the maximum variation in dent depth for each cell wall thickness. The variation in dent depth increases from 0.152 to 0.176mm as the cell wall thickness increased from 0.0254 to 0.1016mm. This shows that the variation is minimal and does not change with cell wall thickness.

3.3.2.5. Impactor Velocity Study

Impact velocities of 677.15mm/s, 1354.3mm/s, 2031.45mm/s and 2708.6mm/s were considered for all positions for this series of sixteen simulations. To ensure that the impactor velocity and corresponding impact energy was the only factor being changed, all other base model parameters were kept constant.

Figure 3-16 a) shows how the residual dent depth changes with impactor velocity for the four impact locations. The maximum dent depth increases with increasing impact velocity for all impact locations, as increasing impact velocity increases the impact energy, which causes more localized buckling in the facesheet and crushing in the core hence more damage. At position P3, the residual dent depth increases by 0.629mm as the impactor velocity increases from 677.15mm/s to 2031.45mm/s, while at positions P1, P2 and P4, the residual dent depth increases by only 0.419mm as the cell walls provide more stiffness and support for the facesheet. This shows that impacts occurring directly on top of cell walls and the center of the cell are both sensitive to changes in the impact velocity.

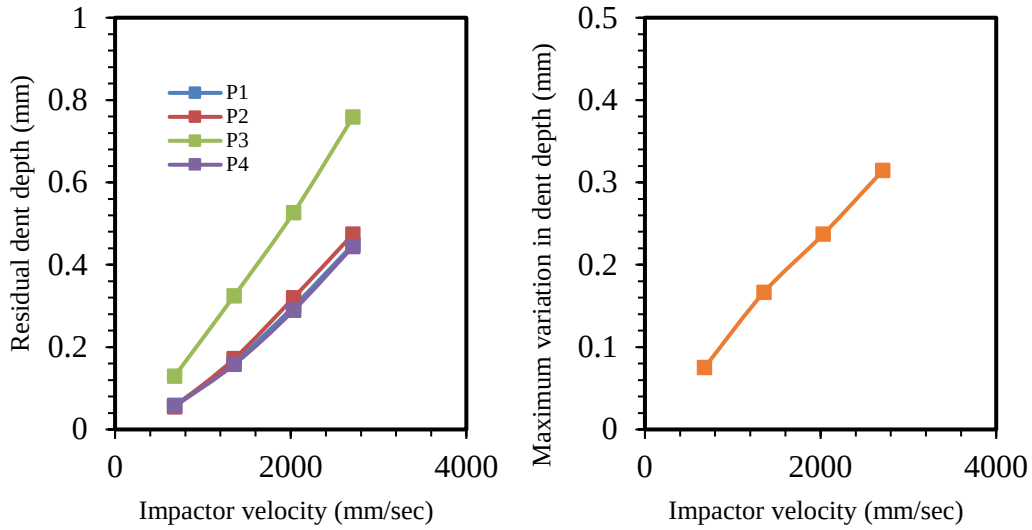

Figure 3-16: a) Residual dent depth and b) Maximum dent depth variation for different impactor velocity and impact locations.

Figure 3-16 b) shows the maximum variation in dent depth for each impactor velocity. The variation in dent depth increases from 0.075 to 0.314mm as the impactor velocity increased from 677.15 to 2708.6mm/s.

3.4. Discussion

This section discusses the interpretation of the variation in dent depth with impact location with the aim of identifying the most critical panel and impact parameters. This section will also show the maximum and minimum variation (upper and lower bound) based on impact location that could be present in physical tests depending on which impact and panel parameters are used.

Impact location has a larger effect on dent depth when facesheet thickness, impactor radius, impactor velocity and cell size are varied; a lesser effect of the cell wall thickness was observed. For example, Figure 3-17 shows that when the cell size increased from 3.175mm to 9.285mm (2.91 times), the variation in dent depth between P3 and P1,2 and 4 increased by 0.187mm (271%) compared to the smaller cell size. However, when the cell wall thickness increased from 0.0254mm to 0.1016 (4 times), the variation only increased from 0.152 to 0.177 (only 16%).

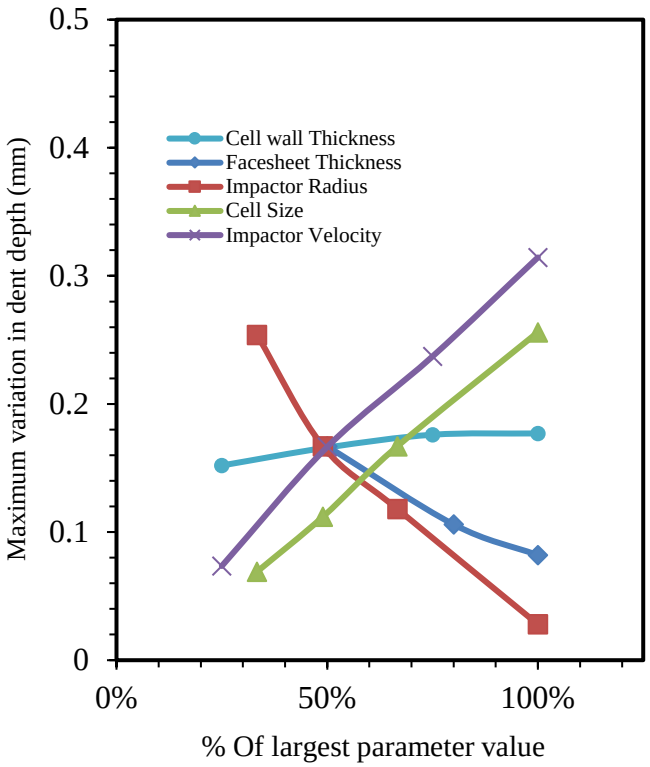

Figure 3-17: Comparison of the maximum variation in dent depth for the five parameters (cell size, facesheet thickness, impactor radius, cell wall thickness and impactor velocity).

The variations with impact location occur when one location is highly affected by the parameter, and the other locations are not. For example, P3 is located in the center of the cell. The residual dent depth is more affected by facesheet thickness and any characteristics that localize the dent, such as larger cell sizes and smaller impactor radii. P1, P2 and P4 are located on the top of the cell walls and are primarily affected by the characteristics of the cells (wall thickness, cell size). Figure 3-17 shows large variations with facesheet, impactor size, impactor velocity, and cell size

because they affect the dent depth for P3 highly compared to the other locations. Cell wall thickness shows minimal change because neither P3 nor P1, P2, P4 are affected more than the other locations.

3.4.1. Expected Maximum and Minimum Variation

Two additional studies were conducted using the values of the parameters that produce the minimum and maximum damage variations to give the range of scattering that could be expected during physical testing. These two series predict the upper and lower bound for the expected variations due to impact location for any combination of panel configurations considered in this study.

3.4.1.1. Minimum Variation

The minimum variation in the dent depth was assumed to be achieved by combining the parameters producing the minimum variation from each study: largest impactor radius, lowest impactor velocity, smallest cell size, thickest facesheet and thinnest cell wall. Table 3-4 shows the panel and impactor configurations that were used to minimize the damage variation.

Table 3-4: Panel and impactor configuration for minimizing the damage variation.

Impactor Radius (mm)	Impactor Velocity (mm/s)	Cell Size mm (inch)	Facesheet Thickness mm (inch)	Cell Wall Thickness mm (inch)
33.4	2031.45	3.175 (1/8)	1.016 (0.04)	0.0254 (0.001)

Figure 3-18 and Table 3-5 show that the four different impact positions result in minimal variation in the residual dent depths for the same panel and impact configuration. When the parameters producing the minimum variation are combined, the dent depth variation between impact locations is decreased to a negligible value of 0.0036mm (2%). Figure 3-19 shows a cross-sectional view for the different impact locations, illustrating that the largest impactor radius and the smallest cell size means that the impact damage is distributed over a larger area covering multiple cell walls and the damage is not localized within the cell even if the impact centred within the cell.

Table 3-5: Residual dent depth for a model producing minimal variation.

Residual dent depth (mm)				
Model P1	Model P2	Model P3	Model P4	Max Variation of damage
0.1837	0.1817	0.1853	0.1829	0.0036

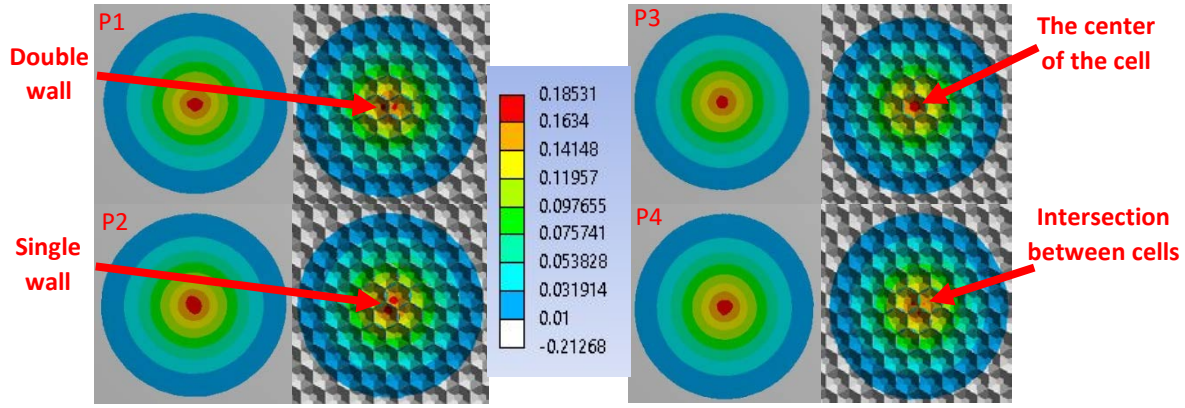

Figure 3-18: Residual dent depth for models with parameters that produce minimum variation in mm and the contour values of vertical displacement (mm), the red shows the deepest dent and grey shows deformation less than 0.01mm.

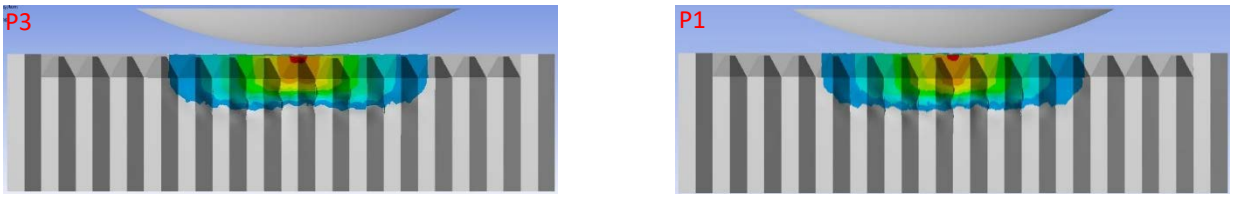

Figure 3-19: Cross-sectional view for P3 and P1 for models with parameters that produce a minimum variation. Contour values of vertical displacement (mm), the red shows the deepest dent, and grey shows deformation less than 0.01mm.

3.4.1.2. Maximum Variation

The maximum variation in the dent depth was assumed to be achieved by combining all the parameters producing the maximum variation from each study: smallest impactor radius, highest impactor velocity, largest cell size, thinnest facesheet and thickest cell wall. Table 3-6 shows the panel and impactor configuration.

Table 3-6: Panel and impactor configuration for maximizing the damage variation.

Impactor Radius (mm)	Impactor Velocity (mm/s)	Cell Size mm (inch)	Facesheet Thickness mm (inch)	Cell Wall Thickness mm (inch)
5.3	2708.6	9.525 (3/8)	0.508 (0.02)	0.1016 (0.004)

Figure 3-20 and Table 3-7 show that the four different impact positions result in different residual dent depths for the same panel and impact configuration. When parameters producing the maximum variation are combined, the dent depth variation is increased and could vary by 0.749mm (151% compared to the smallest value P4). Figure 3-21 shows a cross-sectional view for the different impact locations, illustrating the increase in damage variation because one position is highly more affected than the others, as the smallest impactor radius and the largest cell size localize the dent damage within one cell. The cell walls may only minimally deform.

Table 3-7: Residual dent depth for a model producing maximal variation.

Residual dent depth (mm)				
Model P1	Model P2	Model P3	Model P4	Max Variation of damage
0.5213	0.5131	1.2442	0.4952	0.749

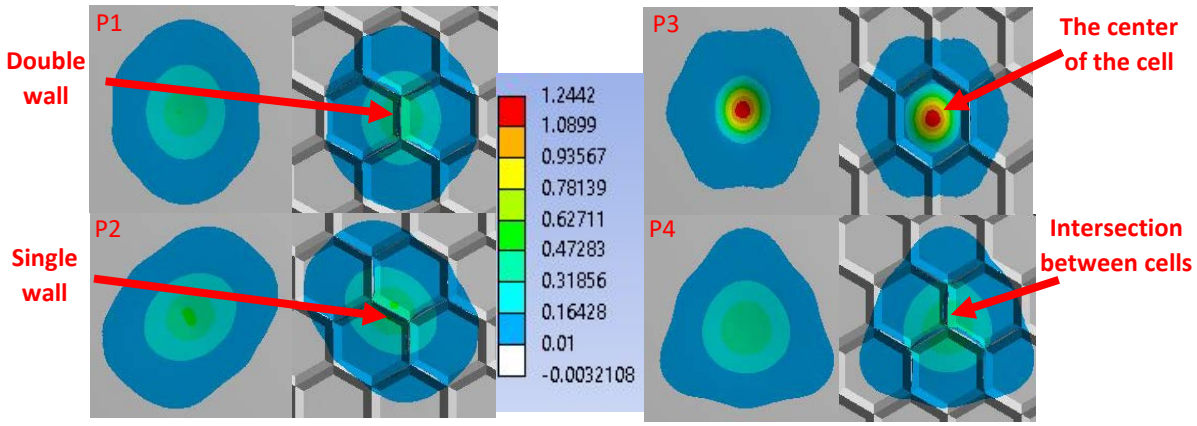

Figure 3-20: Residual dent depth for models with parameters that produce maximum variation in mm and the contour values of vertical displacement (mm), red shows the deepest dent and grey shows deformation less than 0.01mm.

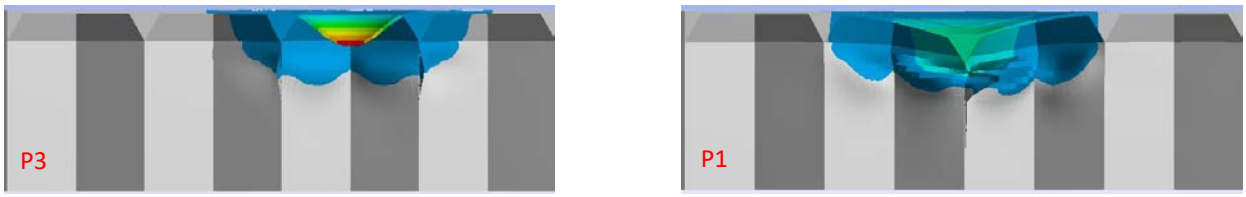

Figure 3-21: Cross-sectional view for P3 and P1 for models with parameters that produce a maximum variation. Contour values of vertical displacement (mm), the red shows the deepest dent, and grey shows deformation less than 0.01mm.

3.5. Conclusion

A systematic procedure was conducted to investigate the variation in residual dent depth that can be expected for different impactor positions on the surface of a metallic honeycomb sandwich panel during a low-velocity impact event.

Dynamic, finite element simulations were conducted for various impact scenarios using a spherical indentor at different locations relative to the cells. The analysis was performed on four different impact locations: the center of a double-wall (P1), the center of a single-wall (P2), the center of the cell (P3), and at the intersection between cells (P4). In addition, 84 additional simulations included a wide range of different panel and impact configurations.

It was determined that for low-velocity impact events that produce barely visible impact damage resulting in residual dent depths between 0.1 and 1.25 mm, the impact location is expected to cause variations between 0.0036 and 0.749 mm in the dent depth. Also, it was determined that thicker facesheets, larger impactor radii, thinner cell walls and smaller cell sizes cause a decrease in dent depth variation across a panel, and the damage could vary by as little as 2% over a panel under the conditions that are considered in the current studies.

When the impactor is large enough to span multiple cell walls, the damage mechanism at any location within the panel is dominated by cell wall buckling. This means that the dent depth will be independent of the impact location. The variation in dent depth measurements during physical or virtual testing can be reduced by either keeping the impact location the same between tests or by using a larger impactor, smaller cell size, thicker facesheet and thinner cell wall.

4. Study 2

"Effect of the Interaction between Multiple Dents on the In-Plane Compressive Residual Strength in Aluminum Honeycomb Sandwich Panels".

4.1. Introduction

Honeycomb sandwich panels are widely used in multiple applications in the aerospace and space industries due to their low density, high energy absorbing capability, higher specific strength, and stiffness. While in service, panels often contain multiple dents that are caused by such events as falling objects and bird collisions. In some cases, multiple damage sites are created which may be in close proximity to each other and may even overlap, which can reduce the structural strength and stiffness. The SRM specifies the minimum distance required between the edges of two dents, but this does not consider the size, shape, depth, or orientations of the dents. It is a general metric and has not been optimized for each panel. For example, the SRM for the Gulfstream, specifies that the minimum distance between the edges of two dents shall not be less than 101.6mm (4in) [18]. A better understanding of the interaction between dents in terms of the residual strength under post-impact loading is required in order to maintain safety standards while potentially avoiding premature repair or replacement.

Several studies have been carried out to investigate the compressive strength of honeycomb sandwich panels after low-velocity single impacts, as mentioned before in Section 2.7. However, there are very few researchers that have investigated the effect of multiple impact sites on honeycomb panels. Tariq et al. [70] studied the effects of multiple impact sites on the in-plane compressive strength in aluminum honeycomb sandwich panels with different impactor diameters. The author showed that multiple dents with 5mm diameters or less have a minimal reduction of the CAI strength of 1-3% compared to a single dent. Larger impactor diameters of 10mm and 15mm reduced the CAI strength by 7-11% and 9-21%, respectively, when the distance between the center of the impacts was 30mm. The larger impactor diameters produced larger and deeper dents which allowed more facesheet and core damage and resulted in greater strength reductions. Cromer et al. [71, 72] studied the effects of multiple non-coincident impacts on laminate sheets. When dents are separated by 50.8mm, the authors found that they do not interact and behave as individual dents. At a distance of 12.7mm apart, the dents are interacting, the damage areas overlap, and the dent depth increases, resulting in a reduction in compressive strength of 8% compared to a single impact.

In the current study, the main objective is to investigate the effect of the interaction of two dents on the residual strength of aluminum honeycomb sandwich panels subjected to in-plane compressive loading. Residual strength hereby refers to the dented panel's residual capacity to support in-service loads. The dents were created from low-velocity impacts that produced dent depths between 0.18 and 0.7mm. This size range was chosen as it lies within typical allowable damage limits, meaning that the aircraft is allowed to continue operation with a dent of this size. The objective will be achieved through simulations of panels with multiple impact sites with different sized dents at different proximity to each other. The dent depth and the dented area were also investigated to explain the relationship between the damage state formed from multiple impacts and the reduction in panel strength.

4.2. Methodology

4.2.1. Introduction

In order to predict the effects of multiple impact sites and the interaction between them on the residual in-plane compressive strength, a two-stage dynamic model was developed. The first stage consisted of modelling the impact event, followed by the second stage, which consisted of the post-impact in-plane compressive loading. This chapter provides details on the finite element models used for the first and second stages.

The purpose of this study was to determine the reduction in the in-plane residual strength for a panel loaded in compression with existing damage from multiple low-velocity impacts. This was achieved using a two-stage sequential loading simulation consisting of an impact stage followed by a compressive loading stage. During the first stage, it was assumed that two impactors hit the panel simultaneously at a specified velocity. Once the impactors had rebounded, and the facesheet had sprung back, the post-impact load was applied. During the second stage, an in-plane compressive load was applied to the panel through a given displacement. Both stages were incorporated into a single continuous run. A series of simulations were conducted to determine the influence of the proximity between damage sites on the residual strength in the honeycomb sandwich panel by varying the distance between the impactors while keeping all other aspects of the model the same.

Explicit dynamic simulations were performed using the finite element analysis software ANSYS to predict the residual strength following compressive loading of a rectangular aluminum honeycomb sandwich panel coupon containing two impact damage sites created by spherical objects. The simulations included a full geometric representation of the impactors, the top facesheet, the core and the adhesive. As the focus is on the damage to the top facesheet, the lower facesheet is ignored as it does not contribute to the local stiffness in the damage region. The model simulation represented a 3ms overall runtime divided into a 2ms long impact event and a 1ms long compressive loading stage. The solution included geometric and material non-linearity through local buckling of the core and plasticity in the facesheet and core. Contact was defined between all surfaces within the model in order to capture the interaction between the impactor and the facesheet, between the facesheet and cell walls and between adjacent cell walls as they collapsed.

4.2.2. Geometry

The models consisted of a 48 mm x 93 mm (1.9" x 3.7") panel with two spherical surfaces impacting the top of the panel. Figure 4-1 shows the four main components of the model: impactors, honeycomb core, facesheet and adhesive. This panel size was chosen to be large enough to capture the damage caused during the impact event and avoid edge effects. The initial impact velocity was chosen to produce dent depths between 0.1mm and 0.7mm, which would fall within the allowable dent limits of a typical aircraft panel.

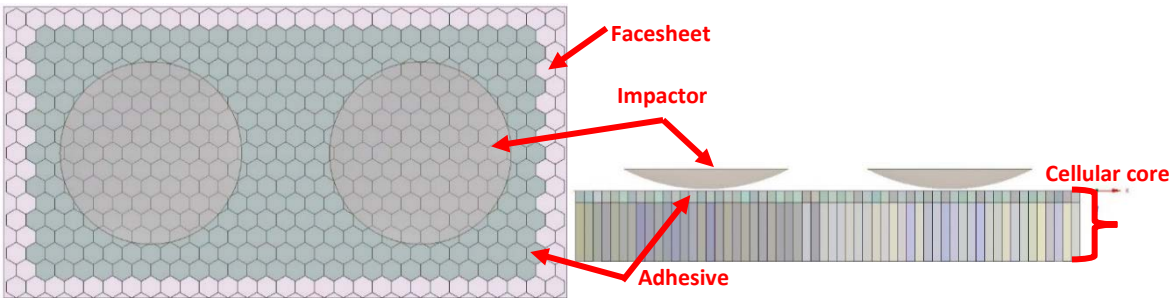

Figure 4-1: The four main components of the model: impactors, honeycomb core, facesheet and adhesive.

The geometry of the panel coupon modelled in ANSYS consisted of one 1.016 mm (0.04") thick aluminum facesheet and a 12.7mm (0.5") thick section of the aluminum honeycomb core; these are configurations that produced a minimum variation on residual dent depth as discussed previously in Chapter 3. The core has a hexagonal cell size of 3.175mm (0.125") measured across flats with a cell wall thickness of 0.0254mm (0.001") and a doubled wall thickness of 0.0508mm (0.002") in the ribbon direction. The entire adhesive layer encased the top 2.17mm of the core as the adhesive is essential for predicting the correct residual dent depth as it prevents the top of the cells from crushing and provides stiffness to the facesheet. The surface of the spherical indentors were modelled as a spherical shell with a radius of 33.4mm (1.315") and a shell thickness of 0.5mm (0.0197"). These dimensions are illustrated in Figure 4-2.

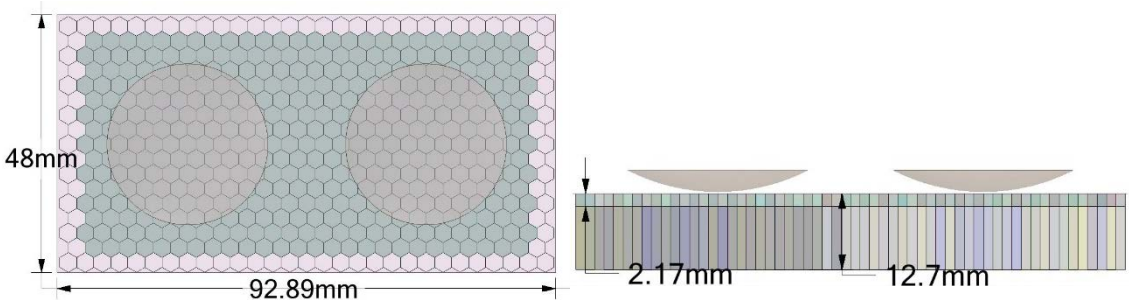

Figure 4-2: Model dimensions in millimetres

The top of the cell walls and the entire adhesive representation were modelled the same way as previously detailed in Chapter 3, Section 3.2.1.

4.2.3. Material

The facesheet was made of 2024-T3 aluminum and the honeycomb core of 5052- H34 aluminum. The spherical impactors were assumed to be made of steel, and the density was adjusted, so the impactors had a mass of 0.25kg. The impactors were modelled using a linear elastic material model, as the impactors were not supposed to yield given the relative stiffness of the two components in contact. Bilinear strain-hardening models were used for both the facesheet and core as the bilinear material model sufficiently captures the impact response while reducing the solver run times [5].

The top 2.17mm of the core geometry was given linear elastic material properties to represent the constraint that the adhesive provides as this region was not expected to yield. This included one set of material properties for the regular cell walls (denoted by "Single-wall adhesive") and another for the doubled cell walls in the ribbon direction (denoted by "Double-wall adhesive"). The wall thickness and the material properties at the top of the cell walls were adjusted to reach a stiffness equivalent to the adhesive and cell wall combined [2]. Table 4-1 shows the material properties of the model for the impactors, facesheet, core and adhesive.

Table 4-1: Material properties of the multiple impact site series models [2].

	Impactors, structural steel	Facesheet, 2024-T3 [68]	Core, 5052-H34 [63]	Adhesive, epoxy material [69]	Single-wall adhesive	Double-wall adhesive
Density [kg/mm^3]	0.00066569	2.78E-06	2.68E-06	1E-06	1E-06	1E-06
Young's Modulus [MPa]	2E+05	73100	71700	3700	6678	9402
Poisson's ratio [-]	0.3	0.33	0.33	0.3	0.3	0.3
Yield Strength [MPa]	-	345	345	-	-	-
Tangent Modulus [MPa]	-	811	305	-	-	-

4.2.4. Element Meshing

Lower-order elements were used in this simulation because the Explicit Dynamic solver in ANSYS does not support higher-order elements. Shell elements with 6 degrees of freedom were used for the facesheet and the honeycomb core cell walls, which allowed for the elements in those structures to carry axial, shear, torsional and bending loads. Solid hexahedral and tetrahedral elements were used to capture the adhesive fillet geometry. Figure 4-3 shows the free mesh used for the facesheet and adhesive and the mapped mesh used for the cell walls. Element sizes of 0.48 mm, 0.6 mm, 0.6 mm, and 1.5 mm were used for the core, adhesive, facesheet and indentor, respectively. The model had 225703 nodes and 383560 elements. The element size in the core was determined based on the result of convergence studies presented in Reference [2].

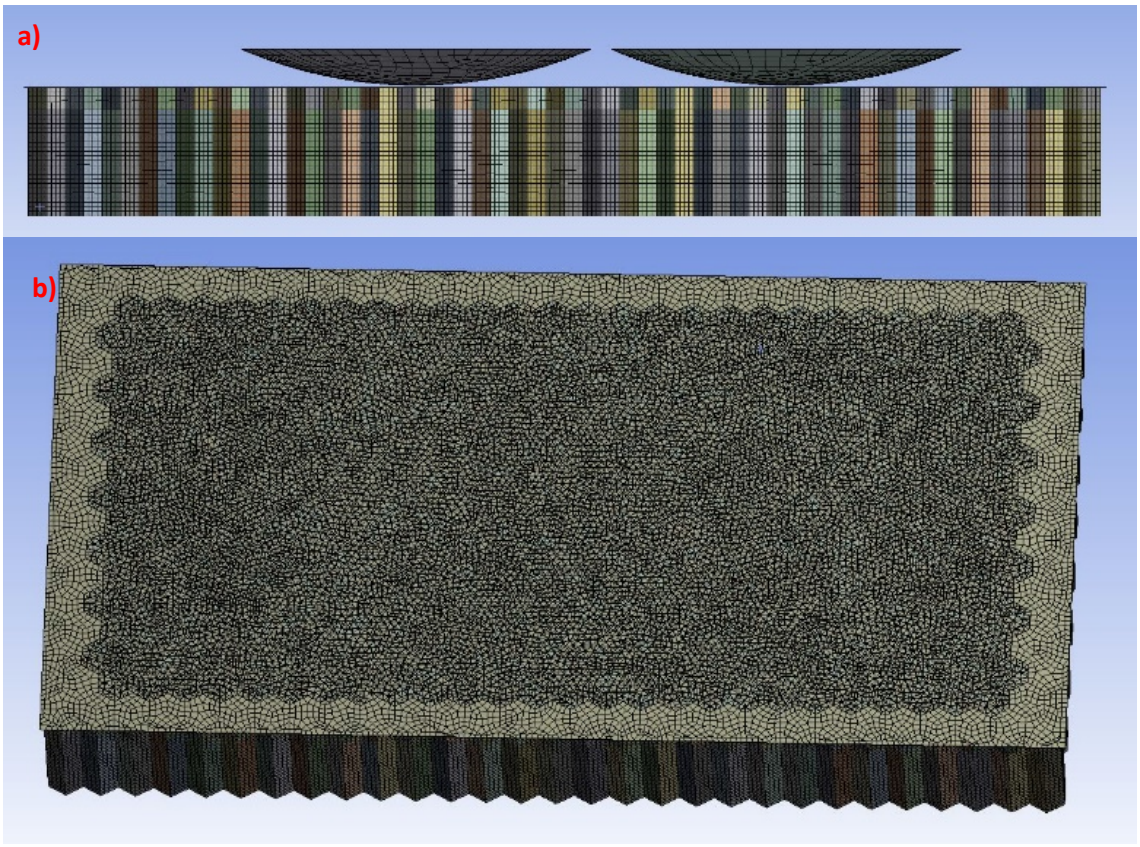

Figure 4-3: Final shape mesh a) Mesh in cell walls and b) Mesh in facesheet and adhesive.

4.2.5. Loading and Boundary Conditions

The numerical model described herein was performed in two loading stages: the first stage involved simulating the damage caused by two impactors at varying distances apart. The second stage simulates post-impact compressive loading, and the residual strength is taken as the peak of the force-displacement curve from the second stage of loading.

4.2.5.1. Impact Stage (Stage 1)

The two impactors hit the facesheet at the same time with a prescribed initial velocity of 2031.45 mm/s and equivalent impact energy of 0.5J in the facesheet normal direction. The impactors were constrained from moving in either lateral direction. This velocity was chosen to produce a residual dent between 0.18 mm and 0.7 mm to fall within the BVID limits. The effect of gravity was neglected, as its overall effect would be minimal given the short duration of the impact simulation.

The bottom of the honeycomb core was constrained in its normal direction to represent a panel sitting on a rigid surface. Although in reality, the bottom of an aircraft panel wouldn't be supported, however, with low impact velocities that produce BVID, the damage state is expected to be the same. The sides of the panel, including the outer core and facesheet edges, were constrained from translating in their respective normal directions to represent an infinitely large panel. The stage duration was 2ms to allow for complete spring-back to occur and the final residual dent to form. The loading and boundary conditions for stage 1 are shown in Figure 4-4.

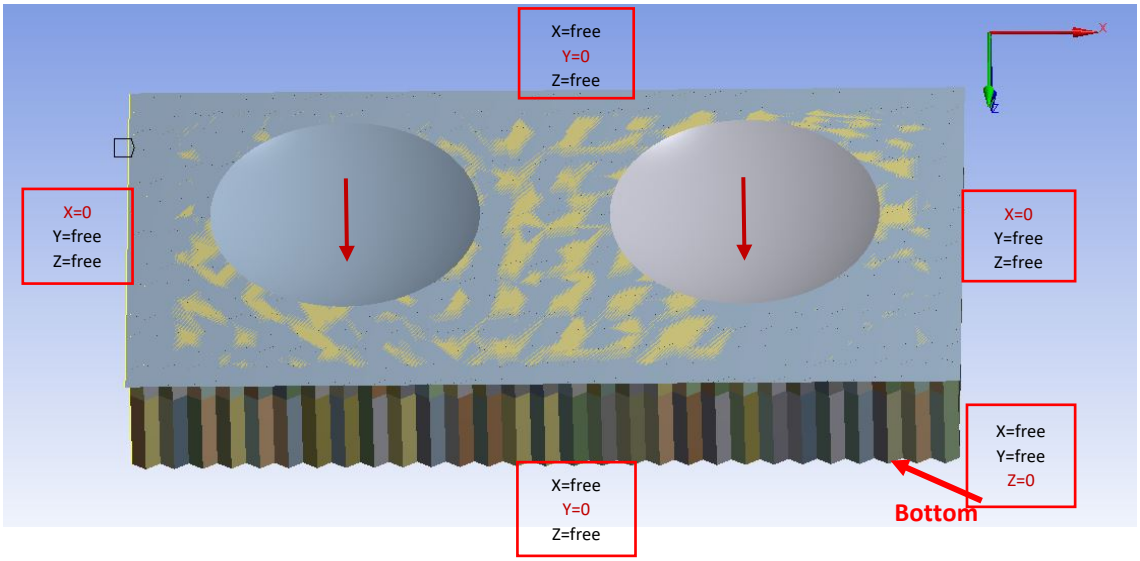

Figure 4-4: Loading and boundary conditions for impact stage (Stage 1).

4.2.5.2. Post-Impact Stage (Stage 2)

The post-impact load case was considered to be in-plane compression as most of the literature has been focused on CAI strength for a single impact event, and only a few studies were found on

multiple impacts sites in aluminum honeycomb sandwich panels. For this reason, more investigation is required for CAI strength for multiple impact sites in aluminum honeycomb sandwich panels, especially because in-service panels typically exhibit multiple dents or clusters of dents.

In this stage, it was assumed that the bottom of the surface is constrained in the normal direction to ensure that the failure initiates in the damaged region for all cases rather than failing due to overall buckling or bending of the panel or premature failure near the load application. Even though in reality, the bottom surface of an aircraft panel would not be constrained, this would not be expected to significantly affect the prediction of residual strength. Residual strength is based on local wrinkling that initiates in the top facesheet under compression. The boundary conditions remained the same as the impact stage, with the bottom surface and three of the sides constrained in their normal directions. The only change was that the constraint was removed from one side and replaced with an 8mm applied displacement to induce the compressive loading, as indicated in Figure 4-5. The peak load is determined by extracting the reaction force at the X=0 boundary condition at the opposite face from the applied displacement.

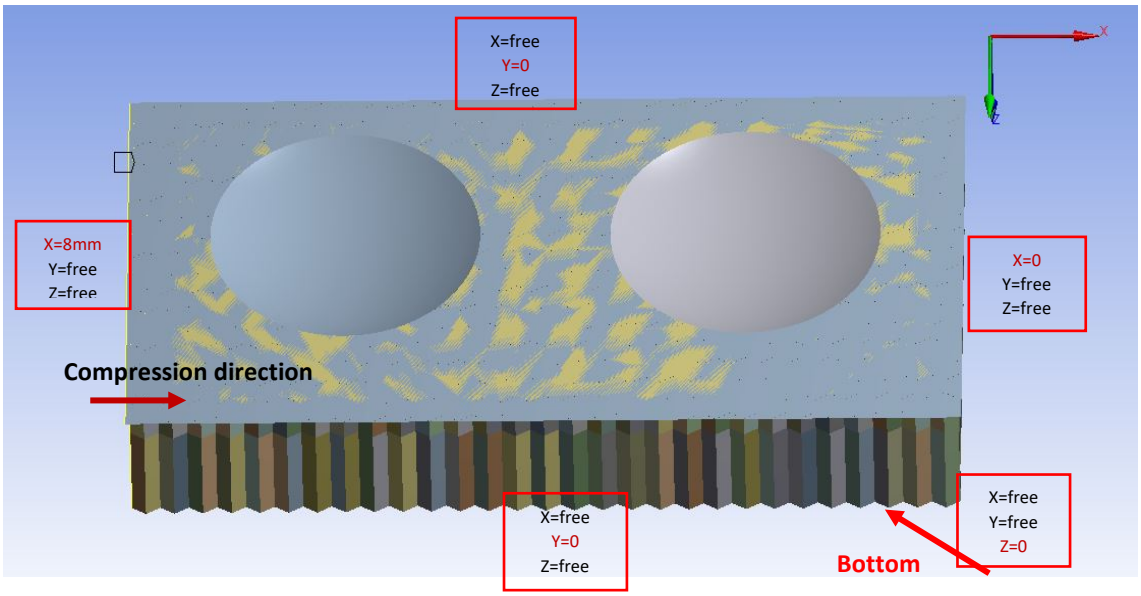

Figure 4-5: Loading and boundary conditions for the post-impact stage.

The compressive loading stage had a duration of 1ms, which was a sufficient length of time for representing a static load using an explicit solver. In the literature, explicit solvers have been used to model the impact and post-impact loading. Fischer et al. [73] conducted numerical CAI tests using an explicit solver, and a two-stage modelling approach showed good agreement with experiments regarding residual strength predictions and damage growth.

Frictionless contact was defined between all the surfaces to capture the interactions between the impactor and facesheet, facesheet and cell walls, and the bends in the cell walls during crushing. Since all the contact was expected to be between surfaces normal to each other rather than

tangential, the effects of friction were expected to be negligible, and a frictionless contact model is considered for ease of convergence.

4.3. Additional Model Development

A preliminary study for stage 1 was performed in order to determine the most effective method for representing the proximity of the impact sites in the first stage of the two-stage model. The results of these studies are presented in this section.

A series of 11 simulations were completed with the distances between the two impact sites varying from 0 mm to 20 mm apart at intervals of 2 mm to determine the distance between them when interacting with each other and when they behave as separate single dents. In the case of a 0 mm distance between the two impacts, it was modelled as one impactor with double the mass, representing two coincident impacts occurring at the same time. The focus of the preliminary study was to determine the residual dent depth, which was assessed by the deepest point of the facesheet displacement of the entire dented region. It was anticipated that as the distance between the impact sites increases, the dent depth would gradually decrease until they are far apart enough and behave as individual dents. At this point, the dent depth versus spacing curve would plateau. Figure 4-6 shows the preliminary results for residual dent depth versus distance between the center of the dents, The graph does not show a smooth curve, and the distance at which the two dents start to behave as individual dents is not clear. Also, it shows that point A is lower than point B, even though point A occurs when the damage regions are interacting, and point B occurs when they are far apart. The reason for this discontinuous curve is that the impacts occurred at different locations on the panel relative to the cell walls, as shown in Figure 4-7.

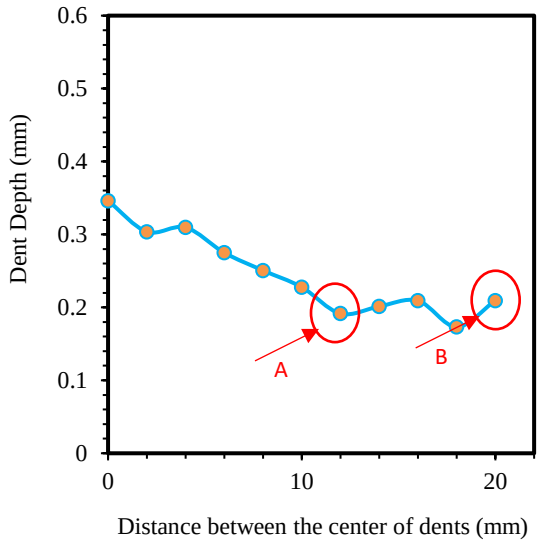

Figure 4-6: Preliminary results of the dent depth for multiple impact sites when varying the distance between them. Point A is at a 12mm spacing between the center of two dents and point B is at a 20mm spacing between the center of two dents.

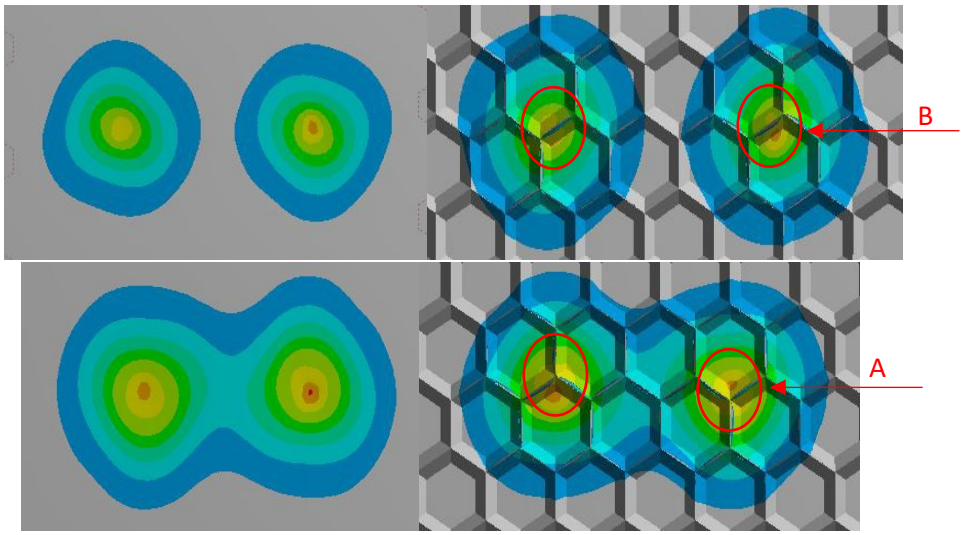

Figure 4-7: Preliminary results for two impact sites on a different location on the cell wall. Label A and B refer to the points on the graph in Figure 43. Point A is at a 12mm spacing between the center of two dents and point B is at a 20mm spacing between the center of two dents.

Figure 4-7 a) show the impact sites being on the center of the cell wall while b) shows impacts on the intersection between the cell walls. When the impactor hits the intersection between cells (the corner point), it produces a smaller dent depth as it is stiffer than when it hits on a single wall.

As discussed previously in Chapter 3, the impact location causes variations in the dent depth. In order to remove the effect of the impact location, the distance between the two impact sites was varied according to the number of cells between them. This kept the location of the impactors on the top of the center of the cell for every impact site in every simulation. In addition, a smaller cell size, thicker facesheet thickness and larger impactor radius were chosen to minimize the variability in the dent depth due to impact location as per the recommendations from Chapter 3.

4.4. Results

Low-velocity impacts on aluminum honeycomb sandwich panels cause permanent deformation of the facesheet and crumpling of the core. When impact sites are close together, the damaged regions of the panel overlap and interact. The results presented in Section 4.4.1 show the residual strength from the single dent. Section 4.4.2 shows the effect of the distance between impact sites on the resulting dent depth and dent area from Stage 1 of the finite element analysis. Section 4.4.3 shows the effect of the distance between impact sites on the residual strength of the panel due to post-impact in-plane compressive loading as determined from Stage 2 of the finite element analysis.

4.4.1. Residual Strength for a Single Dent

After the panel is impacted, it is exposed to post-impact, in-plane compressive loading by applying a prescribed displacement to the end of the panel. Figure 4-8 shows the initiation and propagation of the damaged region of the panel with a single impact site with applied displacement from 0 mm to 8 mm. Under in-plane compression, the facesheet in the dented region starts to bend inwards toward the core and the cell walls experience further folding and crushing. Figure 45 shows that the residual dent is still circular at a 2 mm applied displacement, but its depth has increased from the initial dent. The dented region becomes more elliptical and starts to expand across the facesheet transverse to the compressive loading direction, as shown between 5 to 6.46 mm of applied displacement. At the critical compressive load (6.46mm applied displacement), the facesheet becomes unstable, and buckles as the core crushes completely and lose its ability to support the facesheet. Then the overall failure of the panel occurs as the localization propagates to the edges of the panel, as shown at 8mm of applied displacement.

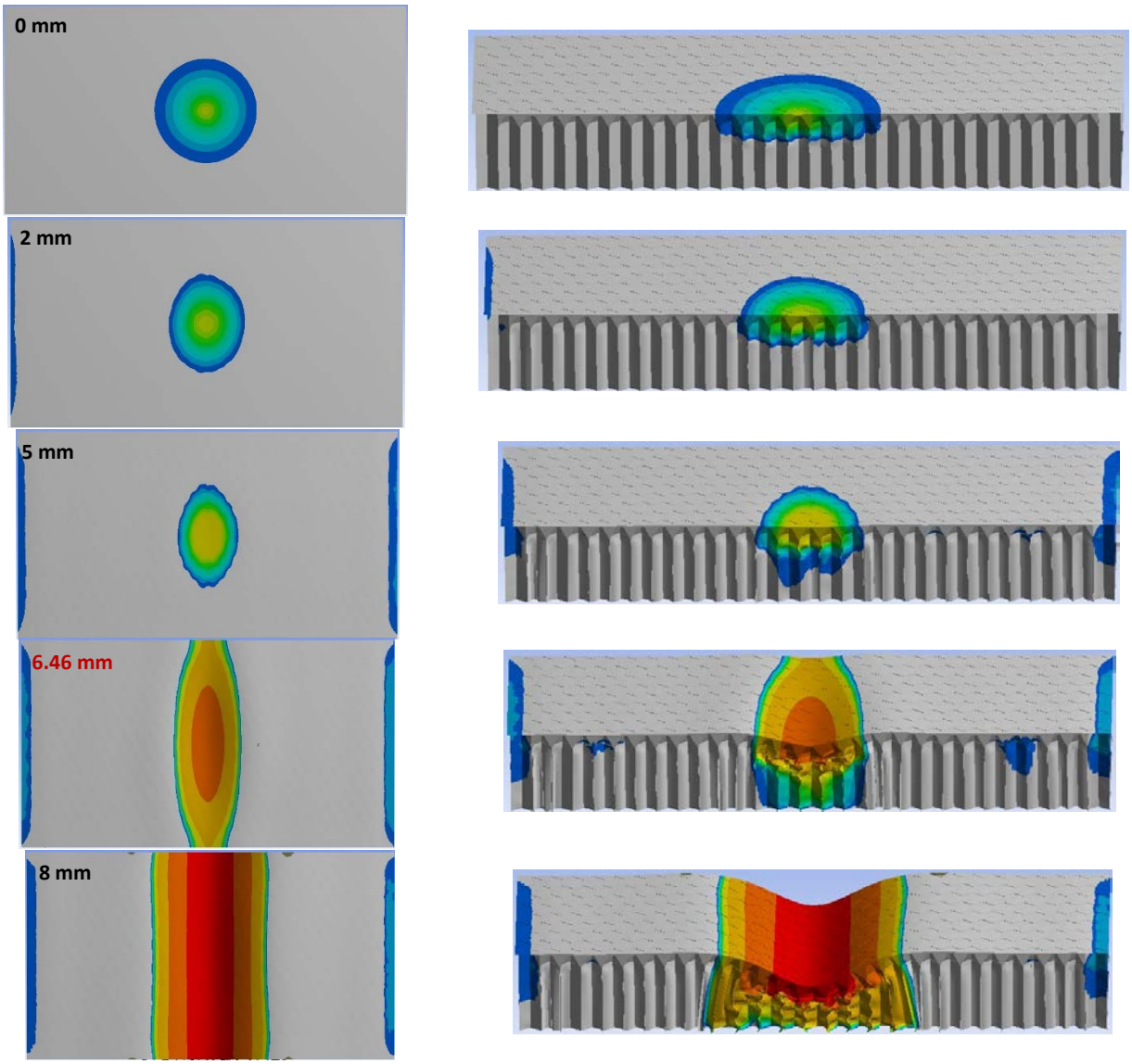

Figure 4-8: Failure mechanism for post-impact compressive loading for a single impact. The contour bar shows the out-of-plane deformation in mm. The red shows the largest out-of-plane deformation, and the grey shows deformation less than 0.0125mm. The number in red shows the amount of applied displacement corresponding to the peak reaction force.

The results from simulations are in good agreement with the published experimental results in the literature in terms of the process by which failure progresses [37, 45, 70]. Figure 4-9 shows the progression of failure in a dented panel in compression from experimental test results published by McQuigg et al. [37]. Figure 4-9 a) shows the initial circular dent in the panel, b) shows that under in-plane compression, the facesheet bends inwards towards the core and the dent deepens and becomes more elliptical, c)-d) shows the buckling of the facesheet and the region expanding across the facesheet transverse to the compressive loading direction, e) shows the overall general failure mode as the localization has propagated to the edges of the panel.

Figure 4-9: Failure mechanism for post-impact compressive loading from the experimental test in the literature. The dent gets deeper and expands across the facesheet transverse to the compressive loading direction until it gets unstable and propagates to edges [37].

Figure 4-10 shows the reaction force versus the applied displacement for the single dent with a dent depth of 0.183mm predicted by the finite element simulations. At the beginning of the applied displacement (between 0 and 0.2mm), the panel is experiencing elastic deformation, and the curve rises linearly to 20kN. As more load is applied, the dented region of the facesheet bends inwards, and the cell walls fold and crush further to accommodate this deformation. In this phase, the facesheet is experiencing plastic deformation as the dent deepens and becomes more elliptical in a direction perpendicular to the loading. The curve rises linearly as the compressive loading increases between 20kN and the peak force. At the peak force, the dent growth becomes unstable as the facesheet buckles. After the peak, the panel is bent and compressed as more displacement is applied. The localization propagates to the edges of the panel leading to global failure and results in a catastrophic reduction in the load-carrying capability of the panel, as seen by a drop of nearly 60% in the reaction force.

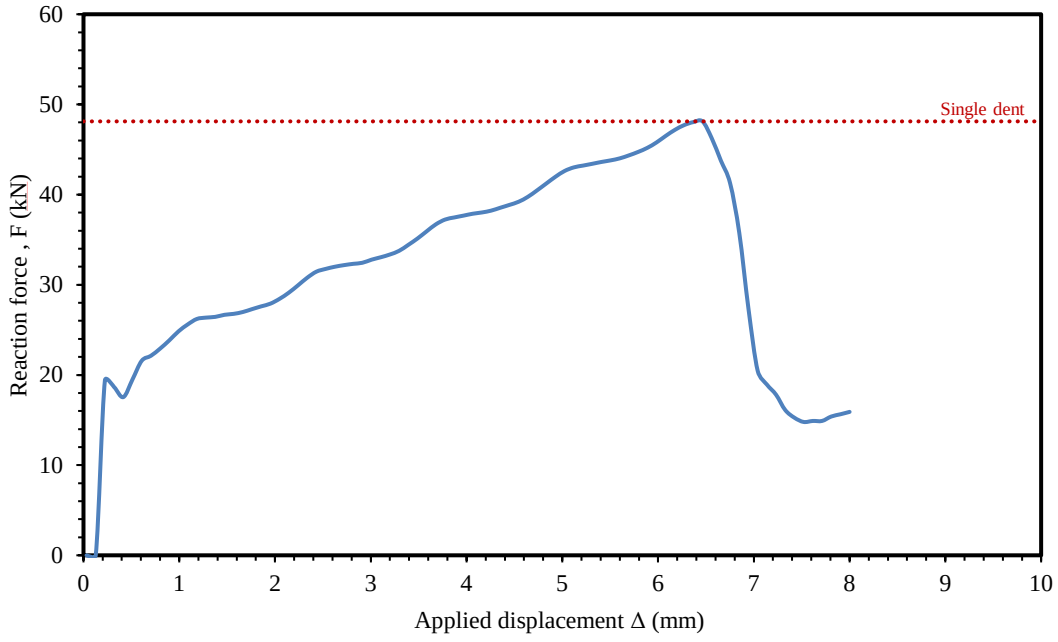

Figure 4-10: Reaction force versus applied displacement for a single dent (solid line). The red dotted line shows the peak force for the single dent.

Gilioli et al. [41] showed that in their experimental tests, the maximum peak force for an undamaged panel with a facesheet thickness of 1mm was in the range of 29.4kN to 80.1kN, and the large variation in this value was due to the panel manufacturing imperfections. Also, when increasing the thickness to 1.5mm, the range of CAI strength increased to the range of 47.9kN to 84.1kN. For dented panels, the authors found that the CAI strength decreased from 38.7kN to 18.3kN, with an increase in impact energy from 16.3J to 141.6J. Figure 4-10 shows that the numerical simulations predicted a CAI strength of 48.12kN for a single dent in a 1mm thick facesheet produced using impact energy of 0.5J. This energy falls within the range of 0J to 16.3J from Gilioli's tests, resulting in CAI strengths of between 38.7kN to 80.1kN. Similarly, Tariq et al. [70] showed that the maximum peak for an undamaged panel with a thickness of 0.5mm in their experimental tests was 32.9kN. The CAI strength only decreased by 5.47% for an impact that penetrated the facesheet.

Tariq et al. [70] used a facesheet of 0.5mm versus the 1mm used in the simulations; therefore, the simulations are expected to produce a higher CAI strength. Tariq's conclusion that having a hole in the facesheet still resulted in a CAI strength of 31.1kN again supports that the finite element predictions of CAI strengths are in the expected range. When comparing experimental results to numerical predictions of CAI strength, the experimental results are expected to be lower due to the imperfections in the panel. These imperfections, along with varying impact locations, will also produce a large variation in the measured strength. Since the literature does not contain results for panels with the same facesheet thickness, panel material, impactor size and impact energy, the simulation can not be fully validated without performing experimental testing for the specific situation simulated here. However, a comparison between published results and the simulations shows that the finite element models are predicting CAI strengths in the expected range.

4.4.2. Effect of Spacing on Damage Area and Depth

Figure 4-11 shows the dents formed by the two impacts. The red numbers indicate the number of cells between the center of the impact sites, where 0 cells apart indicate one impact with twice the impactor mass, representing two impacts directly on top of each other. A dent was identified from contour plots where the out-of-plane deformation in the facesheet was a minimum of 0.0125mm [2]. When the impact sites are 0 cells apart, the damage depth in the facesheet was 0.309mm, and it decreases as dents get farther from each other. When the impact sites are 1-8 cells apart, the impacts interact with each other, and their damage regions overlap, increasing the damaged area. When the impact sites are 9 or more cells apart, the impact sites behave individually with no interaction. The dents in the facesheet are separate, and the regions of the damaged core are also separate.

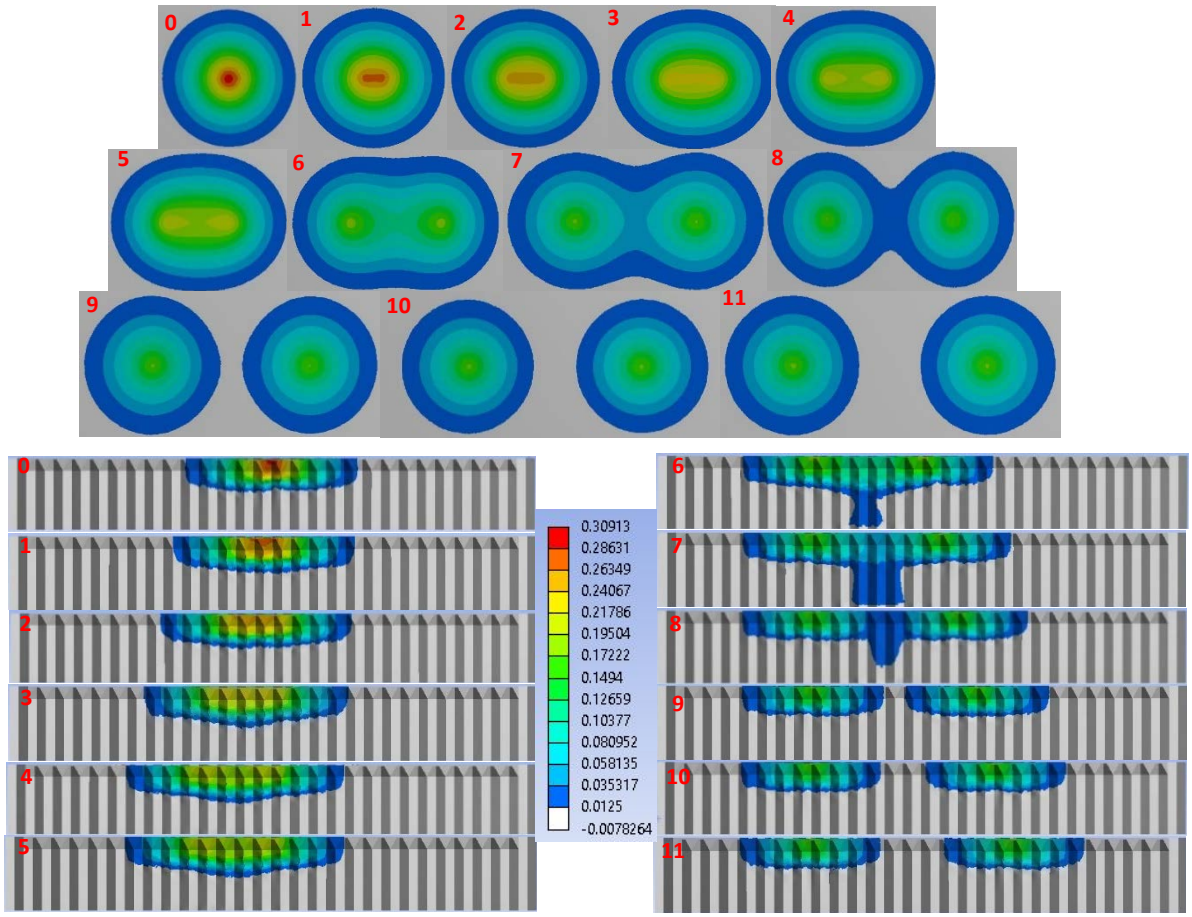

Figure 4-11: Facesheet and core damage from two impact sites as indicated by the out-of-plane deformation (mm). A view of the top of the facesheet and a cross-sectional view through the center of the panel are shown. Red shows the deepest dent, and grey shows deformation less than 0.0125mm.

The damage area and length are analyzed and measured by using ImageJ software. The length is measured from the longest dimension (x-direction) as shown in Figure 4-12. The total length and the total area are defined as being double the single dent length and area and are indicated by the dotted line in Figure 4-13.

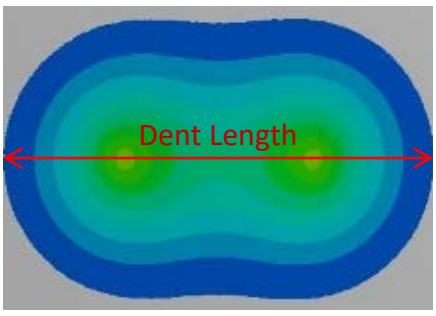

Figure 4: The length of the damaged region.

The graph in Figure 4-13 a) shows that the damaged area increases as the dents move farther away from each other until it overshoots the total area. The dent area then decreases and plateaus when the two dents are far enough apart to behave as individual dents. The graph in Figure 4-13 b) shows that the dent length increases as the dents move farther apart and then plateaus when they are far enough apart to behave as individual dents. Both graphs show the dents behaving independently when the spacing between their centers is at least 9 cells apart.

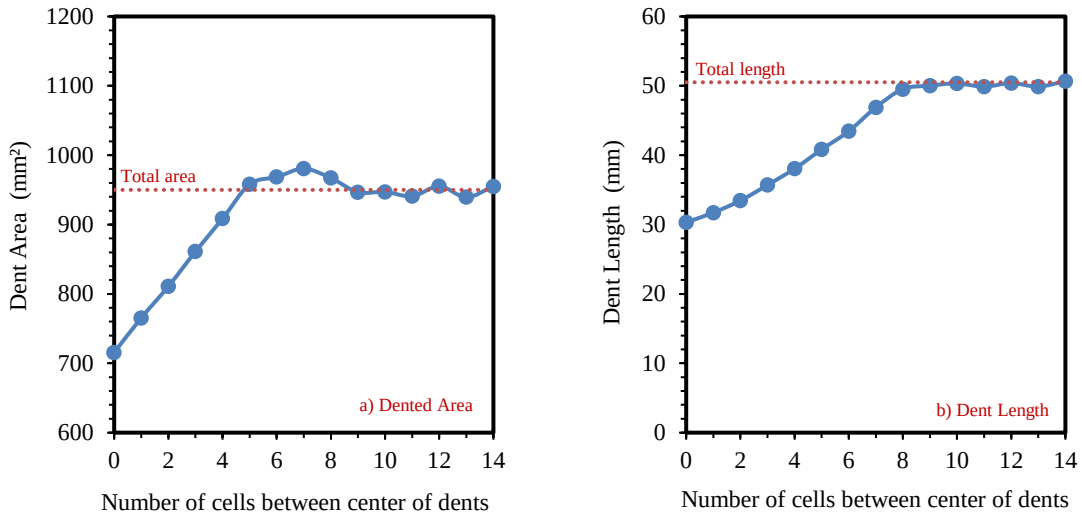

Figure 4-13: Effect of spacing between multiple impacts on a) Dented area and b) Dent length.

Two different images from Figure 48 have been taken and rescaled to show where the center of each dent is located. Figure 4-14 a) shows two dents that are close to each other with a spacing of 5 cells apart, and Figure 4-14 b) shows when they are 13 cells apart and behave as individual dents. When the two dents are close and interacting, they have two local maximum points, and the crushed core is deepest at the center of the damaged region rather than below each dent.

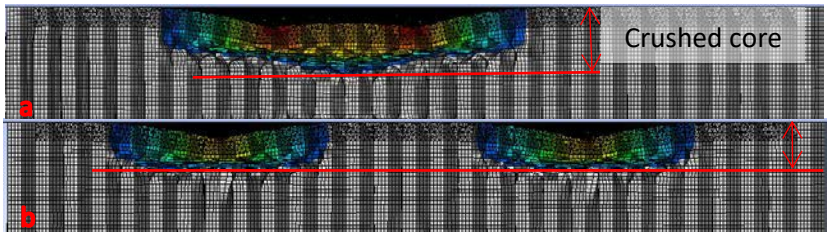

Figure 4-14: Cross-sectional view for two impact sites on the facesheet. a) Two dents spaced at 5 cells apart that are interacting, b) Two dents spaced at 13 cells apart that are behaving separately. The contour values indicate out-of-plane displacement (mm), the red shows the deepest dent, and the grey shows deformation less than 0.01mm.

Figure 4-15 shows the effect of impact site spacing on dent depth. The maximum dent depth of 0.309mm occurs at 0 cells apart, representing two dents overlapping and having the same center point. In this case, the impact energy is doubled that of a single dent, which produces more facesheet and core damage. As the impact sites move further apart, the dent depth decreases as the interaction decreases. At 7 cells apart, the curve plateaus showing the maximum dent depth within the impact region is the same as that of a single dent.

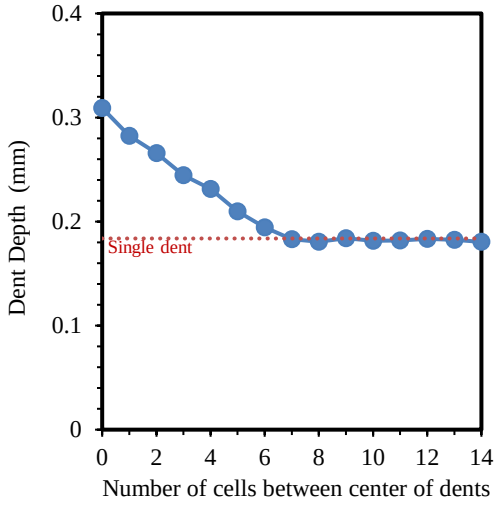

Figure 4-15: Effect of spacing between multiple impacts on residual dent depth.

Table 4-2 shows the dent area and dent depth for the simulations with multiple impact sites. Dent depth increases by 68% from the single impact site when dents are directly overlapping (0 cells apart) due to the impact energy being twice as large. The total damaged area when the dents are directly overlapping is 25% less than the area of two single dents. When the impact sites are 7 or more cells apart, the maximum depth of the impact damage region is the same as that of a single dent. For the dented area, the dents in the facesheet are separate when the impact sites are 9 or more cells apart. At this spacing, the regions of the damaged core are also separate.

Table 4-2: Effect of multiple impacts on residual dent depth and dent area with the percentage of the change compared to a single dent.

Model ID	Distance between Impactors	Dent depth		Dent area	
		(mm)	% Change	(mm²)	% Change
Single Impactor	-	0.183	-	950[1]	-
M-15	14 Cells	0.182	-2%	955	1%
M-14	13 Cells	0.183	-1%	939.4	-1%
M-13	12 Cells	0.183	0%	955.3	1%
M-12	11 Cells	0.182	-1%	940.9	-1%
M-11	10 Cells	0.182	-1%	947.1	0%
M-10	9 Cells	0.183	0%	946.7	0%
M-9	8 Cells	0.181	-2%	967.1	2%
M-8	7 Cells	0.183	0%	980.5	3%
M-7	6 Cells	0.194	6%	968.6	2%
M-6	5 Cells	0.209	14%	958	1%
M-5	4 Cells	0.231	26%	908.5	-4%
M-4	3 Cells	0.245	33%	861	-9%
M-3	2 Cells	0.266	45%	810.9	-15%
M-2	1 Cell	0.282	54%	765.4	-19%
M-1	0 Cell	0.309	68%	715.6	-25%

[1] The total area of 950mm² represents twice the area of a single impact.

4.4.3. Effect of Spacing Between Multiple Dents on Residual Strength

When impact sites are close enough that they interact, the panel's ability to carry in-plane compressive loads is reduced. In order to determine the effect of spacing between two impact sites on the residual strength, a series of simulations were completed with impact sites spaced from 0 to 14 cells apart. The peak force from the reaction force versus applied displacement curve was used as the measure of the panel strength.

Figure 4-16 shows the reaction force versus the applied displacement for two impacts sites with varying spacing between them. The graph shows that they all follow the same overall shape from the start of the applied displacement to the peak force. When dents are closer together, the interaction between them causes the damaged area and depth to increase. This results in a decrease in the peak force that can be sustained by the panel. At 0 cells apart, the dents are directly overlapping, which reduces the maximum reaction force from 48.12kN for a single dent to 42.78kN. At 14 cells apart, the dents behave individually, and the maximum reaction force is 47.85kN. However, the highest reaction force is 51.43kN in these series and is seen when dents are 4 cells apart. This is even higher than the single dent, and the reasons behind this will be discussed in Section 4.5.2.

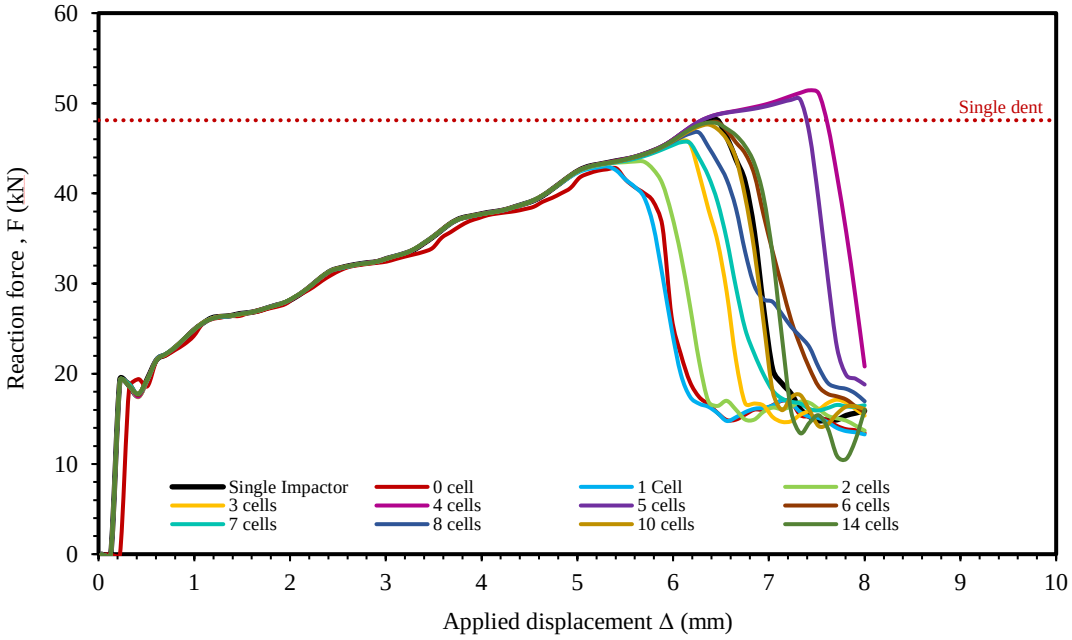

Figure 4-16: Reaction force versus applied displacement for two impact sites spaced at different distances apart. The spacing is noted by the number of cells between the centers of the dents.

The graph in Figure 4-17 shows the effect of the spacing between multiple dents on the peak reaction force. When the spacing is small, 0 to 3 cells apart, the damage sites behave as a single large and deeper dent. There is no interaction at a spacing greater than 10 cells apart, and the dents act as single dents in terms of indentation propagation. In the case where the two impact sites are 4, 5 or 6 cells apart, the compressive strength was higher than a single dent due to the failure location between the interaction of multiple dents, which increased the residual strength. The reasons for this will be discussed further in Section 4.5.2.

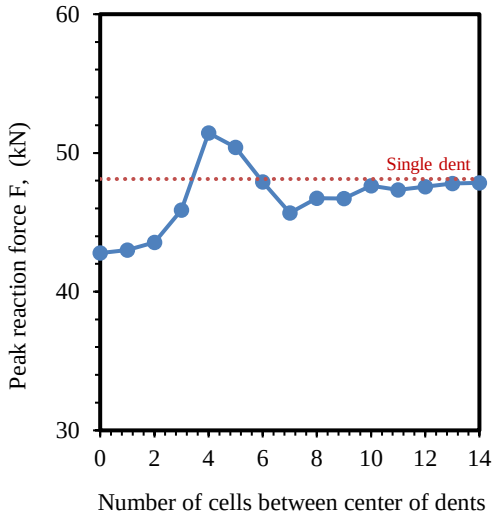

Figure 4-17: The effect of spacing between two impact sites on the CAI strength.

It is interesting to note that the dent depth is unaffected with a minimum spacing of 7 cells, while the dent area requires 9 cells, and the peak reaction force requires 10 cells. This shows that even though the dents may not have visibly overlapping edges, there could still be a reduction in panel strength.

Table 4-3 shows the peak reaction force of the series, the effect of spacing and the percentage change in the peak reaction force compared to the single impact. The applied displacement corresponding to the peak force is also shown. When dents are overlapping, and the spacing is small, 0 to 3 cells apart, the damage sites behave as a larger deeper dent, and the peak reaction force is 10-11% lower than for a single dent. There is no interaction at a spacing greater than 10 cells apart, and the peak reaction force is within 1-2% compared to a single dent. In the case where the two impact sites are 4, 5 or 6 cells apart, the compressive strength was higher than the single dent.

Table 4-3: The peak reaction force and the percentage of change compared to a single dent.

Model ID	Distance between Impactors	Peak reaction force (kN)	Corresponding displacement (mm)	% Change in the Peak reaction force
Single Impactor	-	48.12	6.464	-
M-15	14 Cells	47.86	6.368	-1%
M-14	13 Cells	47.79	6.368	-1%
M-13	12 Cells	47.58	6.368	-1%
M-12	11 Cells	47.33	6.368	-2%
M-11	10 Cells	47.65	6.368	-1%
M-10	9 Cells	46.72	6.464	-3%
M-9	8 Cells	46.74	6.272	-3%
M-8	7 Cells	45.68	6.08	-5%
M-7	6 Cells	47.92	6.464	0%
M-6	5 Cells	50.41	7.328	5%
M-5	4 Cells	51.44	7.424	7%
M-4	3 Cells	45.89	6.08	-5%
M-3	2 Cells	43.55	5.6	-10%
M-2	1 Cell	42.99	5.312	-11%
M-1	0 Cell	42.78	5.408	-11%

When two dents are close enough to interact with each other, the peak force that the panel can sustain is reduced. The peak force is reached when the facesheet becomes unstable, which occurs after a sufficient out-of-plane displacement. Figure 4-18 shows the initial out-of-plane displacement for two impact regions. Figure 4-19 shows a series of images for impact sites at 3 and 14 cells apart. 6 images are shown for applied displacements between 0mm and 8mm. Figure 4-18 a) shows the impact region for two impact sites spaced 3 cells apart, and Figure 4-18 b) shows two impact sites spaced 14 cells apart. This figure shows that when the impact sites are close together, the impact region has one location of maximum depth, but when the impact sites are far apart, there are two locations of maximum depth. The maximum dent depth is larger when the sites are closer together. Since instability of the facesheet occurs once a sufficient amount of out-of-plane displacement is present, impact regions that start with deeper dents will become unstable after less applied displacement. This is shown in Figure 4-19 as the impact sites that are 3 cells apart reach the peak force after an applied displacement of only 5.6mm, while 14 cells apart require 6.37mm of applied displacement.

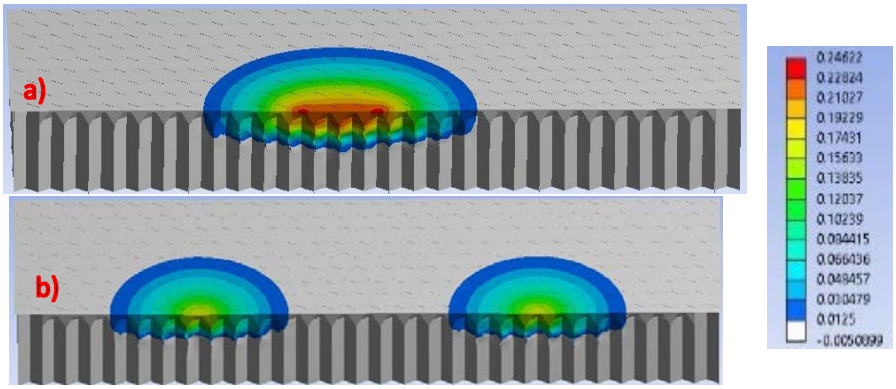

Figure 4-18: Initial depth of impact region a) Two dents spaced at 3 cells apart that are interacting, b) Two dents spaced at 14 cells apart that are behaving separately. The contour values indicate out-of-plane displacement (mm). The red shows the deepest dent, and the grey shows deformation less than 0.0125mm.

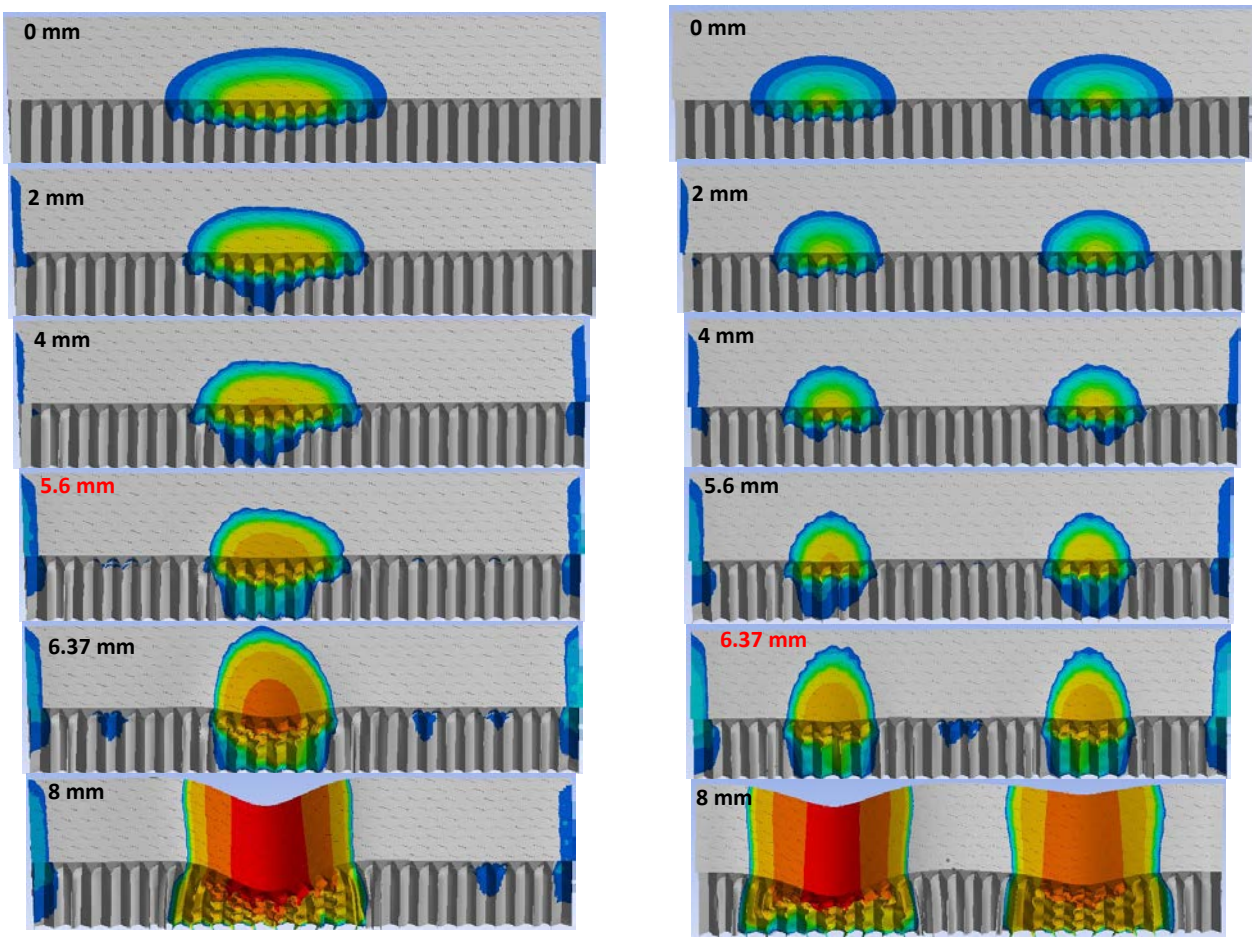

Figure 4-19: Series of comparisons between two impact sites at different applied displacements. a) Two dents interacting together, b) Two dents behaving individually. The contour values indicate out-of-plane displacement (mm). The red shows the deepest dent, and the grey shows deformation less than 0.0125mm. The number in red shows the amount of applied displacement corresponding to the peak reaction force.

4.4.4. Effect of Impact Energy on The Spacing Between Multiple Dents

An additional study was performed to examine the effects of the spacing between the two impact sites on the dent depth, dent areas and residual strength for different impact energies. Three impact energies were studied: 0.5, 1 and 1.5J. As the impact energy increases, the amount of damage to the panel increases, resulting in deeper and wider dents. A single dent at 0.5J resulted in a dent depth of 0.183mm and dent area of 475mm², while a 1.5J impact resulted in 0.415mm dent depth and 865mm² dent area.

Figure 4-20 a) shows the dent depth resulting from multiple impacts at 3 impact energies. All energies showed the same shape of the curve, which has a linear relationship when the impact sites are interacting and a plateau when they behave independently. The difference between the energies is that larger impact energies produce larger dent depths and require a larger distance between the impact sites in order to avoid interactions. An impact energy of 0.5J requires a spacing of at least 7 cells to avoid interacting, while 1.5J requires a minimum of 10 cells.

Figure 4-20 b) shows the dented area resulting from multiple impacts at 3 impact energies. All energies showed the same shape of the curve, which has a linear relationship when the impact sites are interacting and a plateau when they behave independently. The difference between the energies is that larger impact energies produce a larger dent area and require a larger distance between the impact sites in order to avoid interactions. An impact energy of 0.5J requires a spacing of at least 9 cells to avoid interacting, while 1.5J requires 13 cells.

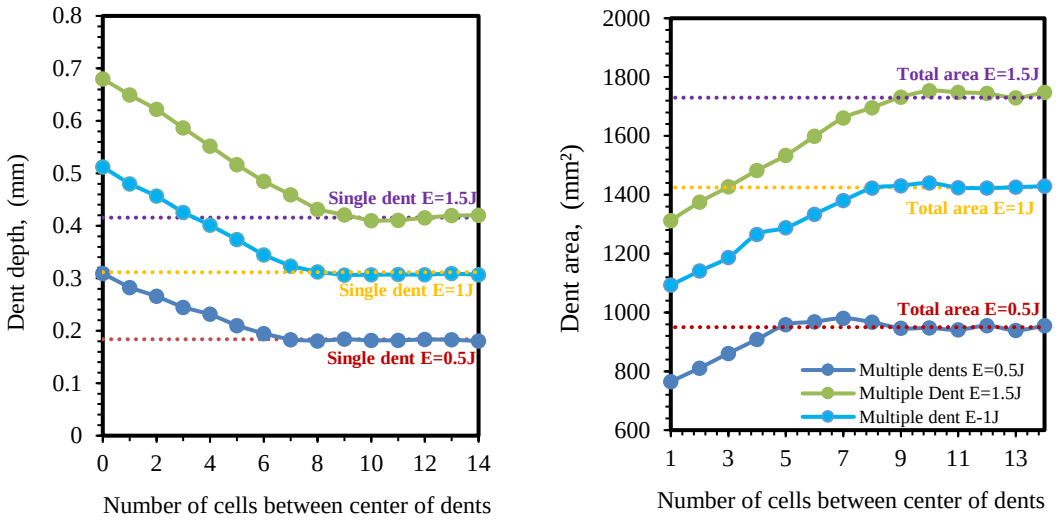

Figure 4-20: Effect of impact energy on the spacing between two impact sites a) Dent depth and b) Dent area.

Increasing the impact energy results in larger and deeper dents that required more spacing between the two dents to avoid the reduction in residual strength as illustrated in Figure 4-21; at 0.5J impact energy, it needs at least 10 cells apart while at 1.5J impact energy, it needs more than 13 cells. The curve for impact energy of 1.5J does not show a stable plateau as the peak reaction force appears

to decrease at spacings of 13 and 14 cells. This is due to the dent areas being larger for this higher impact energy, and they may be starting to interact with the free edges of the panel. A larger panel would be required to avoid these edge effects.

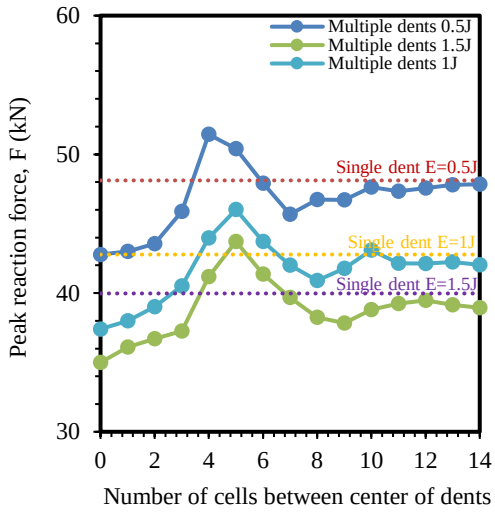

Figure 4-21: Effect of spacing between two impact sites with different impact energy on the CAI strength.

When considering the effects of spacing on the dented area and the panel strength for the 3 impact energies, it can be concluded that the spacing determined by the dented area can be used as a measure of interaction between dents. If the dents are very close but not physically overlapping, as indicated by the total damage area, there will be at most a 1-2% reduction in the panel strength.

4.5. Discussion

Two impact sites that are parallel to the loading direction of a panel influence its residual strength. This section will address three points of interest based on the results presented in the results Section 4.4. It was shown that when impact sites are close together, they interact, resulting in larger dent depths and larger damaged areas and reduced residual strength. However, it is unknown which damage metric is the cause of the reduction in residual strength because they are interconnected. A study that separates the effects of dent depth and dent area was conducted and is presented in Section 4.5.1. Also, it was noted that in Figure 4-17 a spacing of 4-6 cells between the dent centers resulted in a strengthening of the panel. The reasons for this will be discussed in Section 4.5.2. Finally, these results could potentially be used in the field for damage evaluation.

4.5.1. Effect of Dent Area and Dent Depth on The Residual Strength

4.5.1.1. Effect of Dent Area on Residual Strength

In order to determine the effect of dent area on the residual strength, a series of numerical simulations of 7 models were used to increase the dented area while maintaining the dent depth constant. The dented area was isolated as the only source affecting the residual strength. The model had a single ellipsoid impactor with increasing diameter in the x-direction (loading direction) only, as shown in Figure 4-22. An ellipsoid was used so that the length of the damaged area could be extended in the direction parallel to the loading direction (to represent 2 impact sites) while keeping the dimension perpendicular to the loading direction constant. The panel has the same configuration used in the dent spacing study in Section 4.2. Table 4-4 shows the impactor configuration. The impact energy was adjusted to give the same dent depth for the dent area series by changing the impactor density.

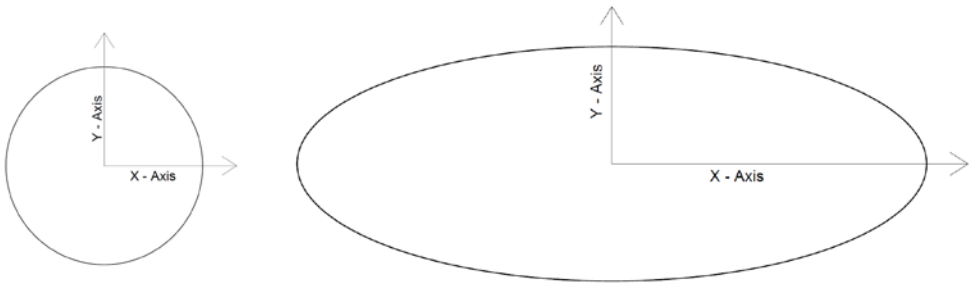

Figure 4-22: Impactor shape for dent area study a) Base model spherical impactor and b) X-direction lengthened and the impactor becomes elliptical in shape.

Table 4-4: The impactor configuration for the dent area study

Model ID	Impactor density (Kg.mm^{-3})	Impactor radius (mm)	
		X-axis	Y-axis
A1 (Base model)	0.00066569	33.4	33.4
A2	0.0005336	48.02	
A3	0.00047064	55.28	
A4	0.00039896	68.14	
A5	0.00037734	75.03	
A6	0.00034025	83.37	
A7	0.00032742	90.05	

Figure 4-23 shows the reaction force versus the applied displacement. There is no difference in the curve up to the peak force, which means the size of the dent does not affect the overall stiffness of the panel prior to localization. Even after localization, all panels behave the same way and reach the same plateau force during propagation (as the wrinkle extends to the edge of the panel).

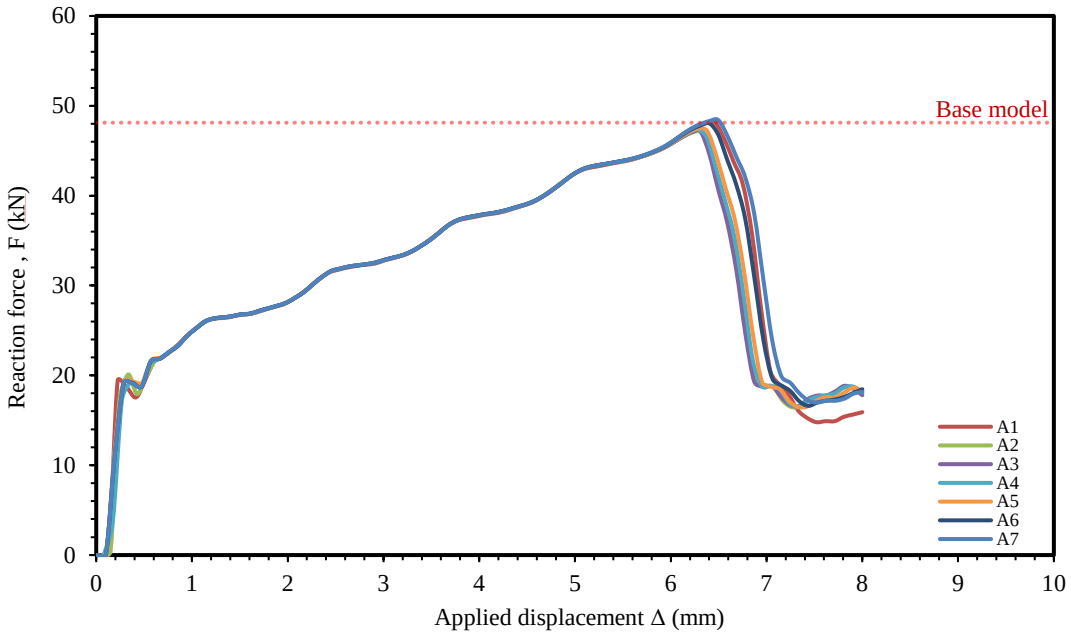

Figure 4-23: Reaction force and the applied displacement for the dent area series.

The graph in Figure 4-24 shows the effect of the dented area on the peak reaction force. When the damaged area increases from 472.3mm² to 728.9mm², the peak force remains constant at 48 kN. This means that the panel strength is independent of the dented area.

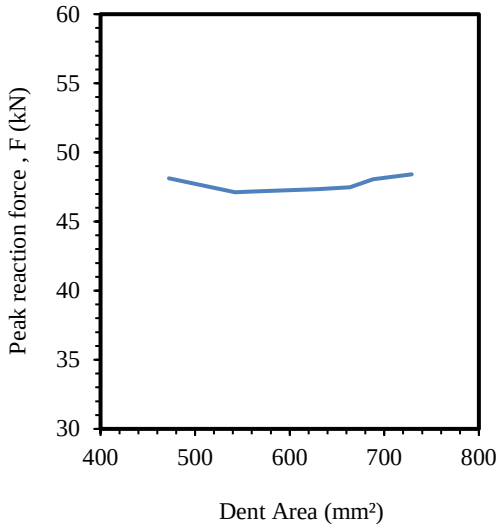

Figure 4-24: Peak reaction force and dent area for the dent area study.

Table 4-5 shows the reaction force of the dent area series and the percentage change in the residual strength compared to the base model. Also, it shows the applied displacement corresponding to the peak force. For dent areas between 472.33mm² and 728.94mm², both the panel peak force and the corresponding applied displacement remain constant within only a 3% variation. For example, when the damaged area increased by 54%, the peak force remains within 2% of the baseline, and the applied displacement required to initiate the localization remains within 3% of the baseline. The peak force occurs when the facesheet has sufficient out-of-plane deformation to become unstable and localize. Since bending of the facesheet would be caused by a moment based on the distance between the loaded facesheet and the bottom of the dent, this would not be affected by the damaged area. It would, however, be affected by the depth of the dent, as demonstrated in Section 4.5.1.2.

Table 4-5: Results for dent area study showing the reaction force and the percentage of change compared to the base model.

Model ID	Dent Depth		Dent Area		Peak Reaction Force		Corresponding Displacement	
	(mm)	%Change	(mm²)	%Change	(kN)	%Change	(mm)	%Change
Base model A1	0.183	-	472.3	-	48.12	-	6.464	-
A2	0.182	-1%	542.3	15%	47.12	-2%	6.245	-3%
A3	0.188	2%	562.9	19%	47.17	-2%	6.307	-2%
A4	0.185	1%	628.9	33%	47.34	-2%	6.282	-3%
A5	0.188	2%	663.5	40%	47.47	-1%	6.287	-3%
A6	0.189	3%	688.1	46%	48.05	0%	6.401	-1%
A7	0.188	2%	728.9	54%	48.42	1%	6.287	-3%

4.5.1.2. Effect of Dent Depth on Residual Strength

This section will show the effect of dent depth on the residual strength. A series of numerical simulations of 7 models were used to increase the dent depth. The model used has a single spherical impactor with the same panel configuration as used in the dent spacing study in Section 4.2. Table 4-6 shows the impactor configuration. The impact energy was increased by increasing the impactor density. Even though increasing the impact energy produces a deeper dent with a larger area, the effect of dent area on residual strength is minimal and can be ignored, as illustrated in Section 4.5.1. Therefore, changing the depth while also changing the area has the same effect as changing the depth while keeping the area constant. The impactor shape is kept constant to achieve the same dent profile for these 7 models.

Table 4-6: The panel and impactor configuration for the dent depth study.

Model ID	Impactor density (Kg.mm^{-3})	Corresponding impact energy (J)
D1	0.00066569	0.5
D2	0.00088759	0.67
D3	0.0011095	0.84
D4	0.0013314	1
D5	0.0015533	1.17
D6	0.0017752	1.34
D7	0.0019707	1.5

Figure 4-25 shows the reaction force versus the applied displacement. There is no difference in the curve up to the peak force, which means the depth of the dent has no effect on the overall stiffness of the panel prior to localization. Even after localization, all panels behave the same way and reach the same plateau force during propagation (as the wrinkle extends to the edge of the panel).

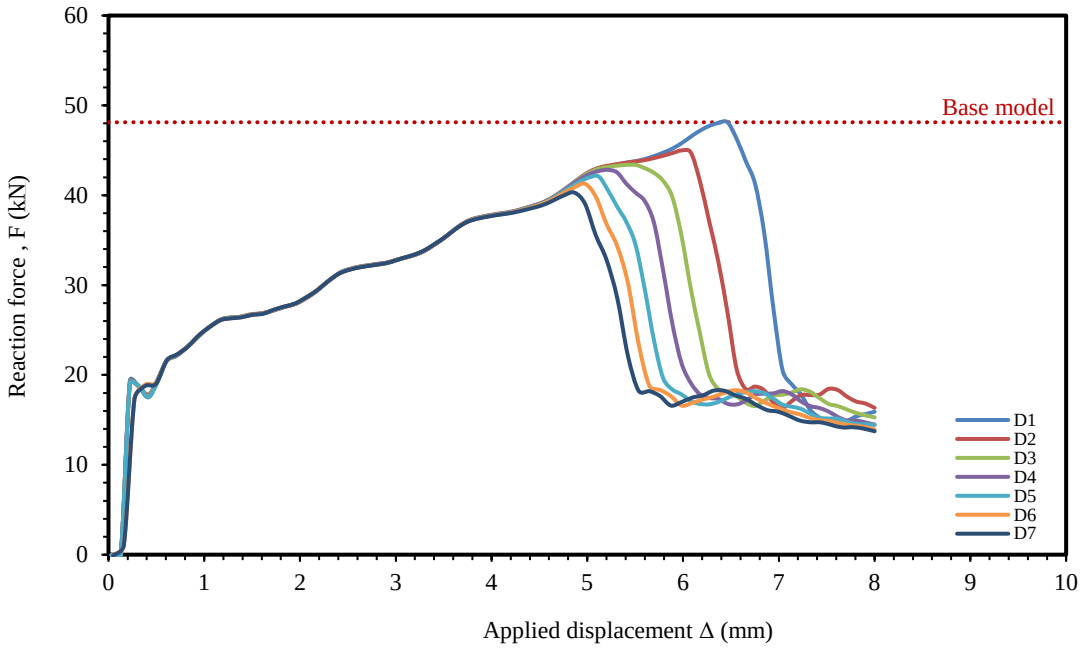

Figure 4-25: Reaction force and the applied displacement for the dent depth series.

The graph in Figure 4-26 shows the effect of dent depth on the peak reaction force. When the dent depth increases from 0.183 to 0.427 mm, the peak force decreases from 48.12kN to 40.29kN.

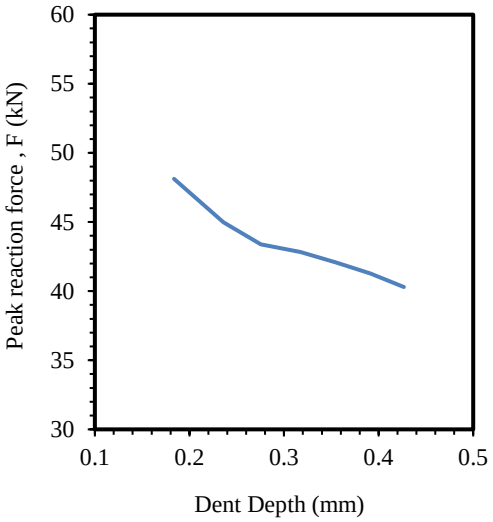

Figure 4-26: Peak reaction force and dent depth for the dent depth study.

Table 4-7 shows the peak force of the dent depth series and the percentage change in the residual strength compared to the base model (the single dent). The applied displacement corresponding to the peak force is also shown. The residual strength decreased by 16%, and the peak force was achieved with 25% less applied displacement as the dent depth increased from 0.183 to 0.427mm.

Table 4-7: Results for dent depth study showing the reaction force and the percentage of change compared to the base model.

Model ID	Dent Depth		Dent Area		Maximum Reaction Force		Corresponding Displacement	
	(mm)	%Change	(mm²)	%Change	(kN)	%Change	(mm)	%Change
Base model (D1)	0.183	-	485.3	-	48.12	-	6.464	-
D2	0.236	28%	536.3	10%	44.99	-7%	5.984	-7%
D3	0.276	50%	601.9	24%	43.38	-10%	5.504	-15%
D4	0.317	73%	667.9	38%	42.83	-11%	5.2161	-19%
D5	0.355	93%	745.6	54%	42.08	-13%	5.12	-21%
D6	0.391	113%	816.14	68%	41.27	-14%	4.976	-23%
D7	0.427	132%	863.9	78%	40.3	-16%	4.864	-25%

Localization occurs when the facesheet bends sufficiently that it becomes unstable and locally wrinkles. In deeper dents, the bending moments are larger than in the shallower dents due to the larger distance between the undamaged facesheet and the bottom of the dent. Localization will therefore happen earlier and with less applied force.

It was shown in Section 4.4.3 that when two dents are close together and interacting, the peak force went down. The reason for the reduction in panel strength is because of the increased dent depth and not the increased dent area, which was shown to have a minimal effect on the peak force.

4.5.2. Effect of Interaction Between Multiple Impact Sites

It has been shown that when the damage regions of multiple impacts overlap, there is a reduction in residual strength of the panel due to the increase in the depth of the dented region. In addition, the spacing required to prevent the interaction between dents changes with the impact energy because increasing the impact energy produces larger and deeper dents that require more distance between them, as presented in Section 4.4.4. However, it was shown in Figure 4-17 that in some cases, the strength of the panel in fact increased above that of a single dent. This occurred for spacing in the range of 4 to 6 cells apart. An example of this can be seen in Figure 4-27 for two impact sites that are 4 cells apart. Figure 4-27 shows that following impact, two local dents can be seen, each with their local maximum dent depth (two initial localization points). Figure 4-28 shows a series of images for applied displacements between 0mm and 8mm. Between 2mm and 6mm, the overall dented region forms one local maximum dent depth. At 7.42mm, the localization occurs at a single site rather than at two sites, as shown in Figure 4-28. It is the transition from two local maximum dent depths to one maximum dent depth that requires a higher force than a single impact site requires.

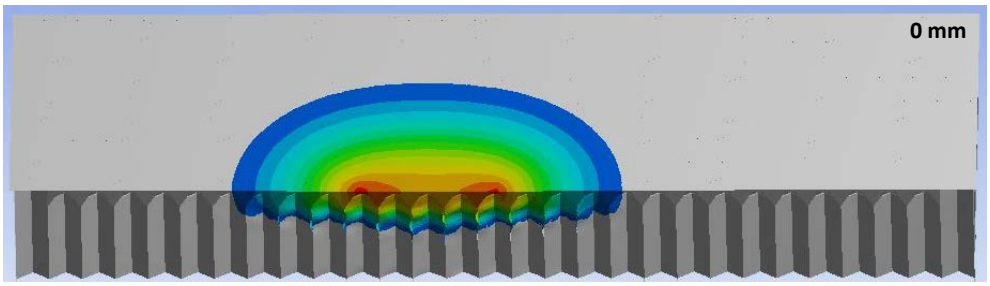

Figure 4-27: Two local dents for two impact sites at 4 cells apart. The contour values indicate out-of-plane displacement (mm). The red shows the deepest dent, and the grey shows deformation less than 0.0125mm.

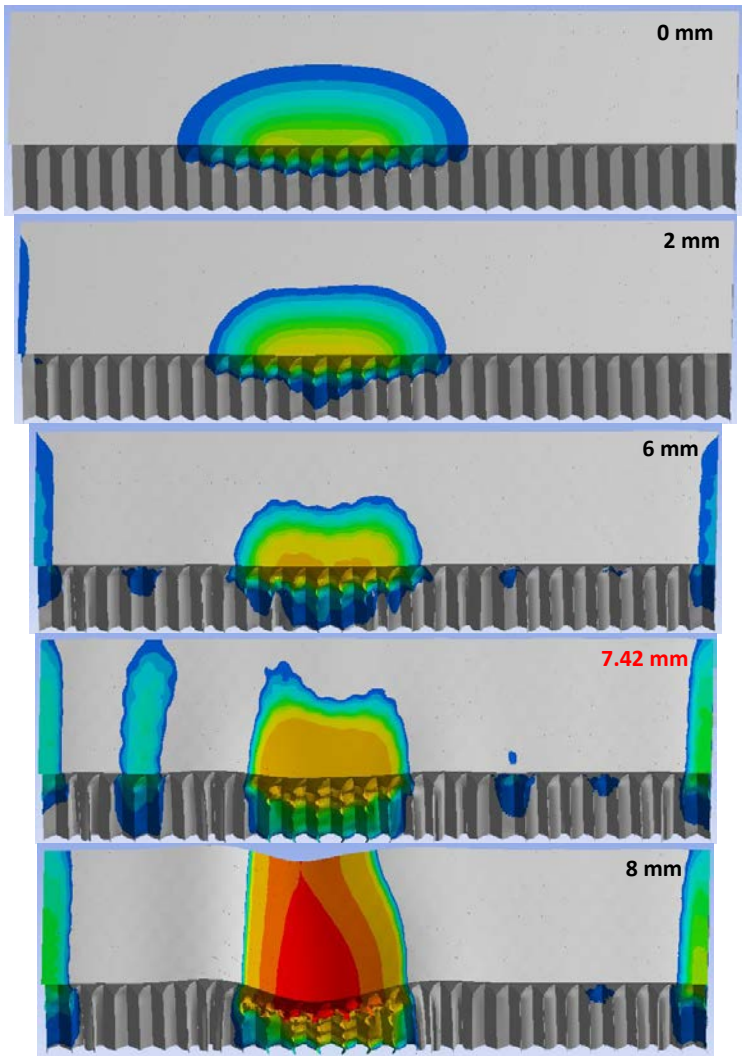

Figure 4-28: Two impact sites with 4 cells apart at different applied displacements. The contour values indicate out-of-plane displacement (mm). The red shows the deepest dent, and the grey shows deformation less than 0.0125mm. The number in red shows the amount of applied displacement corresponding to the peak reaction force.

Figure 4-29 illustrates the difference between the three cases: a) a single localization initiating from a damaged region starting as a single dent, b) a single localization initiating from a damaged region starting as two dents, and c) two localizations initiating from two independent dents. The localization location already exists at the center of the damaged region for a damaged region acting as a single dent, as shown in Figure 4-29 a). Figure 4-29 b) shows that when a dented region has 2 locations with maximum depths, as the compressive load is applied, these two locations merge so that the entire damaged region has the same maximum depth. At this point, the region starts to behave as a single dent, with the deepest point occurring at the center. This process requires a higher force than what is needed to localize from a single impact site. Figure 4-29 c) shows that when two impact sites are spaced far enough apart, each localizes independently as a single dent in Figure 4-29 a).

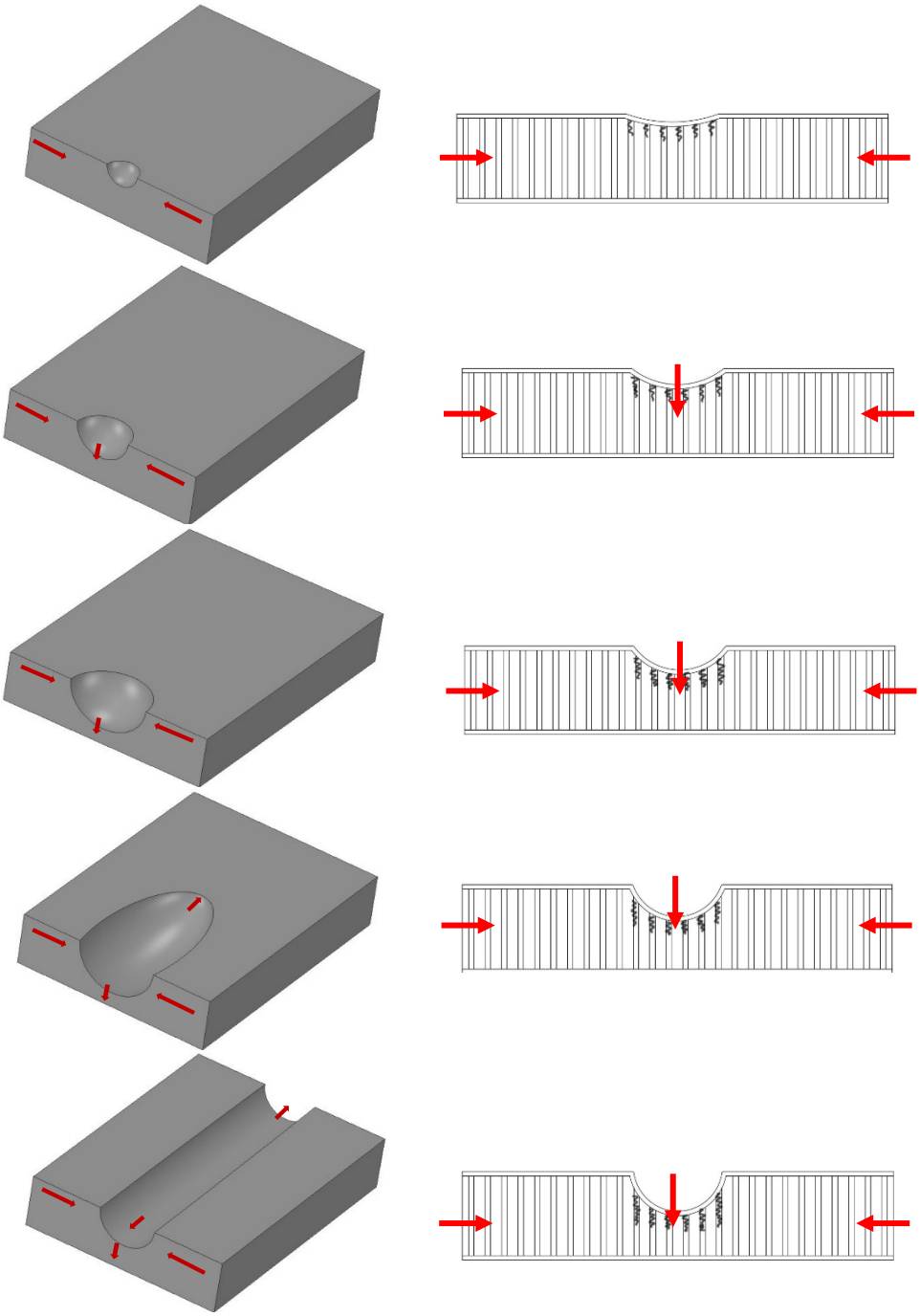

Figure 4-29 a): The failure of a single dent that propagates to the edges of the facesheet.

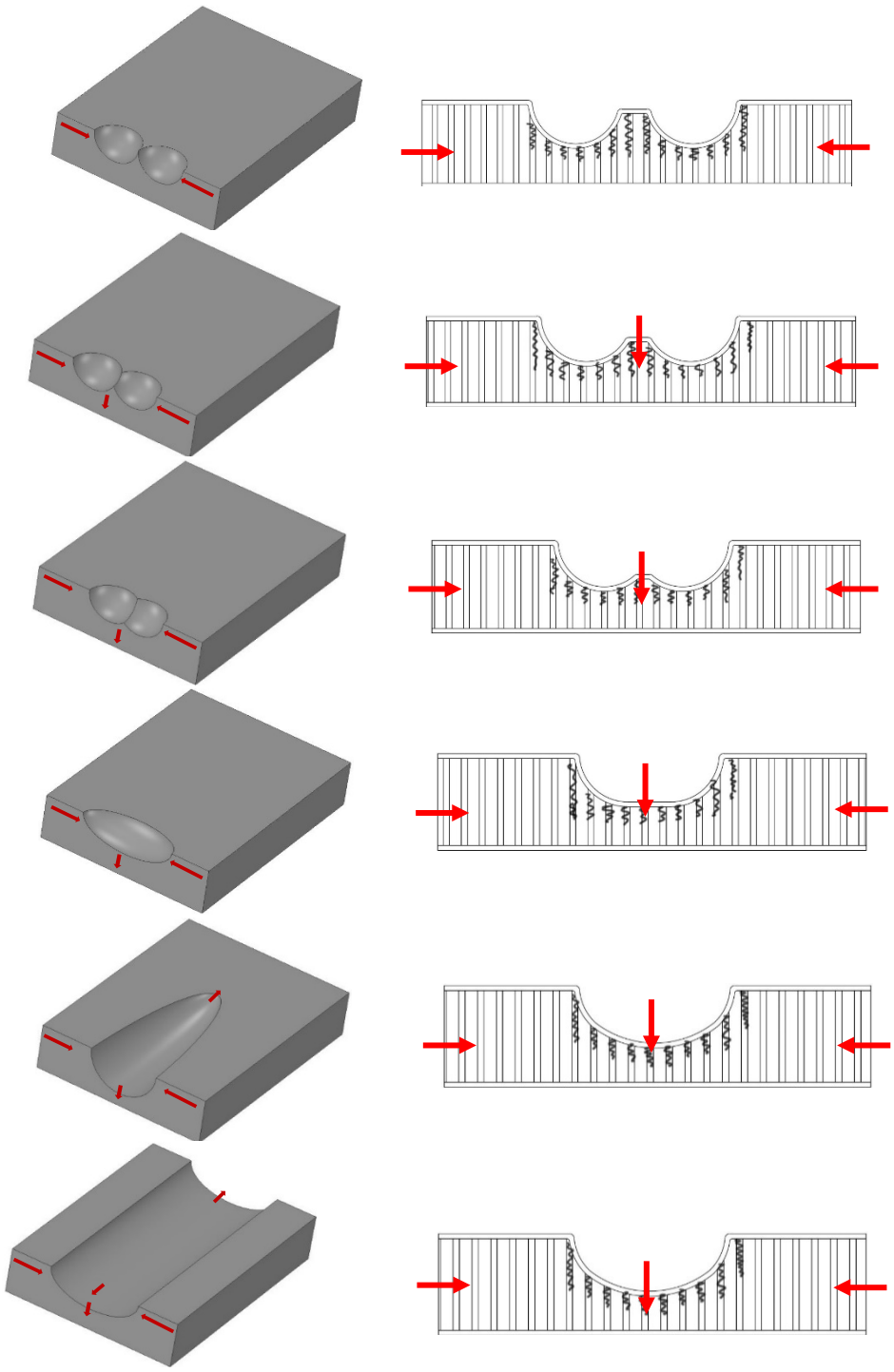

Figure 4-29 b): The failure of two impact sites interacting with each other and propagate to the edges of the facesheet.

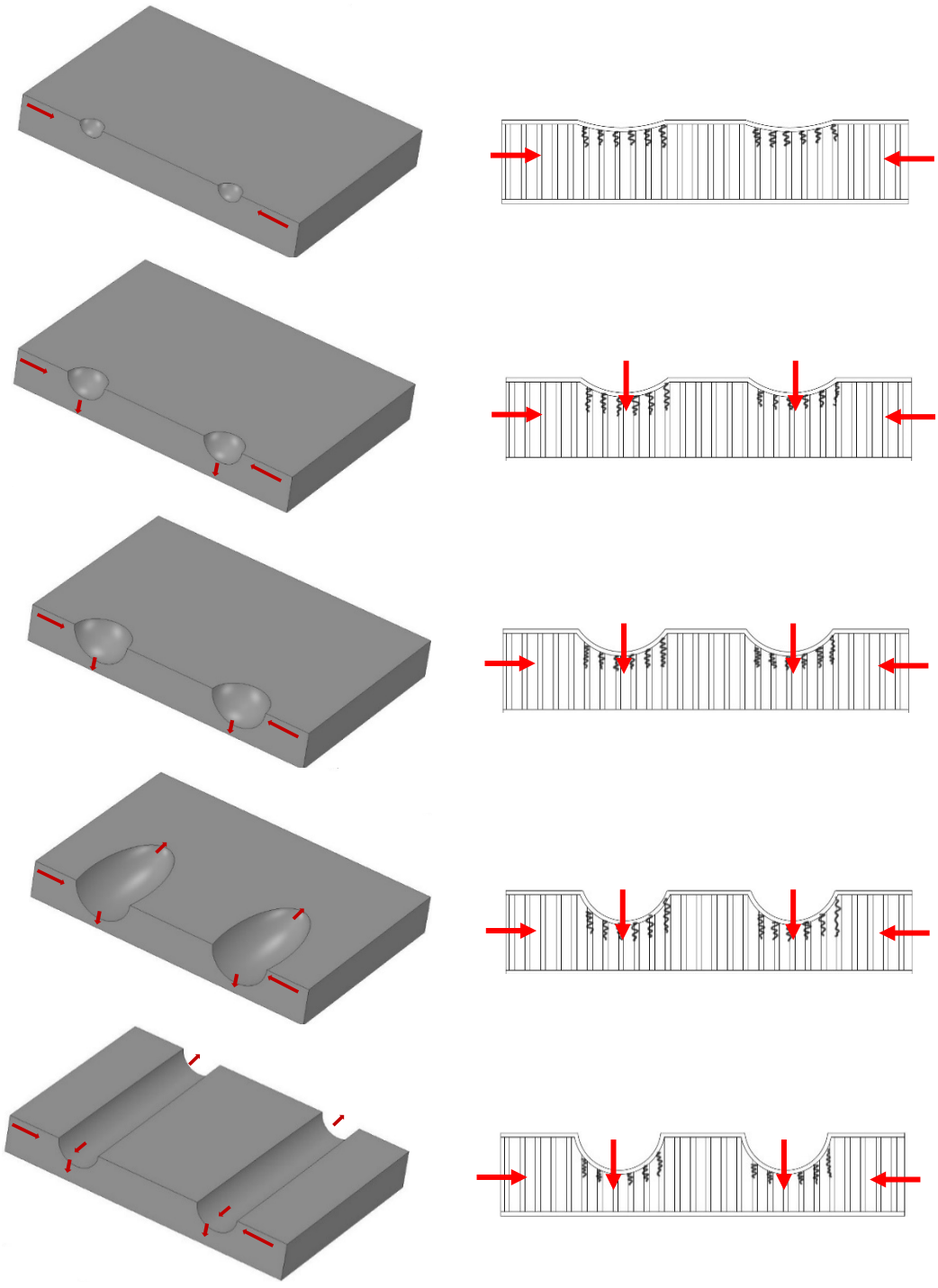

Figure 4-29 c): The failure of two impact sites far apart and behave as individuals dents that propagate to the edges of the facesheet.

4.6. Conclusion

A systematic procedure was conducted to investigate the effect of proximity between multiple dents on the residual strength for metallic honeycomb sandwich panels due to low-velocity impact damage followed by post-impact compressive loading.

Dynamic, finite element simulations were conducted for various scenarios involving two spherical impactors with different spacing between them. The analysis was performed in two loading stages: the first stage for the impact event created the damage between 0.1 and 0.7 mm, and the second stage for post-impact compressive loading. 62 total simulations were performed that also included variations in impact energy.

Six main conclusions can be drawn:

- When impact sites are close together, they interact and produce a deeper dent and a larger area than a single impact.

- Impact sites that are close enough together to interact resulted in a reduction in the panel strength as compared to a single impact site. An impact energy of 1.5J has a maximum reduction of 13%.

- The reduction in panel strength for impact sites that are close together is due to the increased dent depth. The increased area from overlapping impact sites has no effect on the residual strength.

- Dents that are far apart behave individually, and there is minimal reduction in strength as compared to a single dent. For the largest impact energy considered here, the dents must be spaced at least 13 cells apart to avoid reductions in strength.

- When the damage region produces two local dents, but they localize at a single site, the strength of the panel increases.

- If the areas of the two damage sites are not overlapping, then at most, a 1-2% reduction in residual strength is expected as compared to a single impact based on a 0.0125mm threshold for dent depth

5. Summary

This thesis is a part of a larger research project that is concerned with the safety of individuals in the aircraft and extending aircraft panel life, as manufacturing, repairing, or replacing panels is costly. The research develops finite element modelling techniques to predict the effect of spacing on in-plane compressive strength from damage that originates from low-velocity impacts on aircraft sandwich panels with metallic honeycomb core and metallic facesheets. This could be used to help optimize the damage limits in the SRM for in-field implementation within the CAF.

The SRMs are conservative as they define a limit for the distance between multiple dents, which is constant for all damage states (deeper or shallower dents, wider or narrow damaged areas). The current limits considered by maintenance personnel are quite conservative, as the retired panels that are replaced due to these limits still maintain a large degree of their residual strength. It would be beneficial if they were less conservative as it would save in costs and reduce maintenance time. The SRM could be less conservative by revaluating the damage limits for the distance between the edges of multiple dents. This could be done by taking into account specific aspects of the damage rather than having overall rules that must apply to all cases. This would be a challenge, as there would be many parameters to be considered. A systematic analysis would be required to produce the lower and upper bound of the minimum distance between the edges of two dents and then grouping and analyzing these values into a set of simple rules.

The finite element models developed in this thesis could help tremendously in this task, as the parameters could be tested quickly and in a systematic manner. The finite element model has many benefits as it is ideal for handling the fully detailed geometry of honeycomb sandwich panels, cellular core, adhesive layers, and facesheets. It also minimizes the time for performing a large number of studies with various parameters. It can isolate different variables and inexpensively perform virtual testing for many numerical models in order to identify the effects of spacing between the edges of the dents on the residual compressive strength. Critical configurations can be identified before performing costly experimentation. In this thesis, FEA was used to prove that the impactor location could cause variations in the dent depth. This finding could be used to help plan experimental tests so that variability in results can be minimized. Variability can be controlled and reduced in the experimental set-up by using a larger impactor size, smaller cell size, thicker facesheet, and thinner cell wall.

In the field, technicians can detect the damaged area and depth. They are also able to detect the distance between the edges of the dents. The example in the SRM from the Gulfstream lists a minimum spacing of 101.6mm (4”), but the results from this thesis indicate that a spacing less than this would not result in reductions in residual strength. The results indicate that if the areas of the two damage sites are not overlapping, then at most, a 1-2% reduction in residual strength is expected as compared to a single impact based on a 0.0125mm threshold for dent depth. In order to confirm this, the analysis would have to be repeated using the minimum threshold of detection achievable by either manual measurements or by more recent equipment such as laser scanners. It would also have to be repeated for dent depths up to the maximum allowable depth for a variety of panel configurations.

5.1. Future Work

Based upon the research presented in this thesis, recommended topics for future research are as follows:

- A validation of the current results through experimental testing. The current FE model set-up should be replicated as closely as possible in order to confirm the observations concluded herein for the effect of spacing between two impact sites on the compressive residual strength.

- An investigation into other commonly used materials for honeycomb sandwich panels with different facesheet thickness and core density facesheets (especially metal alloys such as 7075).

- A study on the effect of the different orientations of dents with respect to the loading direction. As dents propagate perpendicular to the applied load, dents in close proximity to each other that are aligned in this direction are expected to affect the residual strength differently.

- A study on the effect of the different loading conditions such as tensile, shear and bending loads that may cause different types of failures and different failure modes for dents in close proximity to each other.

- A study on the effect of more than two dents, clusters of dents and random positions. This is more representative of real-life scenarios and would have an effect on the overall panel strength.

- An investigation into dents with non-circular shapes and non-spherical profiles. This could be from different impactor shapes or different impact angles.

6. References

1. Reyno, T., Optical 3D Scanning, Eddy Current Testing, and Destructive Methods for Assessing Surface and Core Damage in Honeycomb Sandwich Aircraft Panels. 2017, Master's Thesis, Royal Military College of Canada, Kingston, ON, Canada.

2. Wowk, D., et al., An experimental and numerical investigation of core damage size in honeycomb sandwich panels subject to low-velocity impact. Composite Structures, 2020. **254**: p. 112739.

3. Zhang, D., et al., Experimental and numerical investigation on indentation and energy absorption of a honeycomb sandwich panel under low-velocity impact. Finite Elements in Analysis and Design, 2016. **117**: p. 21-30.

4. Bitzer, T., Honeycomb technology: materials, design, manufacturing, applications and testing. 1997: Springer Science & Business Media.

5. Benotto, J., Predicting the Effects of Dent Size on the Stress in Aluminum Honeycomb Aircraft Panels Subject to Low-Velocity Impact Damage, 2018, Master's Thesis, Royal Military College of Canada, Kingston, ON, Canada.

6. Handbook–Airframe, A.M.T., Vol. 2 (FAA-H-8083-31). US Department of Transportation, Federal Aviation Administration, 2012.

7. Aircraft Cabins Floor https://www.ainonline.com/aviation-news/business-aviation/2015-05-18/coming-soon-quieter-cabins.

8. Petras, A. and M. Sutcliffe, Failure mode maps for honeycomb sandwich panels. Composite structures, 1999. **44**(4): p. 237-252.

9. Adhesives for Bonding of Honeycomb Sandwich Panels. Masterbond. https://www.masterbond.com/techtips/adhesives-bonding-honeycomb-sandwich-panels

10. The Aluminium Honeycomb Manufacturing Process. Corex Honeycomb. https://corex-honeycomb.co.uk/about/manufacturing-process/.

11. Prior, S., Characterization of sandwich panels subject to low-velocity impact. 2016, Master's Thesis, Royal Military College of Canada, Kingston, ON, Canada.

12. Feraboli, P., Some recommendations for characterization of composite panels by means of drop tower impact testing. Journal of aircraft, 2006. **43**(6): p. 1710-1718.

13. Abrate, S., Impact engineering of composite structures. Vol. 526. 2011: Springer Science & Business Media.

14. Hodges, D.H. and G.A. Pierce, Introduction to structural dynamics and aeroelasticity. Vol. 15. 2011: cambridge university press.

15. Feraboli, P. Damage resistance characteristics of thick-Core honeycomb composite panels. in 47th AIAA/ASME/ASCE/AHS/ASC Structures, Structural Dynamics, and Materials Conference 14th AIAA/ASME/AHS Adaptive Structures Conference 7th. 2006.

16. Reyno, T., et al., Surface profiling and core evaluation of aluminum honeycomb sandwich aircraft panels using multi-frequency eddy current testing. Sensors, 2017. **17**(9): p. 2114.

17. Tomblin, J.S., et al., Impact damage characterization and damage tolerance of composite sandwich airframe structures. 2001, WICHITA STATE UNIV KS.

18. Structral Repair Manual Gulfstream IV https://seb.noaa.gov/pub/engineering/N49RF/SRM/pdf/51-79-00_2re.pdf).

19. Tomblin, J., et al., Review of damage tolerance for composite sandwich airframe structures. 1999, WICHITA STATE UNIV KS.

20. Fawcett, A.J. and G.D. Oakes. Boeing composite airframe damage tolerance and service experience. in Composite damage tolerance & maintenance workshop. 2006.

21. Gower, M., R. Shaw, and G. Sims, Evaluation of the repeatability under static loading of a compression-after-impact test method proposed for ISO standardisation. 2005.

22. McGowan, D.M. and D.R. Ambur, Compression response of a sandwich fuselage keel panel with and without damage. Vol. 110302. 1997: National Aeronautics and Space Administration, Langley Research Center.

23. Clarke, G., D. Wowk, and C. Marsden, Characterization of Low Velocity Impact Damage in Metallic Honeycomb Sandwich Aircraft Panels using Finite Element Analysis. 2017, Master's Thesis, Royal Military College of Canada, Kingston, ON, Canada.

24. Chai, G.B. and S. Zhu, A review of low-velocity impact on sandwich structures. Proceedings of the Institution of Mechanical Engineers, Part L: Journal of Materials: Design and Applications, 2011. **225**(4): p. 207-230.

25. Foo, C., L. Seah, and G.B. Chai, Low-velocity impact failure of aluminium honeycomb sandwich panels. Composite structures, 2008. **85**(1): p. 20-28.

26. Zhang, D., Q. Fei, and P. Zhang, Drop-weight impact behavior of honeycomb sandwich panels under a spherical impactor. Composite Structures, 2017. **168**: p. 633-645.

27. Foo, C., G. Chai, and L. Seah, Quasi-static and low-velocity impact failure of aluminium honeycomb sandwich panels. Proceedings of the Institution of Mechanical Engineers, Part L: Journal of Materials: Design and Applications, 2006. **220**(2): p. 53-66.

28. Aktay, L., A.F. Johnson, and B.-H. Kröplin, Numerical modelling of honeycomb core crush behaviour. Engineering Fracture Mechanics, 2008. **75**(9): p. 2616-2630.

29. Zhou, G., M. Hill, and N. Hookham, Investigation of parameters governing the damage and energy absorption characteristics of honeycomb sandwich panels. Journal of Sandwich Structures & Materials, 2007. **9**(4): p. 309-342.

30. Wowk, D. and C. Marsden, Effects of skin thickness and core density on the residual dent depth in aerospace sandwich panels. International Journal of Computational Methods and Experimental Measurements, 2016. **4**(3): p. 336-344.

31. Zheng, D. and W. Binienda, Effect of permanent indentation on the delamination threshold for small mass impact on plates. International Journal of Solids and Structures, 2007. **44**(25-26): p. 8143-8158.

32. Kurşun, A., et al., Effect of impactor shapes on the low velocity impact damage of sandwich composite plate: experimental study and modelling. Composites Part B: Engineering, 2016. **86**: p. 143-151.

33. Mitrevski, T., et al., The effect of impactor shape on the impact response of composite laminates. Composite Structures, 2005. **67**(2): p. 139-148.

34. Olsson, R., Methodology for predicting the residual strength of impacted sandwich panels. FFA TN, 1999. **8**.

35. Takeda, N., S. Minakuchi, and Y. Okabe, Smart composite sandwich structures for future aerospace application-Damage detection and suppression-: A review. Journal of Solid Mechanics and Materials Engineering, 2007. **1**(1): p. 3-17.

36. Horrigan, D. and R. Aitken, Finite element analysis of impact damaged honeycomb sandwich. FEA Ltd, Surrey, UK, 1998.

37. McQuigg, T.D., et al., Compression after impact experiments on thin face sheet honeycomb core sandwich panels. Journal of Spacecraft and Rockets, 2014. **51**(1): p. 253-266.

38. McQuigg, T.D., et al., Compression after impact analysis on thin face sheet honeycomb core sandwich panels. Journal of Spacecraft and Rockets, 2014. **51**(1): p. 200-212.

39. McGovan, D. and D. Ambur. Damage characteristics and residual strength of composite sandwich panels impacted with and without a compression loading. in 39th AIAA/ASME/ASCE/AHS/ASC Structures, Structural Dynamics, and Materials Conference and Exhibit. 1998.

40. Aminanda, Y., et al., Experimental and numerical study of compression after impact of sandwich structures with metallic skins. Composites Science and Technology, 2009. **69**(1): p. 50-59.

41. Gilioli, A., et al., Compression after impact test (CAI) on NOMEX™ honeycomb sandwich panels with thin aluminum skins. Composites Part B: Engineering, 2014. **67**: p. 313-325.

42. Akatay, A., et al., The influence of low velocity repeated impacts on residual compressive properties of honeycomb sandwich structures. Composite Structures, 2015. **125**: p. 425-433.

43. ASTM C364/C364M-07. Standard Test Method for Edgewise Compressive Strength of Sandwich Constructions. 2008 Annual Book of ASTM Standards, vol. 15.03; 2008.

44. Manes, A., et al., Experimental and numerical investigations of low velocity impact on sandwich panels. Composite Structures, 2013. **99**: p. 8-18.

45. McQuigg, T.D., Compression after impact experiments and analysis on honeycomb core sandwich panels with thin facesheets. 2011, Doctoral dissertation, Virginia Tech.

46. Shyprykevich, P., et al., Guidelines for analysis, testing, and nondestructive inspection of impact-damaged composite sandwich structures. 2003, FEDERAL AVIATION ADMINISTRATION TECHNICAL CENTER ATLANTIC CITY NJ.

47. Tsang, P. and P. Lagace. Failure mechanisms of impact-damaged sandwich panels under uniaxial compression. in 35th Structures, Structural Dynamics, and Materials Conference. 1994.

48. Schubel, P.M., J.-J. Luo, and I.M. Daniel, Low velocity impact behavior of composite sandwich panels. Composites Part A: applied science and manufacturing, 2005. **36**(10): p. 1389-1396.

49. Zhu, S. and G.B. Chai, Damage and failure mode maps of composite sandwich panel subjected to quasi-static indentation and low velocity impact. Composite structures, 2013. **101**: p. 204-214.

50. Zhu, S. and G. Chai, Effect of adhesive in sandwich panels subjected to low-velocity impact. Proceedings of the Institution of Mechanical Engineers, Part L: Journal of Materials: Design and Applications, 2011. **225**(3): p. 171-181.

51. Lee, I., et al., Low velocity impact behavior of aluminum honeycomb structures. Advanced Composite Materials, 2010. **19**(1): p. 19-39.

52. Ivañez, I. and S. Sanchez-Saez, Numerical modelling of the low-velocity impact response of composite sandwich beams with honeycomb core. Composite Structures, 2013. **106**: p. 716-723.

53. Sun, G., et al., Experimental and numerical study on honeycomb sandwich panels under bending and in-panel compression. Materials & Design, 2017. **133**: p. 154-168.

54. Giglio, M., A. Gilioli, and A. Manes, Numerical investigation of a three point bending test on sandwich panels with aluminum skins and Nomex™ honeycomb core. Computational Materials Science, 2012. **56**: p. 69-78.

55. Czabaj, M., et al. Compression after impact of sandwich composite structures: experiments and modeling. in 51st AIAA/ASME/ASCE/AHS/ASC Structures, Structural Dynamics, and Materials Conference 18th AIAA/ASME/AHS Adaptive Structures Conference 12th. 2010.

56. Fan, X., T. Wang, and Q. Sun, Damage evolution of sandwich composite structure using a progressive failure analysis methodology. Procedia Engineering, 2011. **10**: p. 530-535.

57. Meo, M., et al., Numerical simulations of low-velocity impact on an aircraft sandwich panel. Composite Structures, 2003. **62**(3-4): p. 353-360.

58. Xie, Z., A.J. Vizzini, and M. Yang, On residual compressive strength prediction of composite sandwich panels after low-velocity impact damage, in Sandwich structures 7: advancing with sandwich structures and materials. 2005, Springer. p. 363-372.

59. Ratcliffe, J.G. and W.C. Jackson, A finite element analysis for predicting the residual compressive strength of impact-damaged sandwich panels. NASA Technical Memorandum, NASA/TM-2008-215341, 2008.

60. Castanié, B., et al., Modelling of low-energy/low-velocity impact on Nomex honeycomb sandwich structures with metallic skins. International Journal of Impact Engineering, 2008. **35**(7): p. 620-634.

61. Heimbs, S., Virtual testing of sandwich core structures using dynamic finite element simulations. Computational Materials Science, 2009. **45**(2): p. 205-216.

62. Reyno, T., C. Marsden, and D. Wowk, Surface damage evaluation of honeycomb sandwich aircraft panels using 3D scanning technology. NDT & E International, 2018. **97**: p. 11-19.

63. Kendall, P., et al., Experimental investigation of adhesive fillet size on barely visible impact damage in metallic honeycomb sandwich panels. Composites Part B: Engineering, 2020. **184**: p. 107723.

64. Li, K., X.-L. Gao, and J. Wang, Dynamic crushing behavior of honeycomb structures with irregular cell shapes and non-uniform cell wall thickness. International Journal of Solids and Structures, 2007. **44**(14-15): p. 5003-5026.

65. Yang, M.-Y., J.-S. Huang, and J.-W. Hu, Elastic buckling of hexagonal honeycombs with dual imperfections. Composite structures, 2008. **82**(3): p. 326-335.

66. Yang, M.-Y. and J.-S. Huang, Numerical analysis of the stiffness and strength of regular hexagonal honeycombs with plateau borders. Composite structures, 2004. **64**(1): p. 107-114.

67. Tomblin, J.S., et al., Impact damage characterization and damage tolerance of composite sandwich airframe structures-Phase II. 2002, WICHITA STATE UNIV KS.

68. 2024T3. (2019). Matweb, Material Property Data (2024T3) Retrieved Dec 3, 2019, from http://www.matweb.com/search/DataSheet.aspx?MatGUID=57483b4d782940faaf12964a1821fb61.

69. Epoxy adhesive. (2019). Matweb, Material Property Data (epoxy adhesive) Retrieved Dec 3, 2019.

70. Tariq, F., M. Uzair, and M. Shifa, Residual compressive strength of aluminum alloy honeycomb sandwich panel in the presence of multiple impact dents. Journal of Sandwich Structures & Materials, 2021: p. 10996362211036987.

71. Cromer, K., J.W. Gillespie Jr, and M. Keefe, Effect of multiple non-coincident impacts on residual properties of glass/epoxy laminates. Journal of Reinforced Plastics and Composites, 2012. **31**(12): p. 815-827.

72. Cromer, K., Impact and post-impact response of a composite material to multiple non-coincident impacts. 2010, Doctoral dissertation, University of Delaware, USA.

73. Fischer, C., et al. Strategies to investigate the residual strength of impact damaged honeycomb sandwich structures using detailed numerical models. in Conference paper, 21st International Conference on Composite Materials. 2017.